Deciphering the mechanism and function of stage-specific protein association with the membrane cytoskeleton of Toxoplasma gondii

Author: Rashmi Dubey

Persistent link:

This work is posted on eScholarship@BC,
Boston College University Libraries.

Boston College

Graduate School of The Morrissey College of Arts and Sciences

Department of Biology

Deciphering the mechanism and function of stage-specific protein association with the membrane cytoskeleton of *Toxoplasma gondii*

a dissertation

by

RASHMI DUBEY

submitted in partial fulfillment of the requirements

for the degree of

Doctor of Philosophy

Dec 2016

Abstract

Deciphering the mechanism and function of stage-specific protein association with the membrane cytoskeleton of *Toxoplasma gondii*

Author: Rashmi Dubey

Advisor: Prof. Marc-Jan Gubbels

Apicomplexan parasites like *Toxoplasma gondii* have a complex life cycle comprising of transitions between different hosts, different organ systems and between the extracellular and intracellular milieu. The parasite must thus adjust itself and its cellular processes in accordance with its environment. In this dissertation, I have focused on such stage specific behaviors of three distinct intermediate filament-like proteins as well as a glycolytic enzyme, glyceraldehyde-3-phosphate dehydrogenase 1 (GAPDH1). These proteins relocate from the cytosol to the unique cortical membrane skeleton of non-dividing parasites. The intermediate filament-like proteins IMC7, 12 and 14, localize exclusively to the mature cytoskeleton. One model of function was that these proteins differentially stabilized mother and budding daughter cytoskeletons in the division process, but we ruled out this role for the individual proteins, as they are not essential for the lytic cycle of the parasite. However, we determined that IMC7 and IMC14 are contributing to the maintenance of rigidity of the cytoskeleton under osmotic stress conditions in extracellular parasites. In addition, IMC14 is critical in cell cycle progression as its depletion results in the formation of multiple daughters per division round. When the parasite egresses from the host cell, glycolytic enzyme GAPDH1 translocates to the cortex. The functional role of GAPDH1 in the parasite and the mechanism of its cortical translocation are deciphered based on the 2.25Å resolution

crystal structure of the GAPDH1 holoenzyme in a quaternary complex. These studies identified that GAPDH1's enzymatic function is essential for intracellular replication but we confirmed the previous reports that glycolysis is not strictly essential in presence of excess L-glutamine. We identify, for the first time, S-loop phosphorylation as a novel, critical regulator of enzymatic activity that is consistent with the notion that the S-loop is critical for cofactor binding, allosteric activation and oligomerization. We show that neither enzymatic activity nor phosphorylation state correlate with the ability to translocate to the cortex. However, we demonstrate that association of GAPDH1 with the cortex is mediated by Cysteine 3 in the N-terminus, likely by palmitoylation. Overall, glycolysis and cortical translocation are functionally decoupled by post-translational modifications. Collectively, the discoveries made in this dissertation reveal unprecedented detail in mechanism and function of cortical protein translocation and thereby identifying new drug targets.

This thesis is dedicated to my Nanajee and Nanijee (maternal grandparents) and Baba

and Dadi (paternal grandparents), who taught me to dream big and work harder to

achieve them. I love and respect them beyond words.

insightful scientific discussions and support. Alongwith the scientific skills, I have also been immensely fortunate to develop dear friendship during my time in graduate school. It is difficult to put in words how grateful I am to have met Megan, Sudeshna, Anindita, Angela and Klemens. They have been a source of constant support, encouragement and guidance during this PhD journey.

Last but not least, I would like to acknowledge the unwavering support and love of all my family members over the years. They have patiently endured my ups and downs through graduate school and always been there with words of encouragement. I would like to acknowledge my mom, dad, uncle and aunt and all my amazing siblings for believing in me and supporting me during this time. I am also thankful to my in-laws: mother-in-law, father in-law, brother-in-law, sister-in-law and my adorable niece and nephew for cheering me and allowing me to be as ambitious as I wanted. Finally, the one person without whom I would have never started or completed my graduate school is my husband Pragati Tiwary. He has inspired me to be a persistent, resilient and better person everyday. Thank you for reminding me to have faith and standing by me everyday.

Table of Contents

List of Figures and Tables

Dissertation contributions

Chapter 2:

      Figure 2.2. mCherry IMC7 and mCherry IMC14 data for random cycling and
           early G1 done by Tomasz Szatanek Brooke Anderson-White as
           published in Szatanek et al., 2012)

Chapter 3-5:

      Table 3.1. Crystal structure data of TgGAPDH1 compiled by Bart L. Staker as
           published in Dubey et al., 2016.

      Figure 3.1. Secondary structural alignment of GAPDH done by Huan M. Ngô as
           published in Dubey et al., 2016.

      Figure 3.2. Structure of TgGAPDH1 protein done by Huan M. Ngô as
           published in Dubey et al., 2016.

      Figure 3.8. Structure of *Toxoplasma* GAPDH1 catalytic site done by Huan M.
           Ngo as published in Dubey et al., 2016.

      Figure 4.1. Structure prediction for Serine phosphorylation in the regulatory S-
           loop done by Huan M. Ngô as published in Dubey et al., 2016.

      Figure 5.1. Tyrosine phosphorylation in the S loop may be sterically hindered
           predicted by Huan M. Ngô as published in Dubey et al., 2016.

      Figure 5.4. (b-d) GAPDH1 is predicted to be palmitoylated as structurally shown
           by Huan M. Ngô and published in Dubey et al., 2016.

      Figure 5.5. 17ODYA labeling and click chemistry to analyze GAPDH1
           palmitoylation performed by Ian T. Foe as published in Dubey et al.,
           2016.

List of Abbreviation

3-MA	3-methyl adenosine
AIDS	acquired immune deficiency syndrome
ALD1	aldolase
ALP-1	actin like protein-1
AMA1	apical membrane antigen 1
ATc	anhydrous tetracycline
ATP	adenosine triphosphate
A488	Alexa Fluor 488
A594	Alexa Fluor 594
BSA	bovine serum albumin
Cas9	CRISPR associated protein 9 nuclease
cKD	conditional knockdown
CDPK	calcium-dependent protein kinase
CRISPR	Clustered regularly interspaced short palindromic repeats
DAPI	4′6-diamidino-2-phenylindole
DHFR	dihydrofolate reductase
dKO	direct knock out
DMEM	Dulbecco's modified eagle medium
DMSO	dimethyl sulfoxide
FBS	fetal bovine serum
GAP	gliding-associated protein
GAPDH	glyceraldehyde-3-phosphate dehydrogenase
HBSS	Hank's balanced salt solution
HEPES	4-(2-hydroxyethyl)-1-piperazineethanesulfonic acid
HFF	human foreskin fibroblasts
HH	HBSS with 1 mM HEPES pH 7
HIV	human immunodeficiency virus
HiSp	high speed
HiSp-S	high speed supernatant
Hi-Sp-P	high-speed pellet
HR	homologous recombination
HRP	horseradish peroxidase
hTERT	human telomerase reverse transcriptase
IF	intermediate filament
IFA	immunofluorescence assay
IMC	inner membrane complex
IMP	inner membranous particle
ISP	IMC sub-compartment protein
KO	knockout
LDH	lactate dehydrogenase
LoSp	low speed
Mab	monoclonal antibody
MIC2	microneme protein 2
MORN1	membrane occupation and recognition nexus1

MJ	moving junction
MT	microtubule
MTOC	microtubule organizing center
MyoA	myosin A
NaCl	sodium chloride
NAD	nicotinamide adenine dinucleotide
NHEJ	non-homologous end joining
NP-40	4-Nonylphenyl-poly ethylene glycol
NPC-1	Niemann-Pick, type C1-related protein
NTPase	nucleotide triphosphate degrading enzymes
PAGE	polyacrylamide gel electrophoresis
PAT	palmitoyl acyltransferase
PAM	protospacer adjacent motif
PBS	phosphate buffered saline
PI	propidium iodide
PSB	phosphatidylserine-rich binding domain
p*T7S4*	minimal SAG4 promoter preceded by seven-tetracycline operator repeats
p*tub*	tubulin promoter
PV	parasitophorous vacuole
Rab	Ras regulated protein
RB	resuspension buffer
RON	rhoptry neck protein
SAG	surface antigen protein
SAG1	surface antigen 1
SAG4	surface antigen 4
SD	standard deviation
SDS	sodium dodecyl sulfate
SEM	standard error of the mean
TATi	tetracycline transactivator
TX-100	Triton-X 100
YFP	yellow fluorescent protein
WT	wild type

CHAPTER 1: INTRODUCTION

1.1. Introduction

Toxoplasma gondii is a ubiquitous apicomplexan capable of infecting any nucleated cell within a wide variety of warm-blooded vertebrates including human (Frenkel, 1973; Huynh et al., 2003). The phylum Apicomplexa consists of approximately 5000 species (Levine, 1988) which are nearly all obligate intracellular parasites and are defined by the presence of a complex apical cytoskeleton and secretory organelles (Hu et al., 2006). *Toxoplasma* is distinct from nearly all other members owing to the exceptionally wide range of animals that serve as host for its intermediate life cycle (Frenkel et al., 1970). Generally regarded as an opportunistic pathogen, *T. gondii* is responsible for the development of toxoplasmosis-associated encephalitis and congenital toxoplasmosis in humans (Luft and Remington, 1992; Montoya and Liesenfeld, 2004).

Other pathogens in this phylum of medical and economic importance affect humans and livestock. *Plasmodium* is a human pathogen, the causative agent of malaria, and results in the death of half a million individuals annually (Starkl Renar et al., 2016). *Cryptosporidium* species and *Cyclospora cayetanesis* cause severe gastrointestinal enteritis specifically diarrhea (Francia and Striepen, 2014; Mansfield and Gajadhar, 2004). *Neospora caninum* is a livestock pathogen causing clinical disease like neosporosis associated with abortion in cattle and causes significant economic loss to both dairy and beef industries (Larson et al., 2004). *Babesia* and *Theileria* species transmitted by ticks infect wild and domestic animals including dogs, cattle, goats and sheep (Bishop et al., 2004; Schnittger et al., 2012), and infection of poultry by *Eimeria* species results in coccidiosis, causing severe economic loss worldwide (McDonald and Shirley, 2009). Since Apicomplexa are pathogens, the development of new drugs and

drug target candidates is a mainstay driver for studying these parasites and it is inevitable that there will be a big gain by understanding the parasite biology and underlying molecular process.

1.2. Epidemiology and pathogenesis

Infections by the protozoan parasite *Toxoplasma gondii* are widely prevalent worldwide in both animals and human. Currently, one third of the world's population is infected (Montoya and Liesenfeld, 2004) and an estimated 1.1 million persons in the United States are infected each year (Jones and Holland, 2010). It is the second leading cause of death attributable to foodborne illness and leading contributor to loss of quality adjusted life years (Jones et al., 2014). The parasite has a typical heteroxenous life cycle alternating between sexual replication in felids and asexual replication in a wide range of warm-blooded animals that serve as intermediate hosts (Frenkel et al., 1970). Infection occurs by food-borne transmission when the host ingests undercooked or raw meat containing the parasite in tissue cysts or through ingestion of either soil, food or water contaminated by cat feces harboring oocysts (Jones and Holland, 2010). Tachyzoites are the rapidly growing stage formed by asexual reproduction in all the intermediate hosts causing acute infections. Most acute infections pass with mild or no symptoms, but severe disease occurs in immuno-compromised patients (Barsoum, 2004; Luft and Remington, 1992; Sahasrabudhe et al., 2003). In healthy individuals, the infection is usually asymptomatic and results in the formation of dormant encysted bradyzoites that remain in the brain and muscle tissues for life and thus cause chronic infection. Reactivation of such latent infection occurs in immunocompromised HIV/AIDS patients, immuno-suppressed organ

transplant-recipients and patients undergoing anti cancer treatment, affecting the central nervous system, leading to toxoplasmotic encephalitis (Luft and Remington, 1992). Primary infection in naïve pregnant women can lead to transplacental transmission of the parasite causing congenital toxoplasmosis, which may result in abortion, retinochoroiditis, and mental retardation (Wong and Remington, 1994). The current drug therapy is a combination of pyrimethamine and sulfadiazine, which targets the folate pathway and effectively kills the tachyzoite stage; such treatments do not remove the chronic infection and as a result long-term therapy is needed in immunocompromised patients (Rajapakse et al., 2013). These drugs have numerous side effects like nausea, vomiting, diarrhea, fever, rash, bone marrow suppression, neuropathy and hematuria (Kaye, 2011). The toxic side effects combined with their inability to eliminate infection highlights the need for safer and more effective treatments.

1.3. Lytic cycle of the parasite

The pathogenesis of this parasite absolutely depends on its ability to reiterate its lytic cycle, which is composed of invasion, intracellular replication and egress from the host cell (Figure 1.1.). Invasion is a multi-step process consisting of recognition, attachment and active penetration of a host cell. The parasite attaches to the potential host through its surface protein coat SAGs and releases contents of its specialized secretory organelles microneme and rhoptry, to form a tighter interaction called the moving junction (MJ) (Kafsack et al., 2007). The MJ is a ring like structure formed on the interface between the host cell and parasite at the entry point into the host cell. It is a collaboration of rhoptry neck proteins (RONs) assembled in the host cell plasma membrane and microneme

protein apical membrane antigen 1 (AMA1) anchored in the parasite (Alexander et al., 2005). The active penetration of the host cells by the parasite results in the formation of specialized, non-fusogenic compartment termed the parasitophorous vacuole (PV) within which the parasites reside and replicate (Joiner and Dubremetz, 1993; Soldati et al., 2001). A myosin motor complex termed the glideosome powers parasite propulsion into the host cell and is required for efficient invasion. It is not completely understood if motility is a strict requirement of invasion as in absence of many glideosome components some parasites are able to invade and develop normally (Blader et al., 2015). Recent reports claim that host cell membranes are actively involved in the invasion process and specifically host cell actin is critical for parasite internalization (Bichet et al., 2016). Following successful invasion, parasites replicate by internal budding and continue multiplying in the PV until it fills the host cell cytoplasm. The parasite initiates to egress through different mechanisms like increased concentration of abscisic acid, decreased pH and increased secretion of nucleotide triphosphate-degrading enzymes (NTPases). Upon egress from the host cell, the tachyzoites demonstrate actinomyosin based gliding motility to search for the nearby host. Thus, gliding motility, invasion and egress are vastly interconnected though the molecular mechanisms governing these processes are highly diverse.

Division of the parasite occurs via internal budding or endodyogeny where two daughter parasites are formed within a mother (Sheffield and Melton, 1968). The initiation of cell division occurs by the duplication of the Golgi apparatus late in G1 (Hu et al., 2002) followed by the replication of the centrosome early in S phase (Hartmann et al., 2006; Hu et al., 2002; Nishi et al., 2008). The centrosome plays a pivotal role in

coordinating the mitotic and cytokinetic events (Chen and Gubbels, 2013). The centrosome is comprised of an inner and outer core, which involves two functionally distinct regions separately regulating mitosis and cell division, respectively (Suvorova et al., 2015). The outer core provides spatial cues for daughter cytoskeleton assembly driven by recruitment and assembly of the cortical cytoskeletal components forming the new daughter scaffold. Karyokinesis and cytokinesis progress simultaneously as the cytoskeleton grows providing structural integrity (Mann and Beckers, 2001; Striepen et al., 2007). In this process it engulfs the divided Golgi (Nishi et al., 2008), then the apicoplast (Striepen et al., 2000), the nucleus and endoplasmic reticulum (Hager et al., 1999; Hu et al., 2002) and finally the mitochondrion (Nishi et al., 2008). The apical secretory organelles (micronemes and rhoptries) are formed de novo, within the developing parasite (Nishi et al., 2008; Sheffield and Melton, 1968). Division is completed by the breakdown of the mother's cytoskeleton whereas the plasma membrane is recycled onto the daughter parasites (Morrissette and Sibley, 2002). The unencapsulated material of the mother parasite is degraded away in a residual body (Sheffield and Melton, 1968).

Upon completion of replication, the egressing parasite becomes motile to search for new host cells to continue to the lytic cycle (Sibley, 2004). The extracellular parasites are in a biologically distinct state from the intracellular form; they do not divide, are highly motile, and secrete the contents of their microneme organelles (Blader et al., 2015). The switch between the intracellular and extracellular states is accompanied by dramatic changes in gene expression (Gaji et al., 2011; Lescault et al., 2010), mRNA availability for translation (Lirussi and Matrajt, 2011) and translocation of glycolytic

enzymes as described in detail in section 1.5 (Pomel et al., 2008). The activation toward the extracellular stage is in a way first step of host cell invasion (Hoff and Carruthers, 2002).

1.4. Cytoskeleton of *Toxoplasma* and the intermediate-filament like proteins

The tachyzoite is crescent shaped with a pellicle consisting of an outer plasma membrane, an inner membrane complex (IMC) and a microtubule structure (Figure 1.2.) (Foussard et al., 1990). The cytoskeleton provides mechanical strength to the parasite to maintain its structural integrity and in addition is the main driver of cell division (Mann and Beckers, 2001). The IMC is a double membrane system composed of a patchwork of flattened membranous sacs called alveoli which are rectangular and arranged in three rows encircling the entire parasite with a single cone shaped vesicle capping the apical end (Dubremetz and Elsner, 1979; Porchet and Torpier, 1977). There are 22 subpellicular microtubules that originate from the apical polar ring and extend two-third the length of the parasite in spiraling fashion (Nichols and Chiappino, 1987). The subpellicular microtubules are associated with the IMC by microtubule-associated proteins, which are anchored to inner membranous particles (IMPs) (Morrissette et al., 1997; Morrissette and Sibley, 2002). These IMPs are also present on the inner and middle faces of the IMCs in double and single rows with 32 nm periodicity extending along the entire length of the parasite (Dubremetz and Torpier, 1978; Morrissette et al., 1997). The IMC also runs along the entire length of the parasite with gaps at the apical and posterior end. The opening at the apical end allows for the extension of the conoid during invasion while the posterior end is occupied by the basal cup whose functions are still unclear (Del Carmen

et al., 2009; Mann and Beckers, 2001). MORN1 a highly conserved apicomplexan protein localizes to the apical and posterior end of the parasite and to the centrocone, a specialized nuclear structure that organizes the mitotic spindle (Gubbels et al., 2006).

The parasite has an atypical actin cytoskeleton, comprised mainly of the globular form and transient formation of short actin filaments occurs during host cell invasion and gliding motility of the parasite (Dobrowolski and Sibley, 1996). Filamentous actin transiently forms to harbor the motility apparatus called glideosome, which contains Myosin A, Myosin Light Chain 1 and the membrane anchoring protein GAP45 and GAP50 (Keeley and Soldati, 2004). The parasite is able to invade successfully even in the absence of core components of the invasion machinery like actin, MyoA, AMA1, MIC2 (Andenmatten et al., 2013; Bargieri et al., 2013; Egarter et al., 2014) likely due to plasticity between the motor proteins like MyoC and MyoA (Frenal et al., 2014b) or the contribution of host cell membrane to invasion (Bichet et al., 2016). However, actin is essential for apicoplast replication (Andenmatten et al., 2013) and appears to be involved in the step upstream of formation of MJ during parasite invasion (Egarter et al., 2014), but parasites are able to complete cell division indicating actin is not required for contractile ring constriction.

The cytoskeletal network is a complex structure composed of 8-10 nm-interwoven intermediate-filaments located on the cytoplasmic face of the IMC. In the membrane sac are the IMC subcompartment proteins namely ISP1, ISP2, ISP3 and ISP4 localized to the distinct subcompartment of the IMC (Beck et al., 2010). Recently, other novel IMC proteins localizing to the specific IMC compartment or alveolar sutures have also been discovered (Chen et al., 2015). Specifically, the intermediate filament-like (IF-like)

proteins contain a series of conserved repeats called alveolins, which contains valine and proline-rich domains (Gould et al., 2008). These domains are composed of 'EKIVEVP', 'EVVR' or 'VPV' sub repeats (Gould et al., 2008) and *T.gondii* genome has 14 alveolin domain containing genes (Anderson-White et al., 2011). The assembly process of the IMC proteins and other cytoskeleton proteins during budding process has been established in detail (Anderson-White et al., 2012). Different groups are defined within the alveolin IMC protein family: a group localizing exclusively to the basal complex (IMC5, 8, 9, and 13); IMC 15 colocalizing with the centrosome and early daughter buds; a group at the cortex of the mature mother and daughter parasites (IMC1, 3, 4, 5, 6, and 10), and finally a group localizing to the mature cytoskeleton (IMC7, 12, and 14) (Anderson-White et al., 2011). Thus, it is hypothesized that these IMC proteins fulfill different functions in the parasite during cytoskeletal assembly, maturation, maintenance and/or disassembly (Anderson-White et al., 2011).

1.5. GAPDH: more than housekeeping

Glyceraldehyde-3-phosphate dehydrogenase (GAPDH) is a key enzyme of glycolysis and catalyzes the oxidative phosphorylation of glyceraldehyde 3-phophate to D-glycerate 1,3-bisphosphate in presence of NAD^+ and inorganic phosphate during glycolysis. GAPDH has been studied for its pivotal role in glycolysis and is a common housekeeping protein. For its abundant and constitutive expression, GAPDH is used as an internal control for analysis and expression of other genes and proteins. Besides its glycolytic function, GAPDH is an impressive multifunctional protein with diverse activities and distinct sub-cellular localization (Sirover, 1999, 2011). These varied functions include membrane

fusion and transport (Glaser and Gross, 1995; Tristan et al., 2011), cytoskeletal dynamics (Kumagai and Sakai, 1983), post-transcriptional gene regulation (Bonafe et al., 2005; Sirover, 1999), chromatin structure (Demarse et al., 2009; Sundararaj et al., 2004), maintenance of DNA integrity (Azam et al., 2008) and the facilitation of actin polymerization and microtubule bundling (Kumagai and Sakai, 1983; Reiss et al., 1996). The diverse functions are likely regulated by post-translational modifications next to changes in sub-cellular localization and oligomerization (Tristan et al., 2011). For example, the association of GAPDH with vesicular tubular clusters, which function as transport complexes, carrying cargo between endoplasmic reticulum and the Golgi apparatus, is mediated by tyrosine phosphorylation of GAPDH by an atypical protein kinase. Phosphorylated GADPH is recruited to Rab2 and thereby promotes the interaction between microtubules and motor proteins with Rab2-mediated vesicles. Notably, most of these additional roles of GAPDH are independent of its glycolytic function (Robien et al., 2006; Tisdale, 2001, 2002; Tisdale and Artalejo, 2006; Tisdale et al., 2004).

In *Toxoplasma*, all glycolytic enzymes except hexokinase and glucose-6-phosphate isomerase occur in duplicate in the genome (Fleige T, 2007). The complete set of the ten enzymes that form the glycolytic pathway is targeted to the cytosol while the other isoforms localize to the apicoplast or nucleus in case of enolase (Fleige T, 2007). It was further discovered that the glycolytic enzymes like GAPDH1, aldolase and LDH1 are translocated from the cytoplasm to the pellicle of the parasite upon egress from the host cell (Pomel et al., 2008). These enzymes remain pellicle-associated throughout the extracellular phase and during invasion of the host cell (Pomel et al., 2008). The enzyme translocation is triggered by the changes in extracellular potassium and intracellular

calcium ion concentrations during egress from host cell. Upon successful invasion, the localization of GAPDH1 reverts back to the cytoplasm (Pomel et al., 2008). Glycolytic enzymes become peripheral in other organisms as well. In freshly isolated human erythrocytes, many glycolytic enzymes are intimately associated to the inner face of the plasma membrane, but are cytoplasmic in deoxygenated cells (Campanella et al., 2005b). It is hypothesized that this association is related to the generation of highly compartmentalized pool of ATP for the efficient consumption by ion and nutrient transporters. Similarly, the close association of the glycolytic enzymes to the pellicle of *Toxoplasma* is related to the highly localized production of ATP in the extracellular parasites. This is hypothesized to occur for improved delivery of ATP by the active transporter mechanism in the parasite plasma membrane and to the motile apparatus situated in the space between plasma membrane and IMC (Pomel et al., 2008; Sirover, 2011).

The crystal structure of GAPDH has been established for numerous species and in general the enzyme crystallizes as a tetramer with dihedral symmetry. The N-terminus includes NAD^+ binding domain also called the Rossman domain and the C terminus contains catalytic domain (Akinyi et al., 2008). A loop separating the NAD^+ binding cavities of adjacent subunits, called the S-loop, is in close proximity to the catalytic domain. It regulates the activity of the enzyme by creating a wide pocket to centrally position the nicotinamide ring into the active site pocket. The key differences of other GAPDH like *Leishmania* and *Trypanosma* has been extensively explored in relation to the human GAPDH as a putative drug target (Lakhdar-Ghazal et al., 2002; Opperdoes and Michels, 2001). In trypanosomes, the binding site for the adenosine portion of NAD^+

in GAPDH has a hydrophobic cleft and adenosine derivatives competing with this binding site have been developed. These inhibitors can stunt the growth of the parasite in culture at low concentration and future research to optimize the affinity and selectivity of these inhibitors is required to make them suitable for toxicity and in vivo activity (Lakhdar-Ghazal et al., 2002; Verlinde et al., 2001). In *Leishmania* the glycolytic enzymes aldolase and enolase have been reported as possible vaccine candidate against visceral leishamaniasis (Gupta et al., 2014).

1.6. Open questions and thesis synopsis

The pathogenesis of *Toxoplasma* is closely linked to rapid replication rounds, which rely on the proper formation of the cytoskeleton. The spatio-temporal behavior of the proteins associated with the IMC namely IMC7, IMC12 and IMC14 are defined and they localize to the mature cytoskeleton, upon the completion of budding. It has been hypothesized that these IMCs mark the newly formed daughter cells from the degrading mother and thereby are a key to successful internal budding (Anderson-White et al., 2011). In addition to IMC proteins translocating to the pellicle of non-dividing G1 cell stage tachyzoites, the glycolytic enzymes make a similar translocation but upon parasite egress, basically in an arrested G0 state of the cell cycle (Figure 1.3.). Neither the mechanism nor the significance of these translocations to the cortex is currently well understood. A better understanding of the unique features of these translocation events might provide insights for the development of parasite specific drugs. This dissertation sets out to identify the mechanism and potential shared mechanisms in the regulation of translocation, as well as to unravel the functions of these translocations.

Figure 1.1. Lytic cycle of the parasite

The schematic of simplified version of lytic cycle showing invasion, replication and egress of the parasite from the host cell. Reprinted material does not require permission from Annual Reviews: Annual Reviews of Microbiology (Blader et al., 2015).

Figure 1.1. Lytic cycle of the parasite
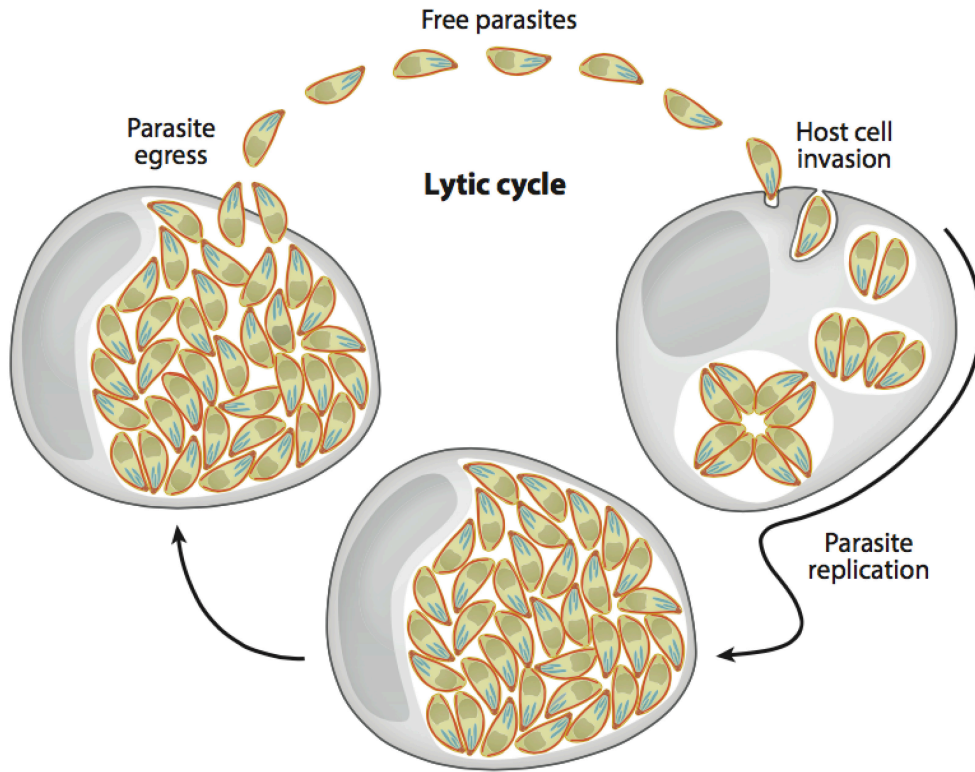
Figure 1.2. Schematic representation of *Toxoplasma* cytoskeleton

Three-part structure of cytoskeleton composed of microtubules on the inner side covered by the IMC meshwork of protein and the alveolar vesicle below the plasma membrane. Reprinted with minor adaptations by permission granted from the Elsevier publisher: International Review of Cell and Molecular Biology (Anderson-White et al., 2012) .

Figure 1.2. Schematic representation of *Toxoplasma* cytoskeleton
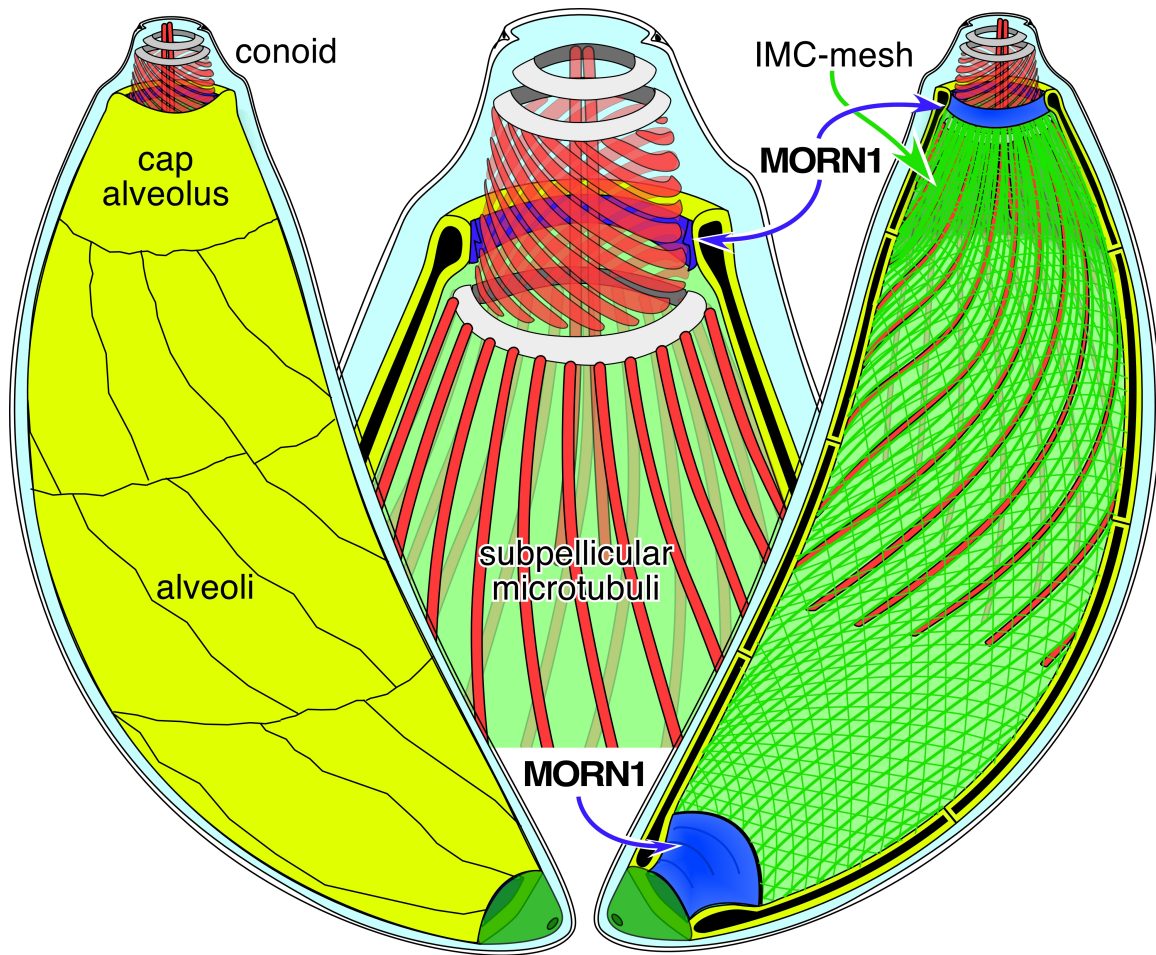
Figure 1.3. Biological stages of parasite: Extracellular and intracellular state.

Glycolytic enzymes like GAPDH1 and cytoskeletal protein like IMC12 is localized to the cortex in the extracellular state of the parasite. The parasite replication and its cell cycle stages are highlighted in the intracellular state. During G1 the centrosome is intact and it duplicates early in S phase to provide cue for appearance of cytoskeleton elements. The daughter buds begin to form as the cytoskeleton grows and fully formed daughter parasites appear (S-M phase) engulfing the mother in a short cytokinesis phase (C-phase). Nucleus: light blue; MORN1: green; IMC: dark blue; tubulin and centrosome: red. Reprinted with minor adaptations by permission granted from the publisher Company of Biologists Ltd: Journal of Cell Science (Gubbels et al., 2006).

Figure 1.3. Biological stages of parasite: Extracellular and intracellular state
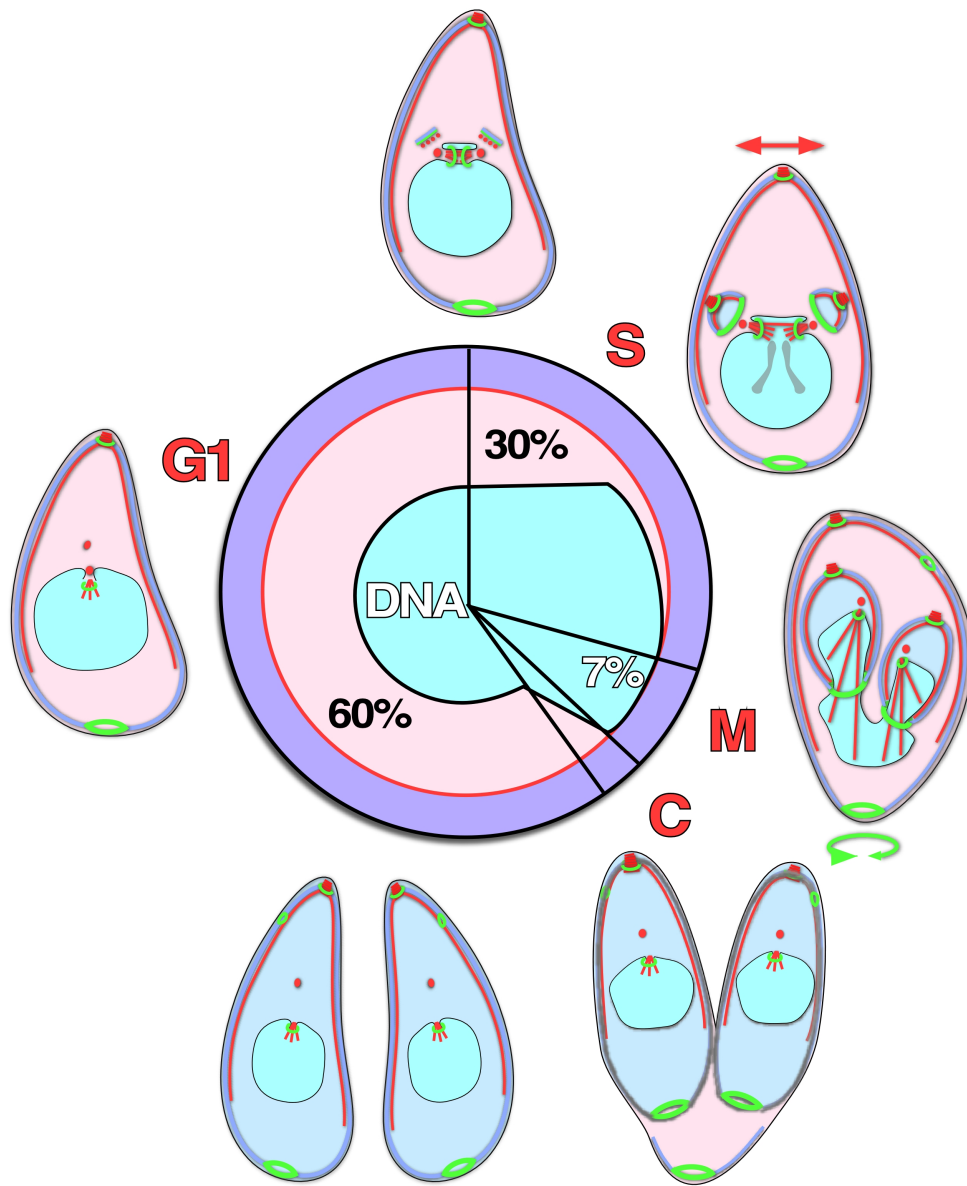
CHAPTER 2: FUNCTIONAL ANALYSIS OF THE GROUP OF INTERMEDIATE FILAMENT-LIKE PROTEINS ASSOCIATING WITH THE CYTOSKELETON AFTER CELL DIVISION IN *TOXOPLASMA*

2.1. Introduction

In *Toxoplasma gondii*, the association of plasma membrane with an IMC (composed of the flattened alveolar sacs) coupled to a supporting cytoskeletal network builds the cortical membrane skeleton (Mann and Beckers, 2001). The IMC plays a critical role in parasite replication (Radke et al., 2001), motility and invasion (Dobrowolski and Sibley, 1997; Meissner et al., 2002). A fine 8-10 nm meshwork of intermediate filament-like proteins arranged below the alveoli are called IMC proteins. A family of 14 IMC proteins shares alveolin domains composed of valine and proline-rich residues (Anderson-White et al., 2011) (Figure 2.1. a). The members of this family are sequentially assembled into the cytoskeleton of budding daughter cells and mark distinct developmental steps in the budding process (Figure 2.1. b) (Anderson-White et al., 2011). A subset of these proteins namely, IMC7, IMC12 and IMC14 only associate with the mature cytoskeleton in the G1 stage of the cell cycle, which makes this group a unique subfamily in the alveolin repeat family (Anderson-White et al., 2011) (Figure 2.1. c). Specifically, IMC7 appears after the association of IMC14 in the early G1 stage (Szatanek et al., 2012) (Figure 2.1. c). None of these proteins have been functionally characterized. Here we aim to decipher the functional significance of these three proteins in the lytic cycle of the parasite.

Two hypotheses regarding the function of this group of non-division IMC proteins are explored here. Firstly, this group of IMC proteins may serve as a mark to differentiate mother and daughter cytoskeleton. This is important during the final phases of cell division when the mother's cytoskeleton is being degraded whereas the daughters mature and emerge (Anderson-White et al., 2011). Alternatively, these IMCs may be involved in maintaining and strengthening the cortical cytoskeleton of the parasite

(Anderson-White et al., 2011) to allow the parasite to survive stresses in the extracellular environment and/or during host cell invasion. We demonstrate here that individual genes are not essential to the parasite per se, but that IMC7 and IMC14 are needed to withstand osmotic stress. Although a role for IMC12 could not be established in our experiments, we discovered that IMC14 is also required to produce two rather than more daughters per division round. This function in division is unexpected and ties structural elements to a role in the cell development cycle.

2.2. Results

2.2.1. *IMC7, 12 and 14 associates to the cortex in late G1 stage*

Although it has been shown that IMC7 appears at the cortex after the association of IMC14 in the early G1 stage using a temperature sensitive mutant arresting in early G1 (Figure 2.2. a) (Szatanek et al., 2012), this timing has not been determined for IMC12. In addition, it is currently unknown whether upon progression of G1 toward S/M phase all these IMC proteins translocate in all parasites, a requirement if these proteins were to function to differentially mark mother and daughter cytoskeletons. To answer these questions, we used exogenous N-terminal and C-terminal fusions of IMC7, 12 and 14 with auto fluorescent YFP protein (Anderson-White et al., 2011). Consistent with the previous report, IMC12 was expressed under a constitutive tubulin promoter but native promoters drove IMC7 and IMC14 to ensure proper spatiotemporal dynamics (Anderson-White et al., 2011).

Like described in previous work, the cortical transition of IMC7 and IMC14 was studied in a temperature sensitive mutant (named FV-P6) of the Cactin gene that arrests in mid G1 (Szatanek et al., 2012). We also subject IMC12 to this analysis (Figure 2.2. c-e). This showed that IMC7 and 12 display similar translocation dynamics, with about 60% of the parasites displaying cortical localization of the protein in both non-synchronized, random cycling parasites (35°C) as well as mid G1 arrested (40°C) parasites. Consistent with the mRNA expression profile maximizing in early G1, the IMC14 translocation goes from just over 60% to nearly 100% upon G1 arrest.

To understand the localization of these IMC proteins upon progression of G1, we treated the parasite lines expressing IMC7, 12 or 14 fused to YFP with 3-methyladenine

(3-MA) to arrest the parasites in late G1 stage and again scored for cortical vs. cytoplasmic localization (Figure 2.2. b) (Wang et al., 2010). Over 90% of the vacuoles contained parasites with IMC7, 12 and 14 at the cortex (Figure 2.2. c-e). Overall, these data fit with the mRNA expression profile for these IMC proteins. In addition, the near uniform translocation at the end of G1 is consistent with a putative role for these IMC proteins in marking the mature mother for degradation, although a role in strengthening the cortex for stress resistance in extracellular parasites cannot be excluded based on these data.

2.2.2. *IMC12 transitions to the cortex in extracellular parasites*

To understand if IMC7, 12 and 14 function in maintaining the rigidity of the cytoskeleton of parasites outside the PV, we scored the cortical localization of parasite lines expressing YFP fused to IMC7, 12 or 14 in the extracellular stage. We mechanically released asynchronously dividing parasites and determined the percentage of vacuoles harboring parasites with cortical YFP signal after increasing time points following release from the host cell. In an asynchronous population at t = 0 hrs, roughly 40% of vacuoles harbor parasites displaying all three IMCs in the cortex (Figure 2.3.). This percentage only slightly fluctuates for IMC7 and IMC14 over a 24 hrs period; however, the cortical IMC12 population significantly increases from 32% to 69% in 24 hrs. These data suggest that IMC7 and 14 are unlikely to function in resisting extracellular stresses, but the doubling of IMC12 over the 24 hr window is consistent with such function.

2.2.3. *Loss of IMC7 shows reduced ability to resist osmotic shock*

To dissect the function of IMC7 in the lytic cycle of the parasite, we created a cKD line by replacing the endogenous promoter of IMC7 with anhydrous tetracycline (ATc) regulatable minimal TetO7Sag4 promoter (Figure 2.3. a). After the verification of the integration of the regulatable promoter and absence of endogenous *pimc7* promoter (Figure 2.3. b), we monitored the downregulation of the IMC7 protein by IFA (Figure 2.3. c) and western blot (Figure 2.3. d). The IMC7 protein was barely detectable after 24 hrs of ATc treatment. Plaque assays show neither a reduction in number nor area of plaques as compared to the parental line (Figure 2.5. a) indicating no evident loss in parasite viability. This result indicates that IMC7 is not required to complete the lytic cycle in vitro. Since plaque assays only measure overall fitness, more subtle defects can be observed by IFA for division markers but these IFA assays identified no division defects (data not shown). Additionally, to test if IMC7 is involved in maintaining the rigidity of the mature parasites in extracellular milieu we asked whether extracellular IMC7 cKD parasites were able to withstand different osmotic stress conditions (Harding et al., 2016). We analyzed parasite integrity through the ability of propidium iodide (PI) to associate with the DNA of ruptured parasites by flow cytometry. To test the assay the parental line was treated with a low concentration of saponin, which is known to create pores in the membrane. We used SAG1 conjugated with Alexa 488 to stain the parasite surface and distinguish the parasites from debris in the assay. We observed that 64% of the parasites were disrupted by saponin treatment indicating that the assay works (Figure 2.5. b). Hypotonic stress conditions were induced by exposure to 0.5X and 0.25X of normal salt concentration (HBBSs diluted with water) and hypertonic conditions were induced by exposure to 1 M sorbitol. IMC7 depleted parasites were two-fold less resistant

to hypotonic conditions than WT (wild type) parasites (Figure 2.5. b), though withstood the hypertonic condition quite well. These results indicate that IMC7 is involved in maintaining rigidity of extracellular parasites.

2.2.4. *IMC12 is not essential for the lytic cycle*

To assess the function of IMC12 we created a dKO line of IMC12 using double homologous recombination aided by the CRISPR technology (Figure 2.6. a). The genotype of the IMC12 dKO line was validated by diagnostic PCR reactions (Figure 2.6. b). Assessment of the viability by plaque assay showed no visible defect compared to the parental line (Figure 2.6. c). Evaluation of parasite division by immunofluorescence assays showed normal, synchronously dividing parasites by endodyogeny (results not shown). Since we observed an increase in IMC12 cortical transition in extracellular parasites we hypothesized a role in stress resistance. However, neither hyper- nor hypo-osmotic stresses results in parasite permeabilization over rates observed for the WT control (Figure 2.6. d). Taken together, IMC12 is not essential for completion of the lytic cycle and acts neither on the progression of endodyogeny nor on resistance of extracellular stress.

2.2.5. *IMC14 is required for maintaining synchronous budding and cell rigidity*

To decipher the role of IMC14, we created a dKO line by double homologous recombination using a CRISPR mediated approach (Figure 2.7. a). The successful replacement of the IMC14 locus with the DHFR selectable marker indicated that IMC14 is not essential for the parasite (Figure 2.7. b). This result was confirmed by testing the

fitness of the IMC14 dKO line by plaque assay where we did not detect a difference in the number or size of plaques when compared to the parental line (Figure 2.8. a). However, upon examination of the dKO parasites by immunofluorescence using the division markers IMC3 to mark the cytoskeleton and centrin to label the centrosomes, we observed a loss in synchronous budding of the parasites in nearly 20% of the population compared to only 3.8% for the WT control (Figure 2.8. b, c). Furthermore, under hyperosmotic conditions we observed a two-fold increase in the percentage of permeabilized parasites in absence of IMC14 compared to WT control (Figure 2.8. d). Additionally, in the hypertonic conditions there is about four-fold increase in the percentage of permeabilized parasites indicating the essentiality of the IMC14 in maintaining membrane rigidity upon osmotic stress. These data suggest a dual role for IMC14 in coordinating the transition of G1 to S/M and cytokinesis phases of the cell cycle in *Toxoplasma* as well as in maintaining parasite integrity under stress conditions.

2.3. Discussion

Our complete analysis of cortical localization of the three IMC proteins shows that IMC14 transitions before IMC7 and 12 to the cortex during G1, but that transition is completed to almost 90% of the parasites by the end of G1. These data thus clearly demonstrate that IMC7, 12, and 14 all translocate before entering S-phase and thereby distinctly mark the mother cytoskeleton from newly forming daughters. In that light, it was surprising to find that in our analysis of the knock-down and knock-out lines none of these three IMC proteins appear to interfere with mother cell turnover. However, at this point we cannot exclude functional redundancy among these three IMC proteins.

Toxoplasma has an armor of flattened vesicles along with subpellicular microtubules and intramembranous particles (Morrissette et al., 1997) which are further decorated with microtubule coating proteins (Liu et al., 2016), to maintain the cell shape and structure that is critical for pathogenesis, most notably host cell invasion (Morrissette and Sibley, 2002). In extracellular parasites, we see that the status quo in cortical vs. cytoplasmic localization is maintained for the situation at the time of egress for IMC7 and 14. It is well known that parasites are able to complete cell division in the extracellular environment and then end up in G1, leading to a G0 arrest (Gaji et al., 2011; Lescault et al., 2010). Our data now show that parasites emerging during G1 largely stay in that stage of G1. We interpret this to mean that egressing parasites in which IMC7 and 14 are already translocated to the cortex do not revert back to the middle of G1, or at least this does not result in the release of IMC7 and 14. On the other hand, for IMC12 we observe that the association with the cortex slowly increases with the time spent outside a host cell. Germane to this, IMC12 was found to be phosphorylated in a calcium dependent

fashion in extracellular parasites in a global phosphoproteomic analysis, but IMC7 and 14 not (Nebl et al., 2011). It is therefore tempting to speculate that one of the unique calcium dependent protein kinases is responsible for this event and furthermore, the phosphorylation of Serine residues 249 and 250 facilitates and/or regulates the cortical association of IMC12. To test this hypothesis we attempted to complement the IMC12dKO line with the auto-fluorescent tagged phosphonull and mimic mutants. Unfortunately, these events were not successful and hint at a potential dominant negative effect when the parasite is asked to rely on a single YFP tagged IMC12 protein in absence of an untagged version. Functionally, we speculated that the translocation of IMC12 would be responsible for resisting stresses faced in the extracellular environment, but our osmotic shock assays do not provide experimental support in this direction. It is again possible that IMC12 acts in concert with other IMC proteins to support this function. Indeed the global calcium dependent phosphoproteome analysis also identified phosphorylation events in IMC1, IMC3 and IMC6, which all are incorporated in the parasites during budding. This again could hint at some form of redundant regulation or function. Alternatively, it is possible IMC12 functions in tensile or deformability stress, as has been shown in malaria gametocytes (Aingaran et al., 2012; Tremp et al., 2008). On the other hand, we show that IMC7 and IMC14, which are not phosphorylated in a calcium dependent fashion, function in resistance to osmotic stress. Thus, it is possible several parallel mechanisms are at work.

It is interesting to note that the IMC filament repertoire in *Plasmodium* parasites is much smaller and that in general, only single IMC protein is expressed in particular live stages. Stage specific roles for individual IMC proteins have been found in

Plasmodium (Tremp et al., 2014). For instance, IMC1a has been shown to be responsible for sporozoite size, stability and infectivity while IMC1b is responsible for ookinete stability and motility (Khater et al., 2004; Tremp et al., 2008). *Toxoplasma* appears to express a much larger repertoire of IMC proteins in the same live stage and therefore appears to have invested in a much more robust and redundant network of IMC proteins. Clearly, this is a challenge in the study of these proteins.

To assess whether Toxoplasma also expresses stage specific IMC proteins with potentially stage specific functions, we assessed the relative abundance of mRNA across tachyzoites, bradyzoites, the coccidian cycle in the cat and sporogenesis in the extracellular environment. These data are available on ToxoDB as microarray data (Gutierrez et al., 2010; Fritz et al., 2012). The expression profiles of IMC7, 12 and 14 across oocysts, sporozoites, tachyzoites and bradyzoites were collected and plotted in Figure 2.9. IMC7 is expressed at low levels in oocysts and sporozoites compared to the tachyzoites and bradyzoites stages of the parasite. Interestingly, IMC12 first peaks in the mature sporozoites and is maintained at relatively higher level than the other two IMC transcripts throughout tachyzoites and bradyzoites stages. Contrastingly, IMC14 has its maximum expression in the oocysts and sporulated sporozoites stages and decreases through tachyzoites and bradyzoites. Hence, it can be noted that these IMC proteins follow a very dynamic expression pattern unique to each life stage, indicating potentially stage specific functions as observed in *Plasmodium* (Tremp et al., 2014). IMC14 may be providing stability to the sporozoites stage along with maintaining the division of oocyst to sporocysts. It is likely that IMC14 also coordinates meiosis and/or sporogenesis in other life stages of *Toxoplasma*.

The most distinct and unexpected discovery of our work was the role of IMC14 in the number of offspring produced per division round. In comparison to the wild type more than a four fold increase was observed in vacuoles with asynchronous budding and multiple daughters within one mother cell. This phenotype is reminiscent of endopolygeny in the cat enterocytes during merogony. The difference in number of offspring is regulated by the differential inner and outer core replication cycles of the centrosome, which controls apicomplexan cell cycle flexibility (Suvorova et al., 2015). The inner core controls the nuclear replication cycle while the outer core regulates the cytokinetic cycle. Thus, IMC14 somehow slows down or interferes with the outer core's coordination of the cytokinetic cycle during endodyogeny of tachyzoites. This results in re-entry into the mitotic cycle without completing cytokinesis and leads to the generation of four centrosomes and four daughters in the next cycle. Taken together, through this first study to functionally characterize the members of the IMC protein family we found evidence for distinct roles for these IMC proteins in tachyzoites.

Figure 2.1. Expression patterns of the IMC proteins

(a) Schematic of Intermediate filament-like IMC proteins containing the alveolin repeat domain in yellow and the N and C terminal ends in green. Typical cysteine residues are marked in red and the asterisks denote predicted palmitoylation sites. (b) Schematic of experimentally validated spatiotemporal localization dynamics of all alveolin domain IMC proteins (Anderson-White et al., 2011). Groups of IMC proteins with a similar behavior are shown in the same color with IMC14 labeling the mature parasite and IMC7 and IMC12 exclusively in the mother parasite. The extracellular parasite outside the box shows the localization of IMC7, 12 and 14 to the mature cortex. (c) The mRNA expression level of all alveolin domain IMC proteins throughout two cycles of tachyzoite development. Expression of the mature group of IMC proteins peaks in early G1 for IMC14 (indicated in yellow) followed by IMC7 (light blue) and IMC12 (navy blue) in mid G1. The primary mRNA data (Behnke et al., 2010) was taken from ToxoDB and the intensity was normalized as described earlier (Anderson-White et al., 2011).

Figure 2.1. Expression patterns of the IMC proteins

a

Palm. sites

(EKIVEVP)$_n$

Cys residues

b

IMC15   IMC1,3,4,6,10   IMC5,8,9,13   IMC14   IMC7,12

c

S   M   G1   S   M   G1

1-6 7 8-11 12 13 14 15

normalized intensity

hours after block release (TK-thymidine)

blk 1 2 3 4 5 6 7 8 9 10 11 12
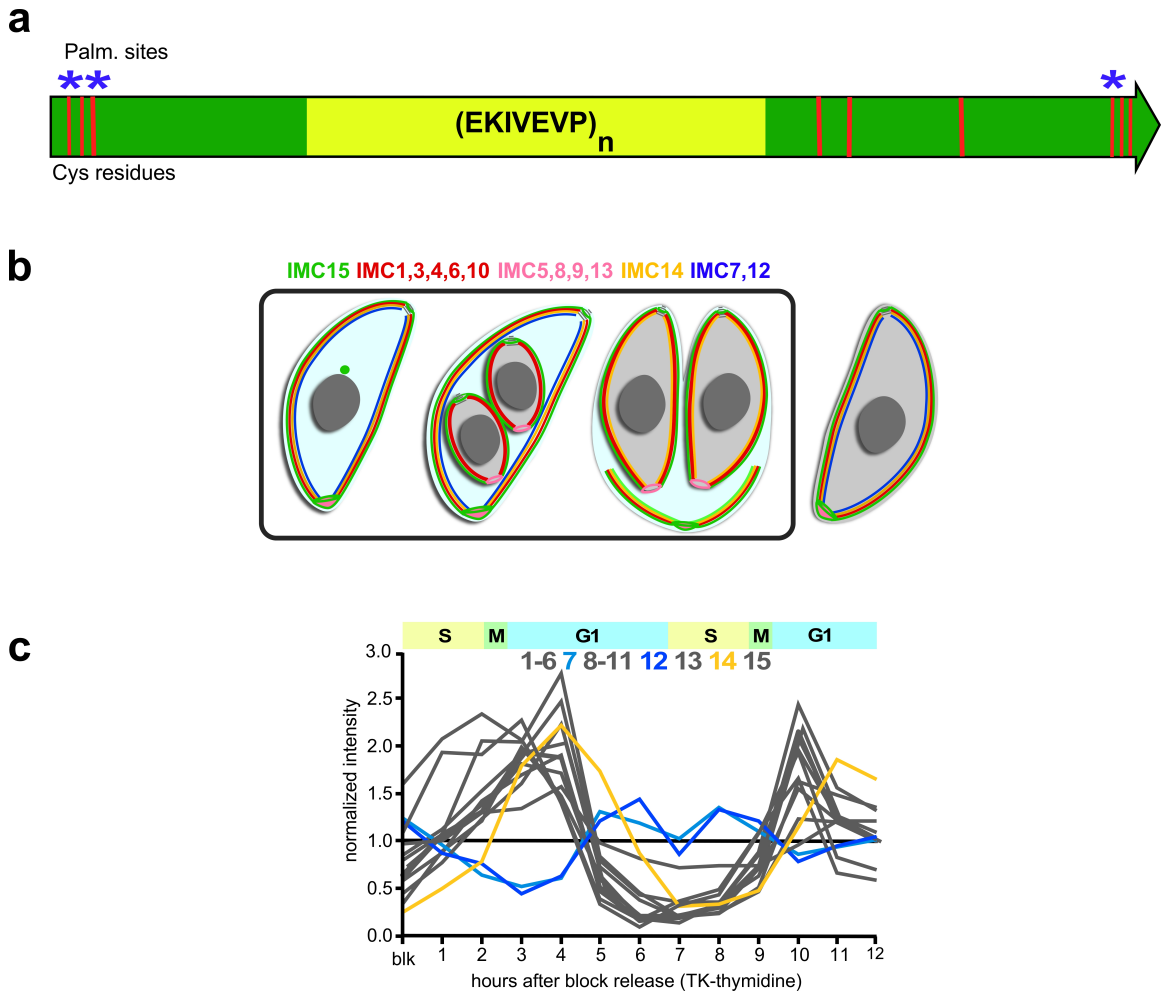
Figure 2.2. Mature group of IMCs completely transition to the cortex in late G1 stage

Pictorial representation of procedure employed to arrest the parasite in (a) mid G1 stage by temperature restrictions and (b) late G1 stage upon 3-MA treatment. Quantification of FV-P6 parasite line expressing mCherry fused to IMC7 (c), IMC12 (d) and IMC14 (e) in the cortex of the parasite after invasion at 35°C (permissive, random cycling parasites) and mid G1 arrest at 40°C. The percentage of parasites with cortical signal of IMC7 (c), 12 (d) or 14 (e) is quantified after 3 -MA block in late G1. All graphs are plotted from the average percentage of cortical vacuoles counted from three independent experiments by quantifying more than 100 vacuoles each time in N=3 ±S.D.

Figure 2.2. Mature group of IMCs completely transition to the cortex in late G1 stage
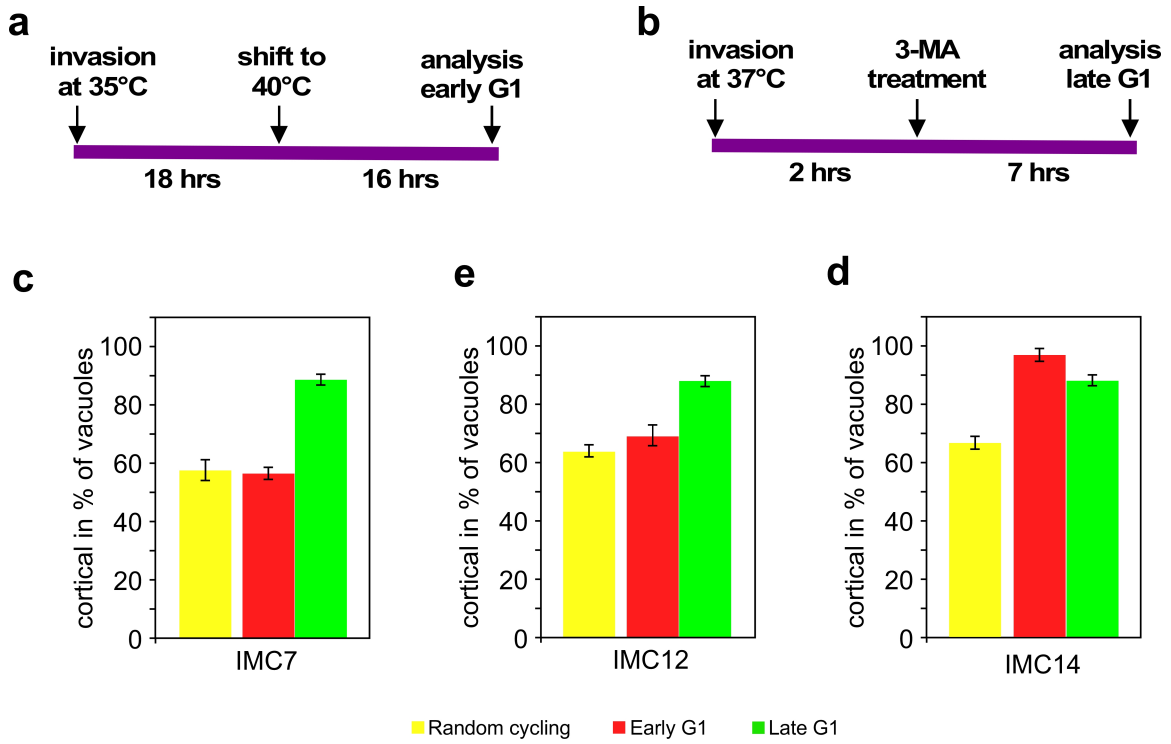
Figure 2.3. Localization of the mature group of IMC proteins in extracellular tachyzoites

(a) Quantification of cortical localization of marked IMC signal in extracellular parasites at 0, 2 and 24 hrs. Graph is plotted from the average percentage of cortical localization of IMC in the extracellular parasites by counting more than 200 parasites in N=3 ±S.D. One-way ANOVA showed a significant $p < 0.002$ for IMC12 between 0-2 hrs and 0-24 hrs time point.

Figure 2.3. Localization of the mature group of IMC proteins in extracellular tachyzoites

Time course of cortical IMC localization in extracellular parasites
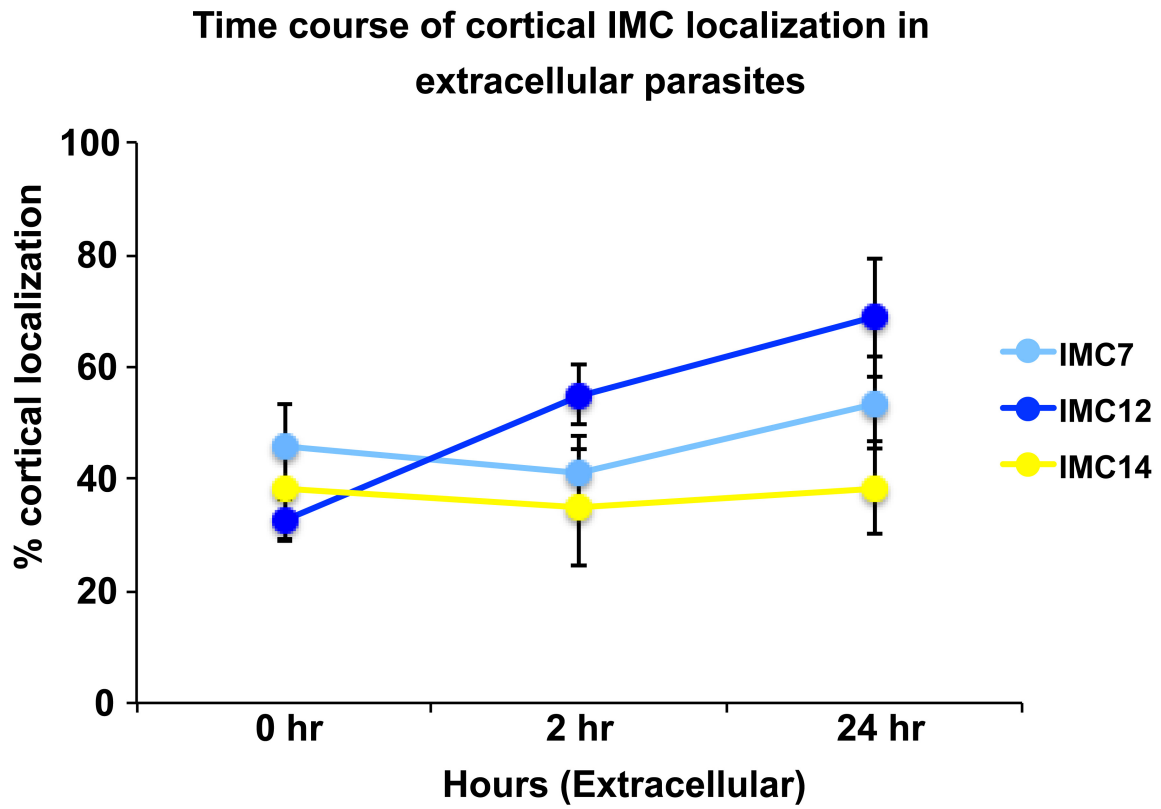
Figure 2.4. Generation and verification of IMC7 cKD line

(a) Pictorial representation of double homologous recombination to replace the endogenous *pimc7* promoter with drug selectable marker and regulatable promoter. Diagnostic primer pairs are numbered 1-3. (b) Integration PCR1 and 2 to verify the 5' and 3' flanks as indicated in panel a in the IMC7cKD line and presence of native promoter in the parental line shown by PCR3. (c) IFA image showing no IMC7 signal after 24 hrs of ATc treatment. IMC1 in green marks the cytoskeleton of the parasites and the DNA material is stained by DAPI. (d) Western blots to show IMC7 protein downregulation after 24 hrs ATc treatment using α–IMC7. α–tubulin (12G10) is used as loading control (lower panel).

Figure 2.4. Generation and verification of IMC7 cKD line
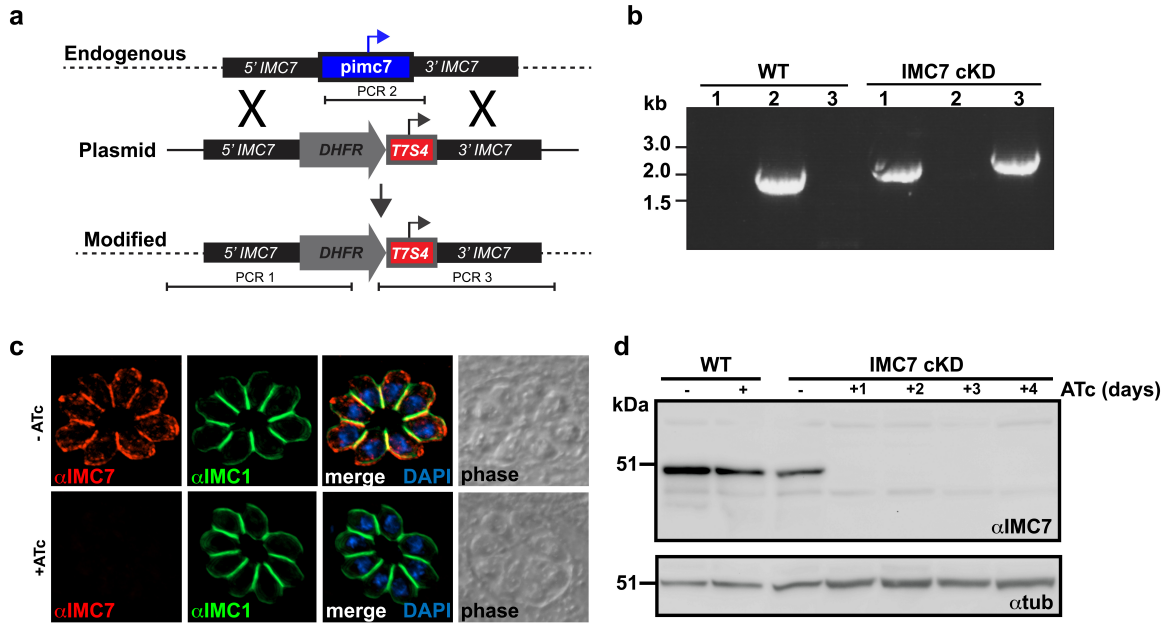
Figure 2.5. IMC7 is required to maintain parasite rigidity

(a) Plaque assay ±ATc of WT and cKD line after incubating it for 9 days and stained with crystal violet. (b) Percentage of permeabilized cells as stained with PI after treatment with 1X HBSS, 0.5 X HBSS, 0.25X HBSS (hypo osmotic) and sorbitol (hyper osmotic) in wild type (WT) parasites and IMC7cKD line. N=1.

Figure 2.5. IMC7 is required to maintain parasite rigidity
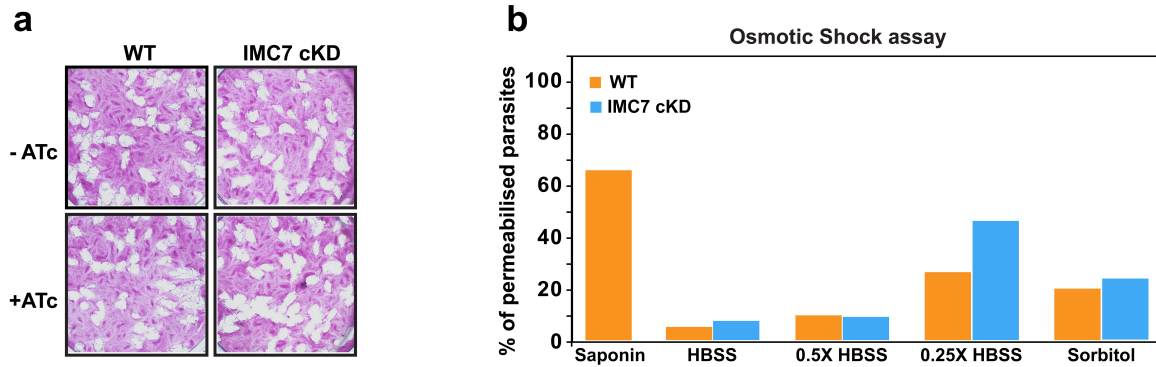
Figure 2.6. Loss of IMC12 is not critical for parasite viability

(a) Schematic of direct knockout line of IMC12 by CRISPR. The genomic locus of IMC12 is cleaved by Cas9 (yellow arrows) and replaced by DHFR resistant marker flanked by the homologous region of IMC12 (red). Diagnostic PCR primer pairs marked I-IV. (b) Verification of correct integration of DHFR cassette in IMC12 locus as indicated by PCR I-III and the absence of reintegration of IMC12 randomly in the genome as shown in panel for PCR IV. (c) Plaque assay after 8 days incubation stained with crystal violet. (d) Percentage of permeabilized cells stained with PI after treatment with hypo osmotic and hyper osmotic buffers in wild type (WT) parasites and IMC12 dKO line. N=1.

Figure 2.6. Loss of IMC12 is not critical for parasite viability
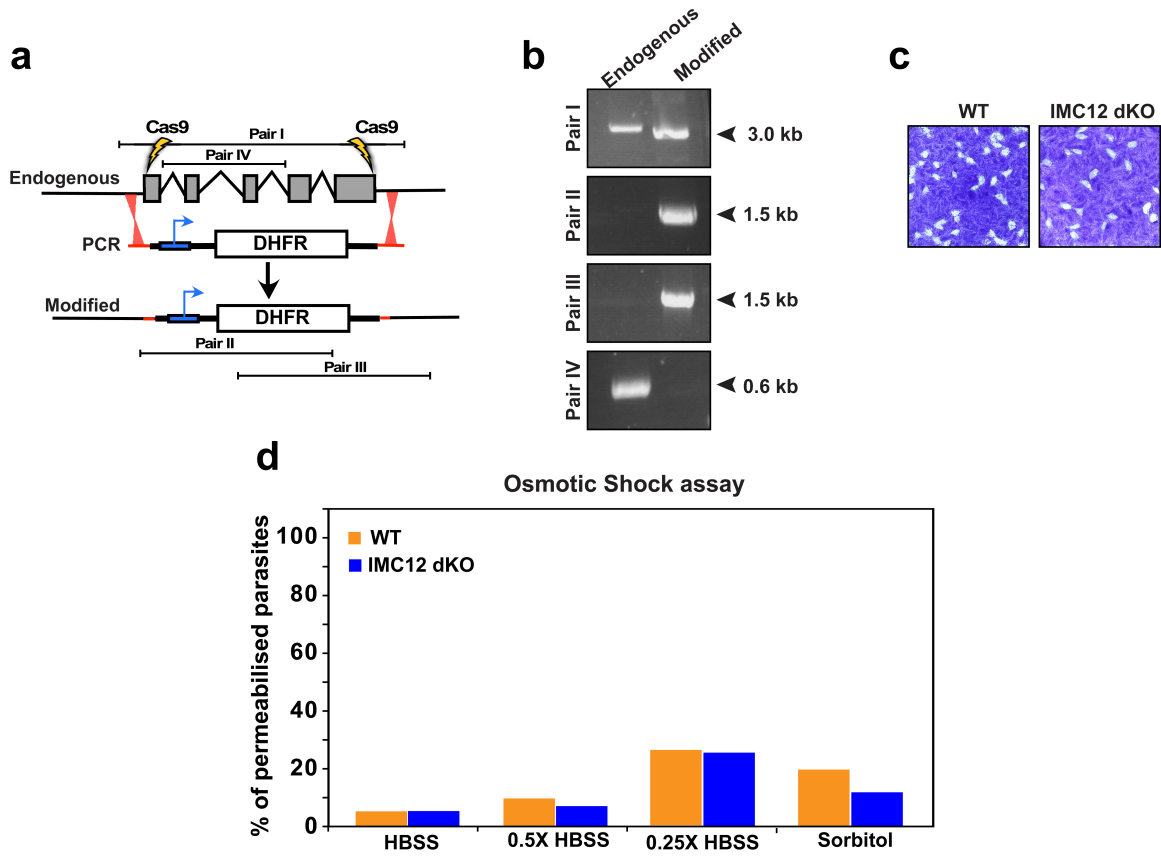
Figure 2.7. Strategy of IMC14 dKO and its verification by integration PCR

(a) Schematic of IMC14 dKO strategy by double homologous recombination using CRISPR/cas9 technology. Cas9 cleaves DNA at the specific sites as marked by the yellow arrows. The PCR product of DHFR flanked by the red highlighted homologous regions of the IMC14 locus replaces the endogenous locus. The location of diagnostic PCR primer pairs is marked I-IV. (b) Diagnostic PCR reactions to confirm the replacement of IMC14 locus (Pair I) and the integration of DHFR locus (Pair II and III). Pair IV marks the absence of IMC14 gDNA indicating the replaced fragment has not randomly reintegrated elsewhere in the genome.

Figure 2.7. Strategy of IMC14 dKO and its verification by integration PCR
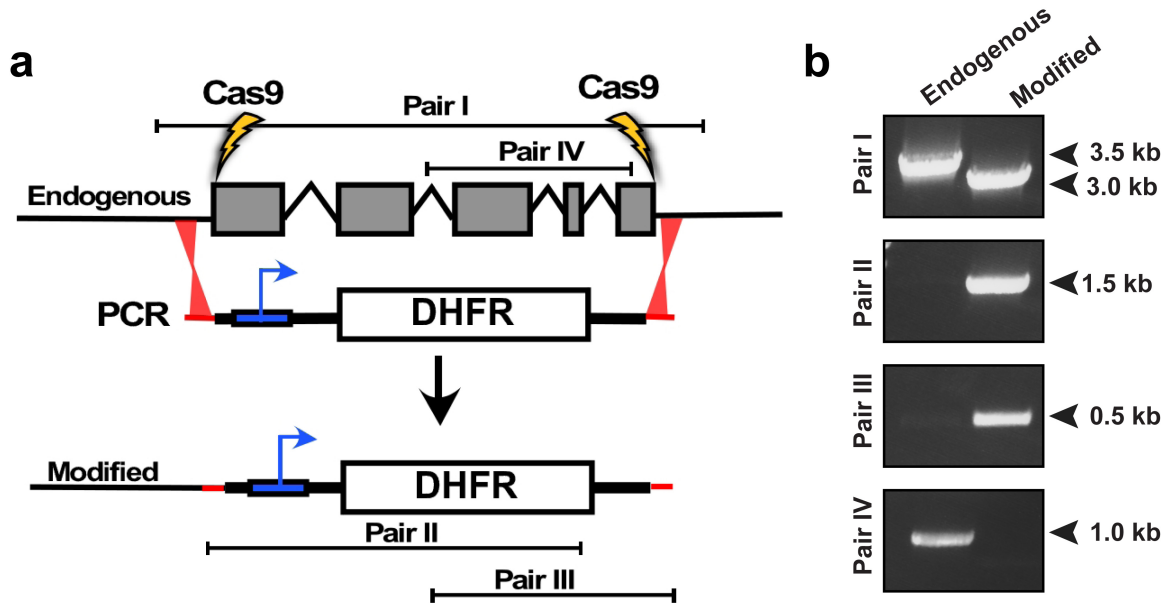
Figure 2.8. IMC14 is required for both synchronous division and membrane rigidity

(a) Plaque assays stained with crystal violet after 8 days of growth. (b) IFA image of parental and dKO line stained with α–IMC3 (red), α–hCentrin (green) and DAPI and the corresponding phase image. The arrowhead indicates the parasite with 4 budding daughters as opposed to 2 in other parasites within the same vacuole. (c) Quantification of loss of synchrony in dKO line compared to wild type by blindly counting about 150 vacuoles in independent experiments. N=3 ± S.D. (d) Increase in percentage of permeabilized IMC14 dKO parasites as shown by PI staining in hypotonic (0.25X HBBS) and hypertonic (1M Sorbitol) conditions. N=1.

Figure 2.8. IMC14 is required for both synchronous division and membrane rigidity
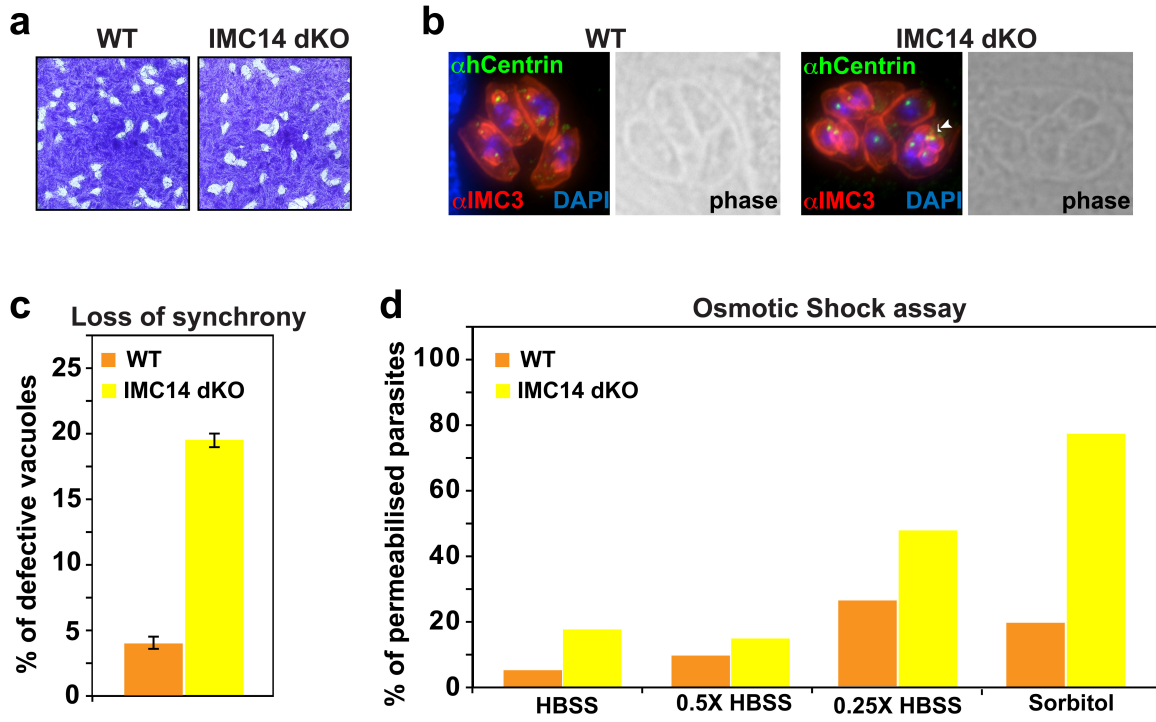
a

WT   IMC14 dKO

b

WT   IMC14 dKO

αhCentrin   αhCentrin

αIMC3 DAPI phase   αIMC3 DAPI phase

c   **Loss of synchrony**

% of defective vacuoles

- WT
- IMC14 dKO

25
20
15
10
5
0

d   **Osmotic Shock assay**

% of permeabilised parasites

- WT
- IMC14 dKO

100
80
60
40
20
0

HBSS   0.5X HBSS   0.25X HBSS   Sorbitol

Figure 2.9. Transcriptomic analysis of oocyst, sporocysts, tachyzoite and bradyzoite development in *Toxoplasma*

Relative mRNA expression levels of IMC7, IMC12 and IMC14 in oocyst indicated by unsporulated and sporulated stages, tachyzoites shown by in vitro for 2 and 4 days and bradyzoites from in vitro 8 days and in vivo 21 days.

Figure 2.9. Transcriptomic analysis of oocyst, sporocysts, tachyzoite and bradyzoite development in *Toxoplasma*

Developmental expression profile of *Toxoplasma*
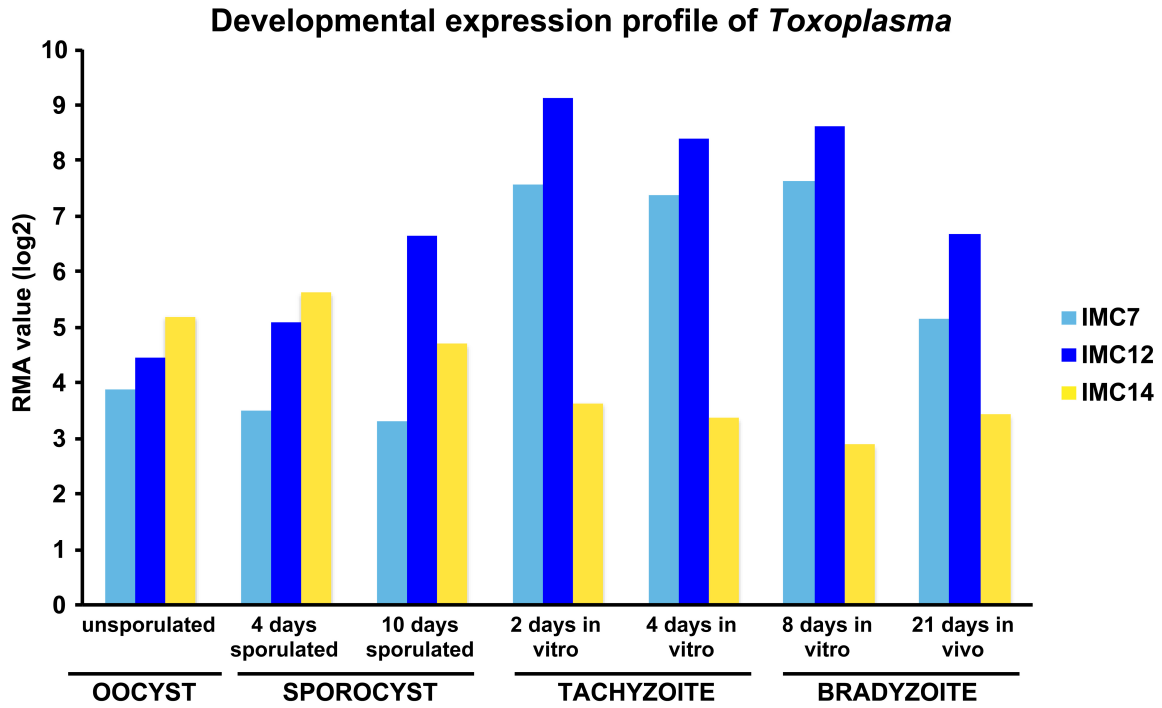
CHAPTER 3: *TOXOPLASMA* GAPDH1 IS ESSENTIAL FOR INTRACELLULAR

REPLICATION

3.1. Introduction

The glycolytic enzyme glyceraldehyde 3-phosphate dehydrogenase (GAPDH) is an archetypical multifunctional protein with diverse activities and distinct subcellular localization (Sirover, 2011) and yet is relatively unexamined in *Toxoplasma*. This key enzyme (EC 1.2.1.12) of glycolysis catalyzes the oxidative phosphorylation of glyceraldehyde 3-phosphate (G3P) to D-glycerate-1, 3-bisphosphate in presence of NAD^+ and inorganic phosphate. Additional moonlighting functions of GAPDH include membrane fusion and transport, cytoskeletal dynamics, iron uptake and transport, heme metabolism, post-transcriptional gene regulation, tRNA export, chromatin structure and maintenance of DNA integrity. These diverse functions are regulated by a combination of post-translational modifications, subcellular localization, conformation dynamicity and protein complex assembly (Tristan et al., 2011). For example, human GAPDH facilitates actin polymerization and microtubule bundling by interacting with tubulin and actin (Kumagai and Sakai, 1983; Reiss et al., 1996). GAPDH is phosphorylated by an atypical protein kinase and recruited to Rab2-coated vesicular tubular clusters to facilitate vesicular retrograde trafficking along microtubule tracks powered by motor protein dynein (Tisdale et al., 2009). A phosphatidylserine-rich binding domain (PSB) localized in the N-terminus of GAPDH is a catalyst for membrane fusion (Nakagawa et al., 2003). The moonlighting roles of GAPDH appear to be uncoupled from its primary function in glycolysis (Tisdale et al., 2004).

To partition the complex GAPDH functions, we take an uncommon approach thus far in *Toxoplasma* research by combining structural information to correlate its functional analysis. With help of our collaborators at Seattle Structural Genomics Center for

Infectious Disease, WA, the X-ray crystallographic analysis of GAPDH1 protein structure was determined. This provided the precise, structural reflection board for a thorough molecular dissection of role of GAPDH1 in the parasite lytic cycle. The crystallographic structure of GAPDH is well documented across several biological kingdoms and the enzymatic mechanism is well studied but the structural basis of its non-glycolytic functions has not been completely explored. GAPDH is a homologous tetramer (~150 kDa) of O-R subunits that exhibits three asymmetric P, Q and R dyads (Roitel et al., 2003). This bilobal structure is universally conserved with the folding of an N-terminal NAD^+-binding domain and a C-terminal G3P catalytic domain (Jenkins and Tanner, 2006).

It has been established that glycolysis is not strictly essential in *Toxoplasma* (Blume et al., 2009; MacRae et al., 2012) and that the extracellular parasites do not require carbon source uptake in the first hour of their extracellular life (Lin et al., 2011). It was also reported that upon parasite egress glycolytic enzymes translocate from the cytosol to the cortex after about an hour in the extracellular stage (Pomel et al., 2008). It was hypothesized that the close association of the glycolytic enzymes to the pellicle is related to the highly localized production of ATP in the extracellular parasites for improved delivery of ATP by the active transporter mechanisms in the parasite plasma membrane and to the motile apparatus situated in the space between plasma membrane and IMC (Pomel et al., 2008).

In this part of the thesis we have established that knockdown of GAPDH1 expression and catalytic site disruption validate the essentiality of GAPDH1 in intracellular replication of the parasite. Complementing it with both small and large

fusions can restore the function of GAPDH1 in the parasite. The relocation of GAPDH1 is blocked in presence of bulky tags due to steric hindrance but the viability of the parasite is not disrupted. It is possible that overexpression of these large fusion tags causes spurious cytoplasmic localization of GAPDH1 in the extracellular stage. Nevertheless, GAPDH1 is critical for parasite viability and active site mutation is not able to restore this phenotype.

3.2. Results

3.2.1. *GAPDH1 is a tetrameric structure*

The *Toxoplasma* genome database (ToxoDB, http://toxodb.org) (Gajria et al., 2008) indicates that GAPDH1 (TGME49_289690) and GAPDH2 (TGME49_269190) are both constitutively expressed in tachyzoite and bradyzoite stages. While the GAPDH2 isoenzyme is targeted to the apicoplast organelle (Fast et al., 2001), GAPDH1 is cytosolic in intracellular parasites (Pomel et al., 2008). The crystal structure of TgGAPDH1 was determined to 2.25Å resolution in the holoenzyme NAD^+-bound state (Dubey et al., 2016). The GAPDH fold was validated by *DALI* analysis of the *Toxoplasma* GAPDH1 structure and reveals its close similarity to the GAPDH oxidoreductase folds with the top scoring hit of *Cryptosporidium parvum* GAPDH (Z-score 55.4, PDB ID 3CIF) (Cook et al., 2009). The secondary, tertiary and quaternary structures of *Toxoplasma* GAPDH1 are very similar to GAPDH structures that have been previously reported (Figure 3.1. and Figure 3.2. a-b).

The tetramer exhibits approximate 222-symmetry (Table 3.1.) with each bilobal subunit composed of a NAD^+-binding domain (residue 4-152, 320-340, Pfam PF00044) and a catalytic domain (residue 153-319, Pfam PF02800). One NAD^+ cofactor is bound per monomer and the average root-mean-square distance (r.m.s.d.) between monomers over all atoms is 0.02 Å as calculated by PISA. The GAPDH1 tetramer exhibits a dihedral symmetry with 3 axes of 'symmetry' (P, Q, R) in which only the P axis is a true symmetry (Figure 3.2. b) (Dubey et al., 2016). The O-R and P-Q dimers are however the most important for optimization of enzymatic activity, since the S-loop (residue 180-207) inserts into the NAD^+-binding cavity of the adjacent subunit (Figure 3.2. and 3.8.). The

most distinct structural feature from human GAPDH is the Lys-Gly dipeptide insertion (Figure 3.2. a) in the S-loop that is also reported in other apicomplexan parasites (Figure 3.1.) (Cook et al., 2009; Robien et al., 2006).

3.2.2. *GAPDH1 relocates to the cortex in extracellular parasites*

Toxoplasma GAPDH1 and other glycolytic enzymes are smoothly distributed in the cytosol in intracellular parasites and are translocated to the pellicle of the parasite upon egress from the host cell (Pomel et al., 2008). This phenomenon was observed only with a small fusion tags but not with large tags like mCherry or YFP. We repeated this study specifically for GAPDH1, with a tandem small c-Myc tag (Myc2: 26 amino acid) and a large YFP or mCherry (GFP: 238 amino acids, mCherryRFP: 226 amino acids) fusion tags at N terminus of the protein. In the intracellular parasites, our IFA results using Myc antibody show a cytosolic localization and in the extracellular parasites there is a clear cortical association (Figure 3.3. a). The YFP fusions bleached instantly making microscopy difficult but the mCherry fusion clearly shows cytosolic localization in both intracellular and extracellular parasites (Figure 3.3. b). Similarly, we also created C-terminus fusions and observed a similar phenotype indicating that this is not an artifact of N-terminal fusion tags (data not shown).

3.2.3. *GAPDH1 is essential for the lytic cycle*

To probe the essentiality of GAPDH1 for the *Toxoplasma gondii* lytic cycle, a GAPDH1 conditional knockdown line (GAPDH1cKD) was generated by replacing the endogenous promoter with anhydrous tetracycline (ATc) regulatable minimal TetO7Sag4 promoter

(Figure 3.4. a-b) (Dubey et al., 2016; Meissner et al., 2002). Expression of GAPDH1 protein in the GAPDH1cKD parasite line decreases upon ATc addition and becomes undetectable within three days of ATc addition (Figure 3.4. c). Plaque assays show that GAPDH1 is essential for completion of the lytic cycle (Figure 3.5. a). Cytoplasmic YFP expressing lines of parent and GAPDH1cKD lines were produced to complement these results and acquire detailed growth kinetics. GAPDH1cKD parasites do not grow in presence of ATc (Figure 3.5. b). Furthermore, microscopic evaluation was used to pinpoint the exact point of arrest in parasite development. In the presence of ATc, GAPDH1cKD parasites replicate at a similar rate to the parent line control up to 60 hrs, at which point the mutant arrests and no further growth is observed (Figure 3.5. c). The parasites arrest while residing in the vacuole without any discernable morphological defects (Figure 3.5. c inset).

We also determined whether GAPDH1 is required for invasion or egress by growing parasites for 60 hrs in the presence of ATc when protein is down regulated. Egress is stimulated by Ca^{2+}-ionophores, whereas invasion is tested by physically releasing parasites from the host cell and testing them for re-invasion of fresh host cells. Invasion and egress are not significantly inhibited in absence of GAPDH1 (Figure 3.6. a-b). The data demonstrate that GAPDH1 is essential for intracellular replication, but is not required to support invasion or egress (Dubey et al., 2016).

3.2.4. *Relocation of GAPDH1 is not essential for parasite viability*

In our optimization of protein reporter tags for GAPDH1, we first genetically complemented the GAPDH1cKD line with both small and large fusion tags. Wild-type

GAPDH1 (WT) was fused to Myc2, YFP and mCherry. Upon quantification of cortical localization we observed that fusion of bulky fluorophores at the N-terminus block translocation of GAPDH1 to the cortex in extracellular parasites, whereas the smaller tandem Myc2 epitope tag does not (Figure 3.7. a). Interestingly this blocking of translocation with bulky fusions of both YFP and mCherry did not impair the viability of the parasites indicating relocation is not essential for the parasite survival (Figure 3.7. b).

3.2.5. *GAPDH1 catalytic site is essential for activity but not translocation*

The active site pocket of *Toxoplasma* and *Cryptosporidium* GAPDH is identical in the G3P residues that form hydrogen bonds with the substrate (S152, T154, T214, G215, N319 in Figure 3.8. a-b). The conserved NAD^+-binding residues include I13, D34, R12, K79 and S121. The NAD^+ binding mechanism in *Toxoplasma* GAPDH1 appears to be stronger than *Cryptosporidium* GAPDH in forming addition hydrogen bonds between residues K79 and N6A of NAD^+ (3.1 Å) and hydrophobic interactions between N319 and N7N of NAD^+ (2.8 Å). Highly conserved in *Toxoplasma* GAPDH1 are the catalytic C152 and H180 residues, which mediate the nucleophilic attacks of carbonyl groups (Figure 3.8. a).

The essentiality of the *Toxoplasma* GAPDH1 enzymatic activity was evaluated by generating a point mutation of the catalytic cysteine (C152G) (Cook et al., 2009). The GAPDH1cKD line was genetically complemented with an allele encoding a tandem Myc2 tagged C152G mutant of GAPDH1. Glycolysis is required for parasite viability since parasite growth is readily rescued by the WT construct but the C152G allele is unable to restore growth (Figure 3.9. a). We also performed a western blot to confirm the

56

downregulation of GAPDH1 in the GAPDH1^{WT} complemented line after ATc treatment (Figure 3.9. b). Additionally, GAPDH1^{C152G} also translocates to the cortex of the extracellular parasites (Figure 3.10.) similar to GAPDH1^{WT} indicating that integrity of active site is not required for this function.

3.2.6. *Glycolysis is bypassed in absence of GAPDH1*

It has been reported that glycolysis can be bypassed by glutaminolysis, as glycolytic intermediates are essential for lipid biosynthesis (Blume et al., 2009). Using a monolayer lysis assay and cell replication assay we observe that in GAPDH1^{C152G} complementation line growth can be restored by glutamine supplementation, but glutamine cannot completely restore the GAPDH1cKD parasites (Figure 3.11. a and b). Direct measurement of GAPDH activity in the parasite indicated a dramatic reduction in the GAPDH1cKD line that was comparable to the loss of GAPDH activity in the GAPDH1^{C152G} complemented line (Figure 3.11. c). This also implies that GAPDH2 does not compensate for the loss of GAPDH1 even if the protein scaffold is present. Additionally, the high level of GAPDH activity compared to the parental line in the GAPDH1^{WT} is not due to the presence of native GAPDH1 as it is clearly down regulated after 60 hrs of ATc treatment (Figure 3.9. b).

To further validate that glycolysis is not essential the overall ATP concentration is measured, as done for other *Toxoplasma* glycolysis mutants (Starnes et al., 2009). The ATP level significantly decreases in the GAPDH1cKD and GAPDH1^{C152G} complemented line but not the parent or GAPDH1^{WT} complemented line (Figure 3.11. d). Hence, the catalytic activity of GAPDH1 is only critical for the glycolytic role of GAPDH1 in the

parasites and is essential for parasite growth under normal conditions. The GAPDH1 protein scaffold if essential for other functions are not critical in the parasites (Dubey et al., 2016).

3.3. Discussion

The crystal structure of GAPDH1 combined with the post-translational modification data and allelic replacement of active site confers its role in glycolysis. Several studies have shown that glycolysis is not strictly essential in *Toxoplasma* (Blume et al., 2009; MacRae et al., 2012), which is also confirmed by our glutamine rescue data. Although our initial data indicated that GAPDH1 is essential, we show that L-glutamine complementation rescues parasite viability to approximately 50%. This partial rescue is consistent with the contribution of glycolysis intermediates to lipid synthesis, which is growth limiting (Nitzsche et al., 2015; Ramakrishnan et al., 2015). Loss of GAPDH1 activity results in the loss of glycolysis, which is essential for parasite growth under normal conditions. Since we observe a trend of increased rescue upon complementation of the complete knockdown with the C152G mutant (albeit not statistically significant), we conclude that there is a hint of moonlighting function(s) of GAPDH1 in the *Toxoplasma* lytic cycle.

GAPDH1, a quintessential multifunctional protein, translocates intriguingly to the unique cortical membrane skeleton. Bulky tags at GAPDH1 termini most likely interfere the interactions with other proteins and complex of the cortical translocation machinery. However, the phenotype of the GAPDH1cKD is rescued by complementation using the large fusions of YFP or mCherry tags. The N-terminus of GAPDH1 protrudes on the surface and could play a role in membrane association that might be blocked by steric hindrance in presence of a large tag. Cortical translocation is nonetheless decoupled from glycolytic essentiality. It has been shown that after prolonged extracellular gliding stored ATP becomes depleted (MacRae et al., 2012) and therefore ATP production at the cortex

59

becomes much more critical in such situation. However, parasite can easily convert other carbon sources to produce energy to survive. The catalytically dead mutant is translocated similar to WT complementation, indicating that this phenomenon is uncoupled from glycolysis. Thus, though GAPDH1 is critical for intracellular replication of the parasite, using our structure-function analysis we have discovered that translocation of GAPDH1 is not essential for parasite viability.

The complemented Myc-tagged GAPDH1 with or without ATc treatment have relatively similar GAPDH activity and translocate to the cortex upon parasite egress. Moreover, the GAPDH1 active site mutant is also readily relocated to the cortex though is not active. It is important to note that although in our complementation experiments the protein levels is relatively similar, it is possible that the overexpression of cytosolic GAPDH1 is able to overcome specific membrane association, as has been shown for CDPK3 kinase anchored to the IMC (Garrison et al., 2012). Overall, our data show that glycolytic activity is prime role of GAPDH1 but is not related to cortical translocation.

Table 3.1. Crystal structure data of TgGAPDH1 Crystal structure data collection and refinement statistics of *Toxoplasma* GAPDH1, PDB code 3STH. Values in parentheses are for highest-resolution shell.

Data collection	
Space group	P 21 21 21
Cell dimensions	
a, b, c (Å)	103.37, 104.32, 146.63
a, b, g (°)	α, β, γ = 90
Resolution (Å)	50-2.25 (2.29-2.25)
R_{sym} or R_{merge}	
I / sI	
Completeness (%)	99.7 (98.7)
Redundancy	5.6 (5.7)
Refinement	
Resolution (Å)	50.0-2.25 (2.31-2.25)
No. reflections	75385 (5199)
R_{work} / R_{free}	0.172/0.216 (0.221/0.299)
No. atoms	
Protein	10169
Ligand/ion	232
Water	751
B-factors	
Protein	23.88
Ligand/ion	27.76
Water	17.54
R.m.s. deviations	
Bond lengths (Å)	0.011
Bond angles (°)	1.277

Figure 3.1. Secondary structural alignment of GAPDH

Apicomplexan parasite (*Toxoplasma gondii, Plasmodium falciparum, Cryptosporidium parvum*), plant chloroplast (spinach), bacterium (*Staphylococcus areus*) and human GAPDH (somatic and sperm) are aligned to the *Toxoplasma* backbone using ESPript 3.0. The two domains as indicated function in NAD$^+$ binding and catalysis. Dashed box indicates the Lys-Gly dipeptide insertion (DI) in apicomplexans that sets it apart from higher eukaryotic GAPDH. Functional residues are identified as C (catalytic residues), P (Phosphorylation), Pa (Palmitoylation), A (Acetylation), G (O-linked N-acetyl Glucosamine), PSB (PhosphatidylSerine-rich Binding), NE (Nuclear Export), and GB (Glutathione Binding). P, Pa and C residues that have been mutagenized for functional assays in this study are underlined. Residues that form hydrogen, hydrophobic and both types of bonds with the cofactor NAD$^+$ are labeled in orange, respectively as H, h and H. Similar labels in green are used for residues that bond with the substrate G3H. Sequences were extracted from UniprotKB database: *T. gondii* GAPDH1 (code Q9BKE2), *C. parvum* GAPDH (code Q7YYQ9), *P. falciparum* GAPHDH (code Q8T6B1), *Homo sapiens* (human) GAPDH1 (somatic, code P04406)*, H. sapiens* (human) GAPDH2/GAPDHS (sperm, code O14556)*, Spinacia oleracea* (spinach) chloroplast GAPDH (code P19866). Crystallographic structures of the seven selected GAPDH proteins are solved and deposited in PDB.

Figure 3.1. Secondary structural alignment of GAPDH
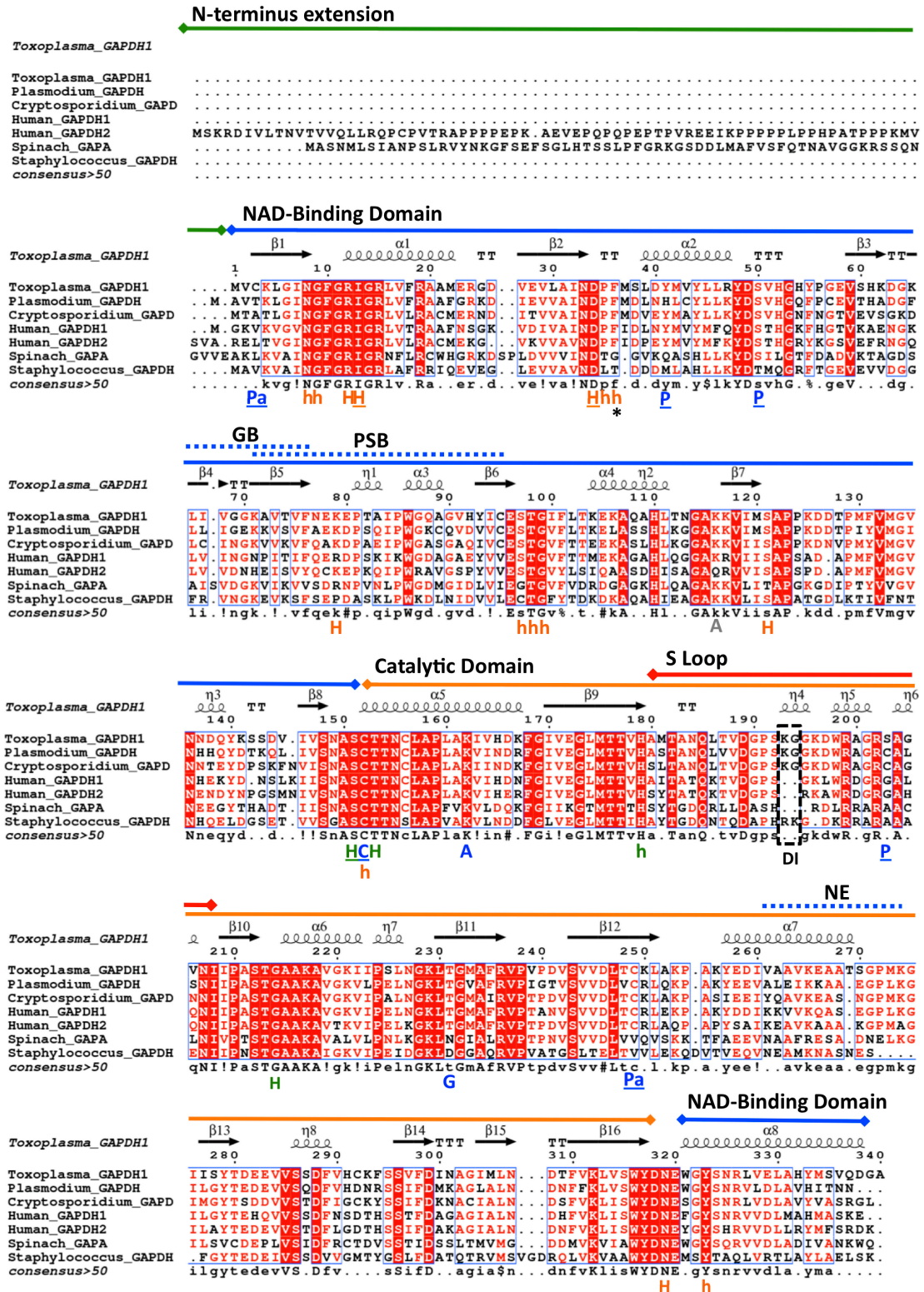
Figure 3.2. Structure of TgGAPDH1 protein

(a) Crystallographic structure of *Toxoplasma* GAPDH1 monomer showing the catalytic and NAD^+-binding domain with a dipeptide insertion (DI) in the S-loop that is unique to apicomplexan parasites. (b) GAPDH1 tetramer exhibits a true axis of symmetry (P axis) (bottom row) and two pseudo (top row) symmetrical axes (Q and R axes).

Figure 3.2. Structure of TgGAPDH1 protein
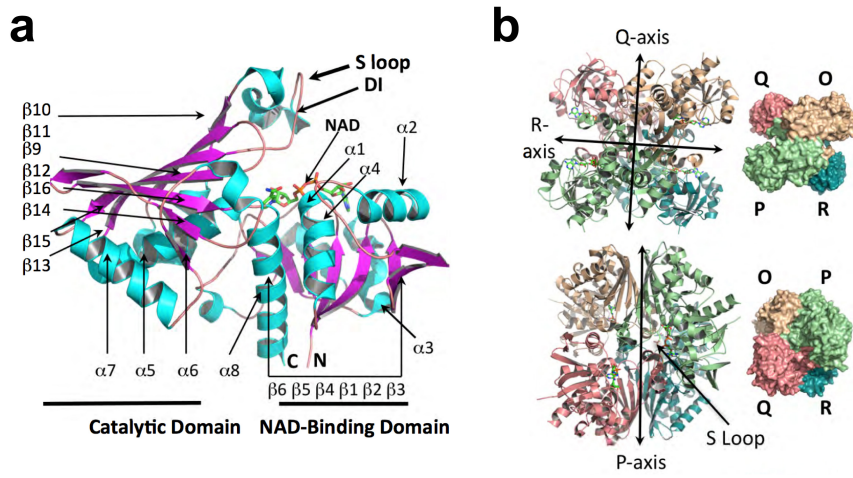
Figure 3.3. GAPDH1 is relocated to the cortex in extracellular parasites

(a) IFA of intracellular and extracellular parasites with c-Myc2 GAPDH1 fusions using α-Myc for visualizing GAPDH1 localization, α−IMC3 to stain the cortical cytoskeleton and DAPI to stain the nuclear material. (b) Live microcopy images of intracellular and extracellular mCherry GAPDH1 fusion at N-terminus.

Figure 3.3. GAPDH1 is relocated to the cortex in extracellular parasites

67
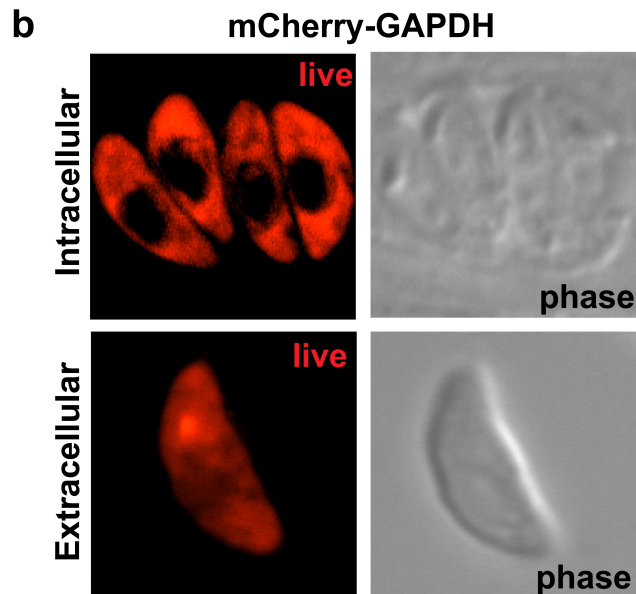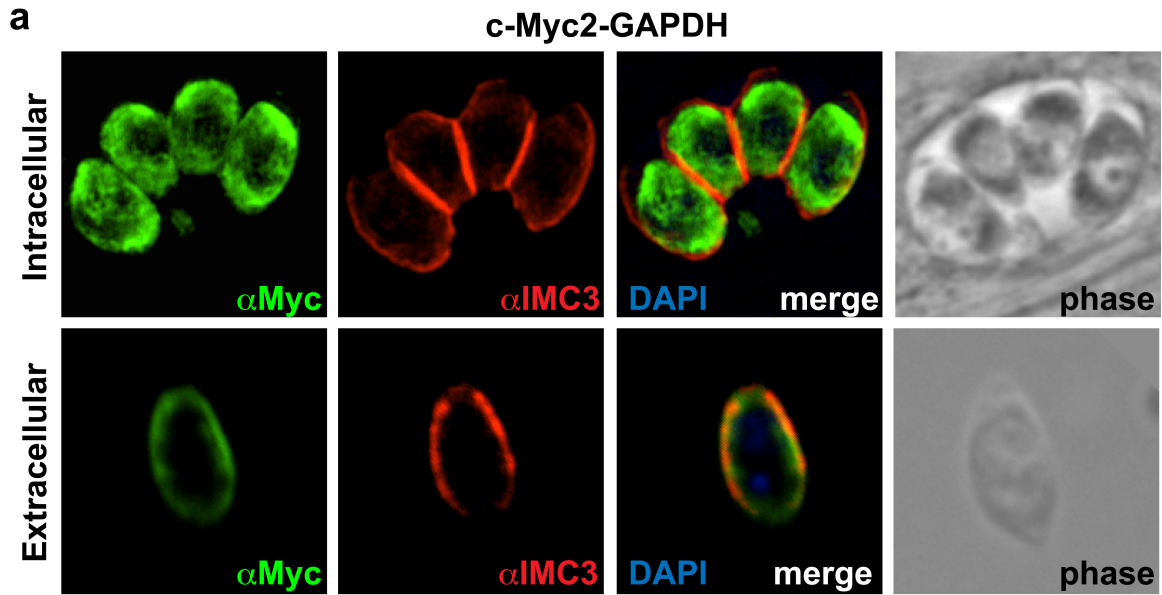
Figure 3.4. Generation and verification of GAPDH1cKD

(a) Schematic of GAPDH1cKD generation. GAPDH1cKD was generated in the TATiΔku80 parental line using the tet-repressible system. A DHFR selectable cassette containing TetO7Sag4 (T7S4) replaced the endogenous promoter of GAPDH1 by double homologous recombination in the 3'HR and 5'HR regions. PCR1-3 regions indicate the diagnostic PCRs to determine correct integration as determined in panel b. (b) Integration PCR shows that endogenous promoter is disrupted. Localization of diagnostic PCR primer pairs provided in panel a. (c) Western blot indicates progressive loss of GAPDH1 protein expression in the GAPDH1cKD parasite line. Parasites were treated with ATc for the indicated time periods. GAPDH1 was detected with anti human GAPDH. A monoclonal antibody recognizing cortical cytoskeleton protein IMC1 was used as a loading control.

Figure 3.4. Generation and verification of GAPDH1cKD
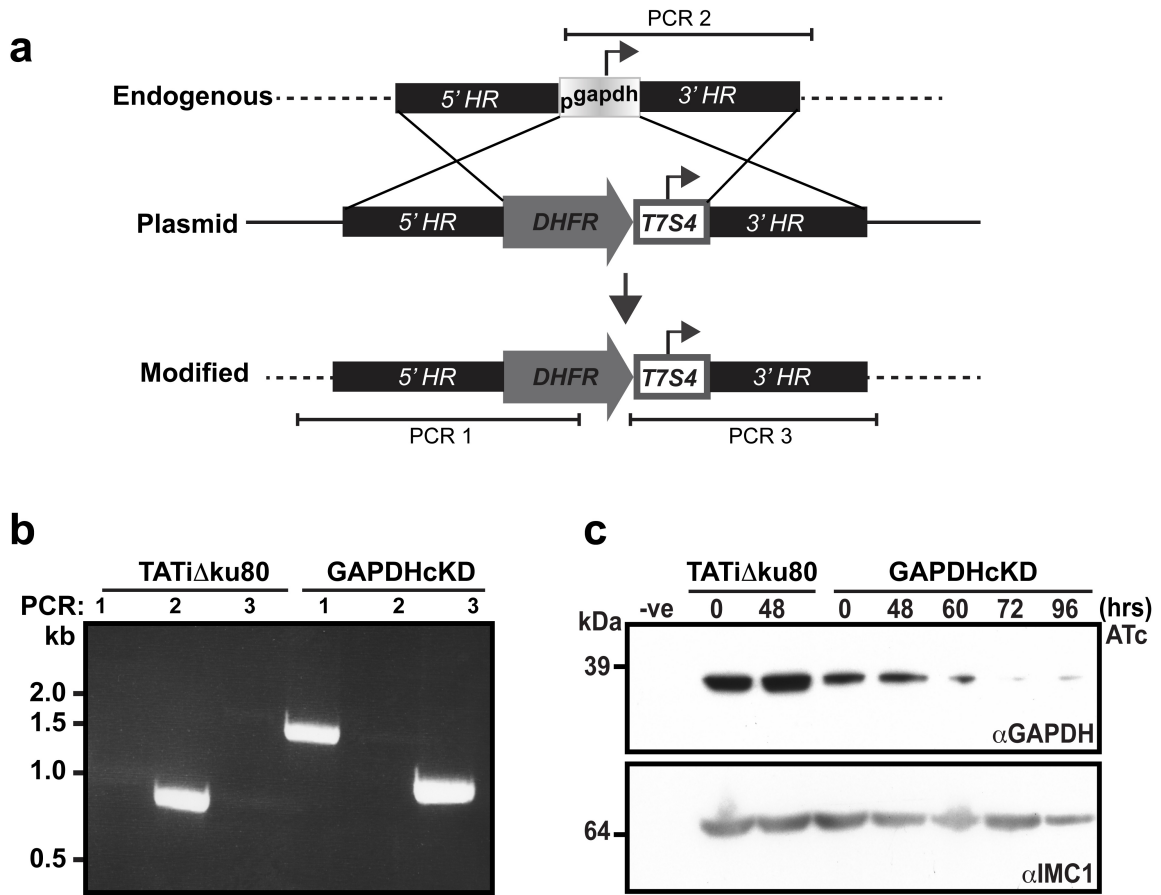
Figure 3.5. Phenotypic analysis of GAPDH1cKD

(a) Plaque assay of parasites grown in the absence (-) and presence (+) of ligand anhydrotetracycline (ATc, 1.0 µg/ml) for 10 days on HFF monolayer indicates that GAPDH1cKD parasites were not viable. (b) Growth assay measures cytosolic YFP fluorescence expressed in parasite strains and shows that GAPDH1cKD parasites did not exhibit growth up to 8 days. (c). Replication assay by microscopic quantification of number of parasites per parasite vacuoles demonstrates that GAPDH1cKD parasites did not replicate further following 60 hrs of induction. Inset shows a vacuole containing four morphologically normal parasites at 96 hrs of ATc induction. More than 100 vacuoles were counted for N=3 ± s.e.m. statistical significance calculated by paired, two tailed *t*-test, **$P < 0.02$.

Figure 3.5. Phenotypic analysis of GAPDH1cKD
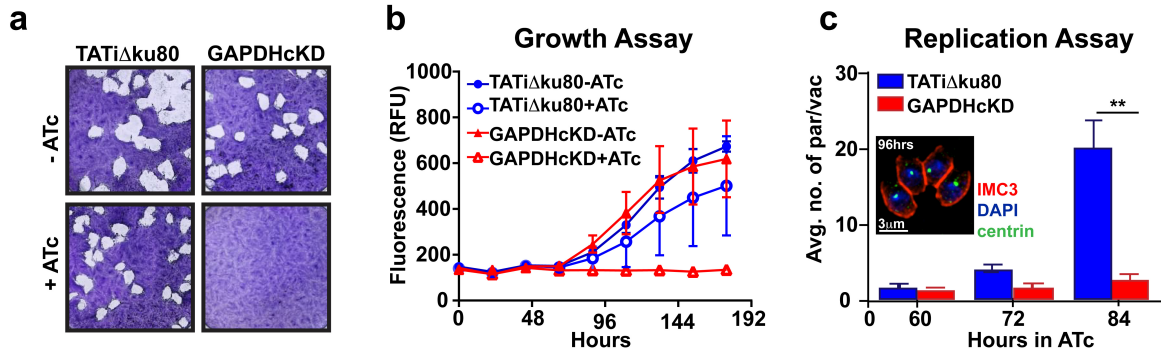
Figure 3.6. GAPDH1 is not required for invasion or egress of the parasite

(a) Invasion assay shows that there is no significant invasion defect. Over 200 parasites per condition were counted to calculate percent invasion and statistical analysis was done by the paired two-tailed *t*-test. N=3 ± s.e.m. (b) Egress assay shows that loss of GAPDH1 does not impair egress. Calcium ionophore A23187 (2 μM) was used to induce egress of GAPDH1cKD and TATiΔku80 parasites after 60 hrs of ATc treatment from the host cell. 15 random fields were counted in N=3 ± s.e.m.

Figure 3.6. GAPDH1 is not required for invasion or egress of the parasite
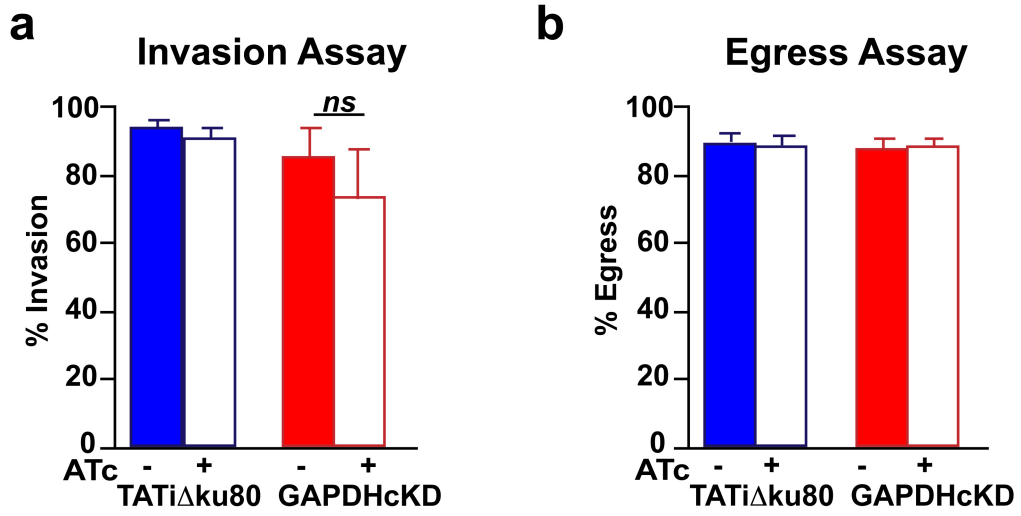
Figure 3.7. Relocation of GAPDH1 is not essential for viability

(a) Cortical localization of N-terminally Myc2 and mCherry fused GAPDH1^{WT} was quantified in the extracellular parasites after counting about 200 parasites in N=3 ± S.D. *t*-test, ***P < 0.0001. Representative image corresponding to the N-terminally fused GAPDH1 with either Myc2 or mCherry. The image of mCherry tagged GAPDH1 (red) is live in extracellular parasites while methanol fixed and probed using α-Myc (green) for Myc2-GAPDH1. (b) Plaque assay of parasites expressing N-terminally-tagged fluorescent fusion of mCherryRFP or YFP to *Toxoplasma* GAPDH1^{WT} after 8 days incubation.

Figure 3.7. Relocation of GAPDH1 is not essential for viability
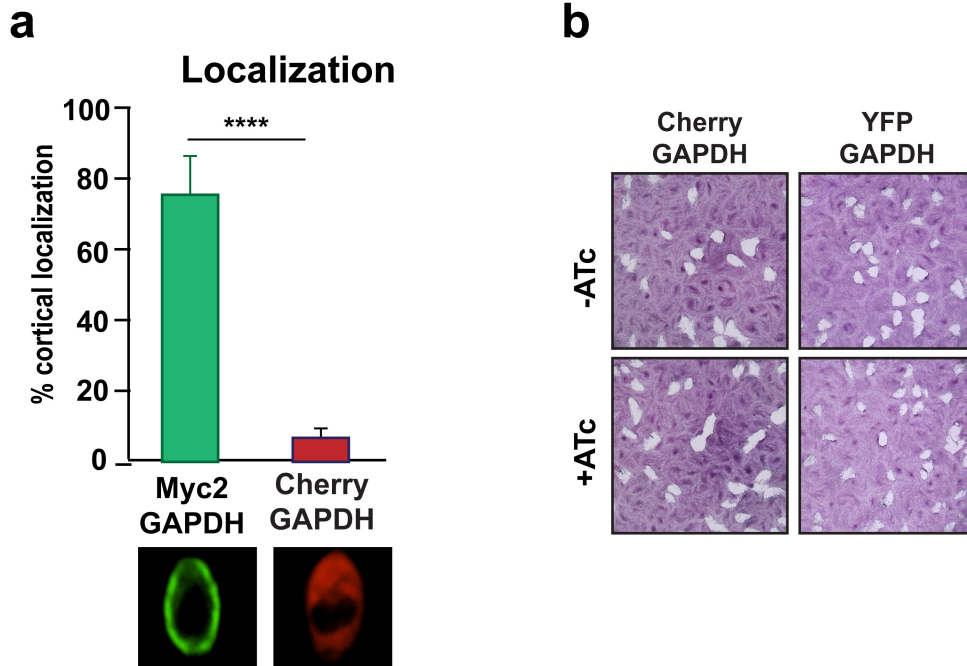
Figure 3.8. Structure of *Toxoplasma* GAPDH1 catalytic site

(a) Superimposition of essential residues that interact with substrate G3P and co-factor NAD$^+$ in the active site of *Toxoplasma* and *C. parvum* (PDB code 3CIF) GAPDH. Residues that form hydrogen and hydrophobic bonds are colored yellow for *C. parvum* and deep teal for *Toxoplasma*. Catalytic residues of G3P are coded as red (*C. parvum*) and green (*Toxoplasma*). *C. parvum* structure has a C151S variant. Unique residues that can form hydrophobic interactions with NAD$^+$ in *Toxoplasma* GAPDH1 are illustrated in purple. (b) Supposition of S-loops in *Toxoplasma* GAPDH1 shown in deep teal (R subunit) and human somatic GAPDH that is expressed in human brain cells are shown in red (PDB code 1ZNQ).

Figure 3.8. . Structure of *Toxoplasma* GAPDH1 catalytic site
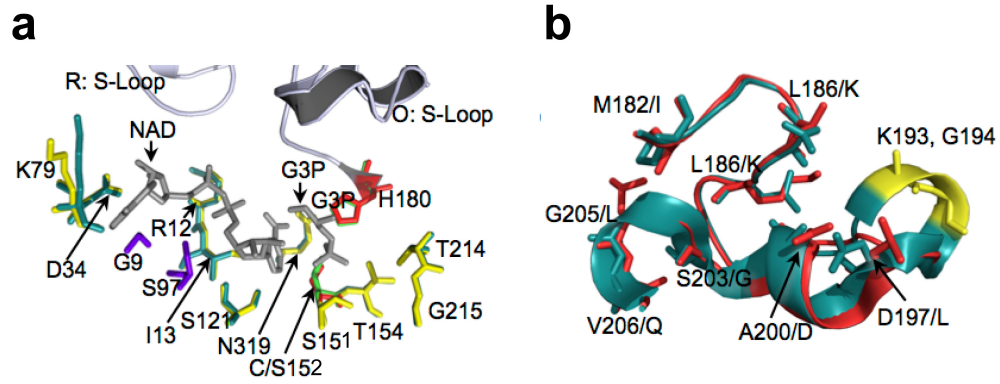
Figure 3.9. Active site mutation is lethal for the parasite

(a) Complementation of GAPDH1cKD was observed with wild type GAPDH1 but not with active site mutant C152G as shown by plaque assay for 10 days. (b) Western blot to ascertain that the native GAPDH1 is the down regulated in the complemented lines upon ATc treatment. Top panel shows endogenous GAPDH1 and the Myc tagged fusion using α-human GAPDH and the middle panel shows the fused Myc2-GAPDH1 as shown by α-Myc antisera. Bottom panel is loading control shown by α-IMC1.

Figure 3.9. Active site mutation is lethal for the parasite
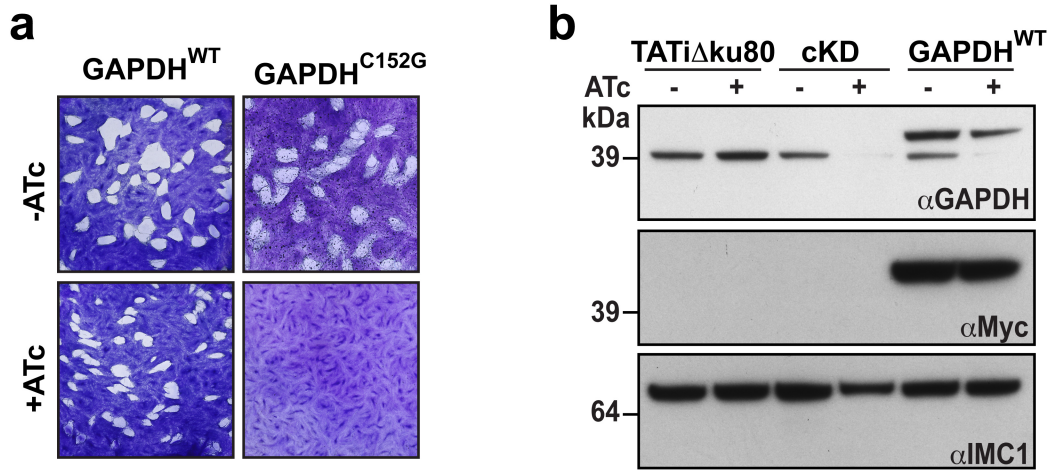
Figure 3.10. Active site of GAPDH1 has no role in translocation

Intracellular and extracellular parasites showing localization of GAPDH1 in the Myc2 tagged GAPDH1^{C152G} variant after methanol fixation. Shown in green is α-Myc staining of tagged Myc2-GAPDH1 and in red is α-IMC3 staining of cortical cytoskeleton, Nuclear material is stained with DAPI.

Figure 3.10. Active site of GAPDH1 has no role in translocation
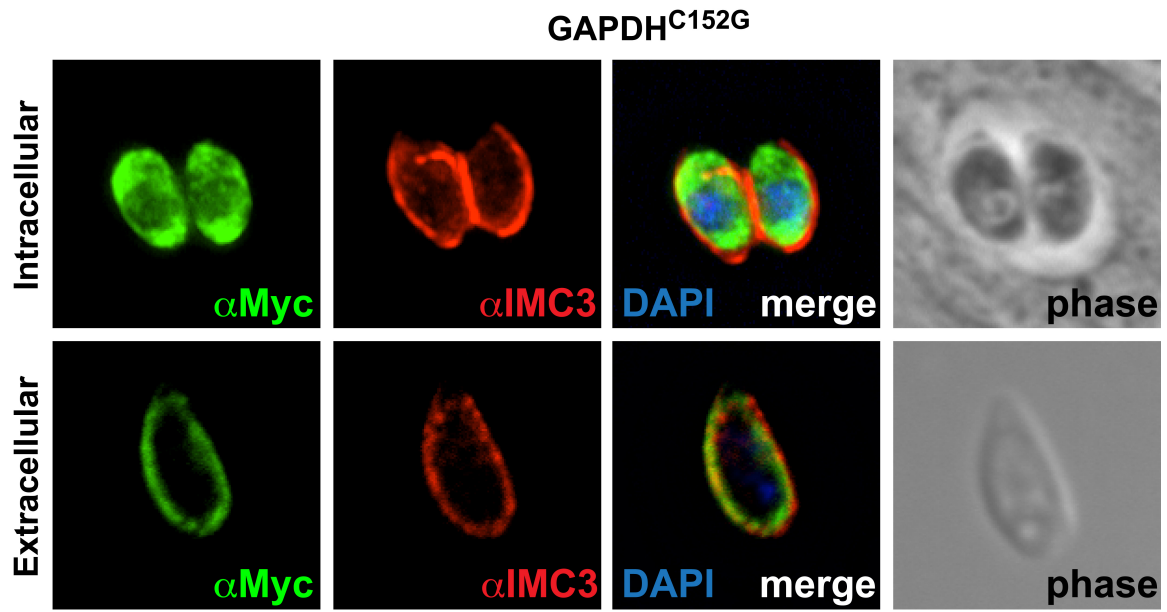
Figure 3.11. Functionality of GAPDH1 active site

(a) Cell monolayer lysis assay measures the capacity of GAPDH1cKD, GAPDH1^{WT} and GAPDH1^{C152G} to proliferate and lyse the host cell monolayer in presence of glutamine replete vs. glucose replete-media. Post 48 hrs incubation the monolayer was fixed and the absorbance after crystal violet staining was measured. One representative experiment of three biological replicates is shown. N=3 ± S.D. (b) Replication assay was done and parasite numbers per vacuole were counted for more than 100 vacuoles and expressed as number of cell divisions post infection in glutamine replete or glutamine-deplete media. N=3 ± s.e.m. t-test, $**P < 0.02$, $***P < 0.002$ (c) GAPDH activity as calculated by measuring the reduction of NADH illustrates the conditional knockdown and catalytic residue mutation inhibit activity. d) ATP measurement was determined by the total amount of ATP per parasite for the parasite lines as indicated grown ± ATc for 60 hrs.

Figure 3.11. Functionality of GAPDH1 active site

a

Cell Monolayer Lysis Assay

b Glutamine Rescue

c GAPDH Activity

d ATP measurement
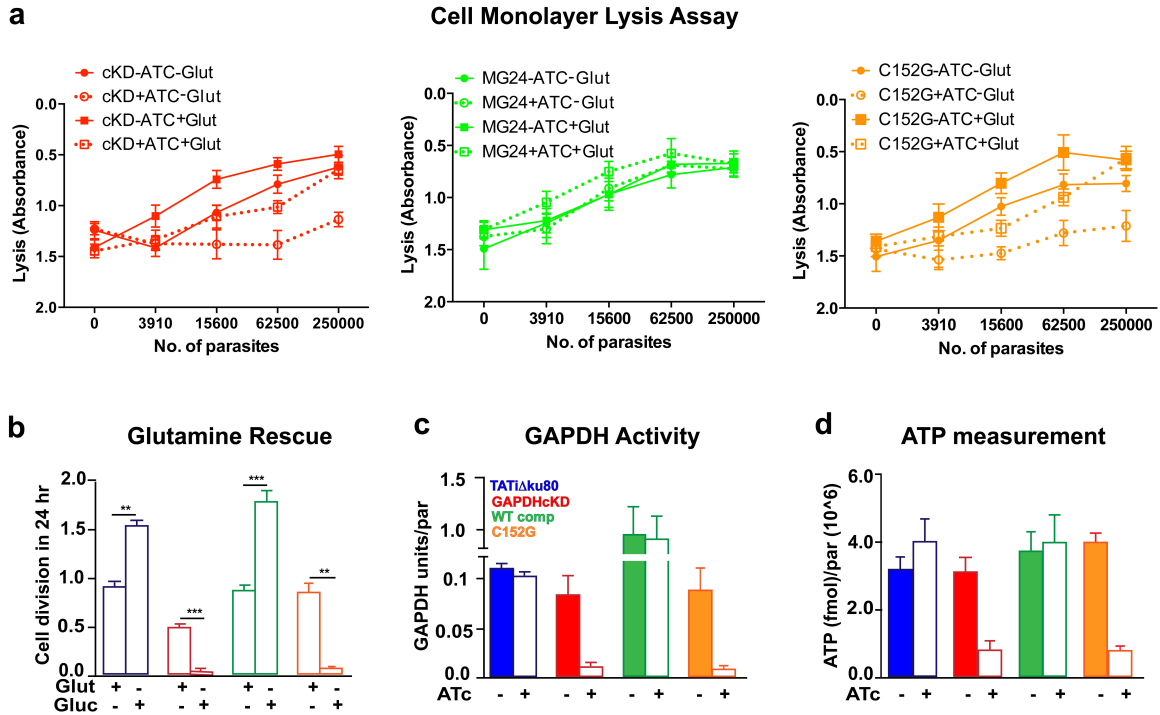
CHAPTER 4: ALLOSTERIC REGULATION OF *TOXOPLASMA* GAPDH1 BY

PHOSPHORYLATION

4.1. Introduction

GAPDH is a highly conserved protein with little variance from species to species (Sirover, 1999). *Toxoplasma* GAPDH1, similar to others, is a tetramer with four independent subunits O, Q, R and P containing the coenzyme NAD^+ (Dubey et al., 2016). GAPDH1 is composed of two folding domains, NAD^+ binding domain and the catalysis domain. Within the catalytic domain is a S-shaped loop called the S-loop, composed of the amino acid residue from position 180 and 210 (Figure 3.1.) The S-loop forms the core of the four subunits and is in contact with NAD^+ on the R-axis and several amino acids across the P-axis. It is pivotal for co-factor binding, allosteric activation and quaternary structure assembly (Biesecker et al., 1977). Interestingly, the phosphoproteome of *Toxoplasma* provides evidence for the phosphorylation of two residues associated with the S-loop of GAPDH1, Ser50 and Ser203 (Treeck et al., 2011a). While Ser50 is highly conserved residue in all across different phylum including humans (Akinyi et al., 2008), Ser203 is unique to *Toxoplasma* and some closely related coccidians like *Hammondia* and *Neospora* (ToxoDB).

It has been known since the early 1950s that GAPDH catalyzes the oxidative phosphorylation of D-glyceraldehyde 3-phosphate to 1, 3-disphosphoglycerate in the presence of NAD^+ and inorganic phosphate (Segal and Boyer, 1953). The homotetramer exhibits a dimerization interface as well as subunit- subunit interactions that occur as dimerized units interact to form the tetrameric structure (Biesecker et al., 1977; Moras et al., 1975). Studies over two decades show that GAPDH is also a multifunctional enzyme with distinct subcellular localizations and diverse activities (Sirover, 1999, 2011). The post-translational modifications are one of the driving forces that modulate the functional

diversity of GAPDH (Sirover, 2011). Phosphorylation of GAPDH is functionally relevant for cytotoxic T-lymphocyte mediated cytotoxicity, cellular trafficking and stress response in cells (Tristan et al., 2011).

In this part of the thesis, we have generated phosphomutant-complemented lines to better understand the significance of serine phosphorylation events in the S-loop. We discovered that dynamic phosphorylation of S50 is required for parasite viability. The phosphomimic form of S203 significantly reduces GAPDH activity likely due to disrupting the possibility for GAPDH1 to form tetramers (Dubey et al., 2016).

4.2. Results

4.2.1. *S-loop of GAPDH1 is phosphorylated*

The GAPDH1 S-loops form a two-plier ridge that separates the NAD^+-binding cavities of

subunits across the R axis (Figure 4.1. a-b). Binding of NAD^+ increases the ordering of

the S-loop and interactions between subunits that are positioned across each other in the

tetramer, leading further to changes in the packing environment at the dyad interfaces

(Figure 3.1. a). The opening to the NAD^+ cavity is more constricted in *Toxoplasma*

GAPDH1 in comparison to human GAPDH due to Lys196 and the bulge created by the

Lys193-Gly194 dipeptide insertion (Figure 4.1. b). Serine 50 is located on the surface

loop that follows α-helix 2 (α2) and can form hydrogen bonds with the S-loop of the

neighboring subunits of the Q-R dyad (Figure 4.1. a). Ser50 in the O subunit can form

contacts with Ser287 in the Q subunit and Asp189 in the S-loop of R subunit. Serine 203

is located directly in the S-loop and can form hydrogen bonds with three S-loop residues

(Thr187, Asp189, Asn207) to configure this flexible loop (Figure 4.3. b). The novel

observation of GAPDH1 S-loop phosphorylation was examined (Treeck et al., 2011a) for

potential regulatory effects by measuring its effect on parasite viability, cortical

localization of GAPDH1 in extracellular parasites and GAPDH activity in the

phosphomutant parasites.

4.2.2. *Dynamic phosphorylation of Ser50 is critical for viability*

To assess the impact of these phosphorylation events on various aspects of the parasite's

biology we generated parasites lines expressing phosphomimetic (Ser to Glu) and

phosphonull (Ser to Ala) point mutations. The alleles were evaluated by genetic

complementation of the GAPDH1cKD line, where the wild type allele can be down regulated by addition of ATc so the effect of the mutant allele can be assessed. We first performed plaque assays to evaluate effects on viability. GAPDH1^{S50E} and GAPDH1^{S203E} did not support parasite growth as is evident by the absence of vacuoles in the ATc treated lines (Figure 4.2.). Additionally, the GAPDH1^{S50A} phosphonull mutation did not support viability but the S203A allele confers complete viability (Figure 4.2.). Parasites stably expressing the double phosphomimetic mutation (GAPDH1$^{S50E, S203E}$) could not be established in the uninduced GAPDH1cKD line, suggesting that this allele has a more severe phenotype and probably acts in a dominant negative fashion (Dubey et al., 2016).

4.2.3. *GAPDH1 translocation is independent on serine phosphorylation*

Since kinase activity is associated with egress (Garrison et al., 2012), we asked whether phosphorylation of these serine residues in the S-loop of the GAPDH1 are involved in cortical translocation. Using the ATc treated mutant parasite lines we did an IFA on the extracellular parasites and quantified the percentage of cortical localization of GAPDH1 mutant. The parasites were scored with either cortical (Figure 4.3. a) or cytosolic (Figure 4.3. b) signal of myc-tagged GAPDH1 mutants as shown by the intensity profiles. Upon quantification, the N-terminally myc tagged GAPDH1^{WT} used as control for the assay, showed cortical localization in 83% of extracellular parasites, indicating that GAPDH1 is relocated to the cortex in these parasites (Figure 3.7. a). Interestingly, none of the phosphomutants displayed a dramatic translocation defect, although the phosphonull mutants trend to show slightly less translocation (Figure 4.3. c). Overall, these data

demonstrate that serine phosphorylation is not the major mechanism regulating relocation of GAPDH1 to the cortex.

4.2.4. *Disruption of S-loop decreases GAPDH1 activity*

Next we assessed whether S-loop phosphorylation had effects on GAPDH1 enzymatic activity. The activity of the phosphomutant complemented lines was measured in parasite lysates and expressed as GAPDH units/par. Interestingly, no decrease in activity for the S50E or S50A mutant was observed upon ATc treatment compared to the S203E. This data indicates that GAPDH1 activity is regulated by dynamic phosphorylation of S50 and both GAPDH1 dimers need to be in different phospho states for complete GAPDH activity (Figure 4.4. a). However, GAPDH1 activity is similar to wild type complementation in case of S203A mutant but decreases significantly upon S203E complementation (Figure 4.4. a). We verified that GAPDH activity was independent of GAPDH1 protein level in the experimental lines (Figure 4.4. b). Although expression levels for all mutant proteins were comparable, we detected a slightly shorter version of the S203A mutant as well as some smaller protein bands suggesting GAPDH1[S203A] might not be stable. Overall, our observations show that serine phosphorylation of the S-loop in GAPDH1 regulates its enzymatic activity, probably by interference with oligomerization assembly and allosteric activation (Dubey et al., 2016).

4.3. Discussion

Our data illustrates that the dynamic S-loop of *Toxoplasma* GAPDH1 is regulated by differential phosphorylation of Ser50 and Ser203 to trans-activate the catalytic pocket of other subunit in the R dyads. Our structure-function data show that dephosphorylated S203 is pivotal for reconfiguring the S-loop to fit into the neighboring NAD^+-binding pocket by forming atomic interactions with three other S-loop residues (Thr187, Asp189, Asn207). Dephosphorylated S50 contributes to homodimerization by hydrogen bonding across the dimer interface with S287 and stabilizes the neighboring S-loop by bonding with Asp189. The phosphorylation events modulate the dynamic motion of S-loop in regulating the NAD^+-binding pocket and oligomer assembly. Glycolysis appears to be regulated by the S-loop phosphorylation as is evident from the decrease in GAPDH activity for the constitutive phosphorylated form of Ser203 (Dubey et al., 2016).

Dynamic phosphorylation of S50 and mimic of S203 affect viability of the parasite. Lytic cycle of the parasite is not disrupted in the absence of phosphorylation of S203. This suggests that phosphorylation of the S-loop of GAPDH1 controls glycolytic activity and henceforth the parasite viability. There appears to be a direct correlation between GAPDH1 activity and viability of the parasite and also the oligomer assembly of GAPDH1. However, based on our data the role of S50 in non-glycolytic roles of GAPDH1 cannot be eliminated and further research may throw some light on this feature. Importantly, the phosphorylation of S-loop has no effect on cortical translocation of GAPDH1 in the parasite. Since GAPDH1 translocation occurs upon egress of parasite which occurs due to increase in and the GAPDH1 phosphorylation is not calcium dependent (Treeck et al., 2011a) so it is not surprising that we did not observe any

significant loss of GAPDH1 translocation indicating that a novel mechanism in underplay for translocation of GAPDH1 in *Toxoplasma*. The specific functions of these serine residues further stress the significance of unique post-translational modifications in the diverse roles of GAPDH1. Interestingly, the other phosphorylation residue responsible for an array of function ranging from cytotoxicity, cellular trafficking and stress response in mammals is not predicted in *Toxoplasma* GAPDH1 (Treeck et al., 2011a).

GAPDH1 S-loop phosphorylation is possibly a universal feature since S50 is a widely conserved residue across GAPDH proteins from different species (Figure 1). The localized effect of catalytic loop phosphorylation on enzymatic activity is a widely conserved mechanism. Hallmark examples include the cis-phosphorylation in the activation loop of the Ephrin subfamily of tyrosine kinase receptors (Overman et al., 2014), phosphorylation of the activation loop in the family of MAP kinases (Akella et al., 2010), and the activation of Aurora A kinase by phosphorylation of its activation loop (Zorba et al., 2014). The allosteric regulation of the *Toxoplasma* GAPDH1 S-loop by multiple intra- and inter-phosphorylation events is a novel mechanism of catalytic loop activation in this class of enzymatic activity regulation (Dubey et al., 2016). Quite surprisingly, no report of GAPDH activity regulation by S-loop phosphorylation has been reported in other systems for this well studied protein. This study also reveals unique amino acid modifications within the S-loop with functionally important roles and provides attractive targets for therapeutic intervention.

Figure 4.1. Serine phosphorylation in the regulatory S-loop

(a) Carbon chain and surface rendering of dimer of the R and Q dyads (O-R, top panels, O-Q, bottom panels) reveals that phosphorylatable Ser50 (magenta) is located on a beta-turn that forms 3 hydrogen bonds with Asp189 residue in the S-loop of adjacent subunit in the O-R dimer. Ser50 of in the α 2 helix also forms a polar contact with Ser287 (cyan) at the interface of O-Q dimer. (b) Phosphorylatable Ser203 is positioned in the S-Loop and is critical to the loop stability by forming polar contacts with three residues (Thr187, Asp189, and Asn207).

Figure 4.1. Serine phosphorylation in the regulatory S-loop
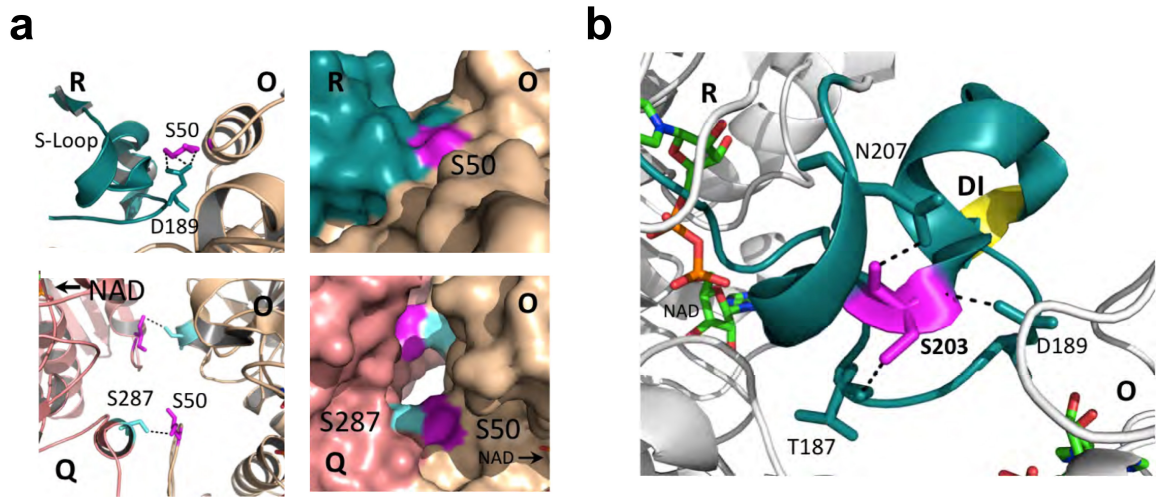
Figure 4.2. Dynamic S50 phosphorylation is required for complementation capacity

Plaque assay after 9 days shows the viability of the phospho-mimic and phospho-null mutants by genetic complementation of a parasite line wherein expression of the endogenous GAPDH1 locus can be down regulated by addition of ATc. The assay was done with a negative control of GAPDH1cKD and a positive control of wild type GAPDH1 complementation not shown in the figure.

Figure 4.2. Dynamic S50 phosphorylation is required for complementation capacity
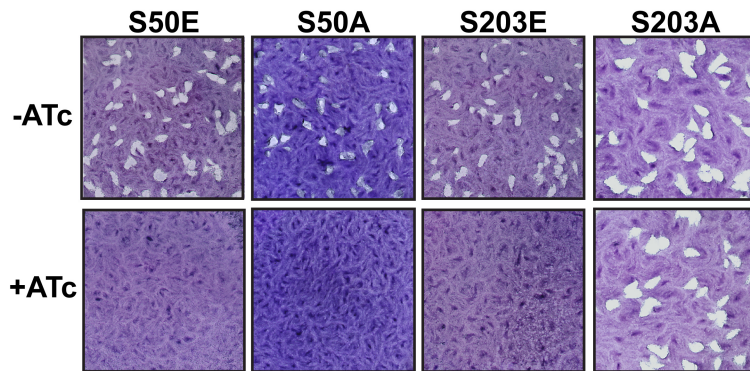
Figure 4.3. Cortical translocation is not effected by phosphomutants

(a) Representative example of cortical localization (green: α-Myc staining of tagged Myc2-GAPDH1; red: α-IMC3 staining of cortical cytoskeleton). The yellow arrow marks the site of the intensity profile of both signals. (b) Representative image indicating the cytosolic localization of mutant GAPDH1 in extracellular parasites with its intensity profile across the yellow arrow. (c) Quantification of percentage of extracellular parasites displaying cortical GAPDH1 localization in the genetically complemented GAPDH1cKD line as indicated for the mutant lines and in three independent experiments for the WT as shown in Figure 3.7.

Figure 4.3. Cortical translocation is not effected by phosphomutants
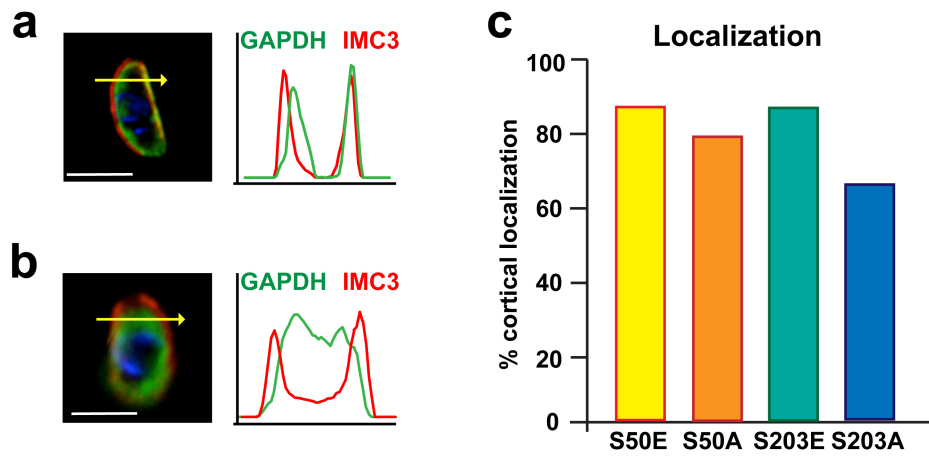
Figure 4.4. GAPDH1 enzymatic activity is significantly disrupted by constitutive S203 phosphorylation

(a) GAPDH1 activity of the phospho-mutants as indicated measured after 60 hrs ± ATc. N=3 ± s.e.m. *t*-test, **P < 0.04. (b) Western blot indicating the level of myc2-GAPDH1 protein in the GAPDH1^{WT} and mutant complemented strains by α-human GAPDH and α-myc antisera. α-IMC1 is used as a loading control.

Figure 4.4. GAPDH1 enzymatic activity is significantly disrupted by constitutive S203 phosphorylation
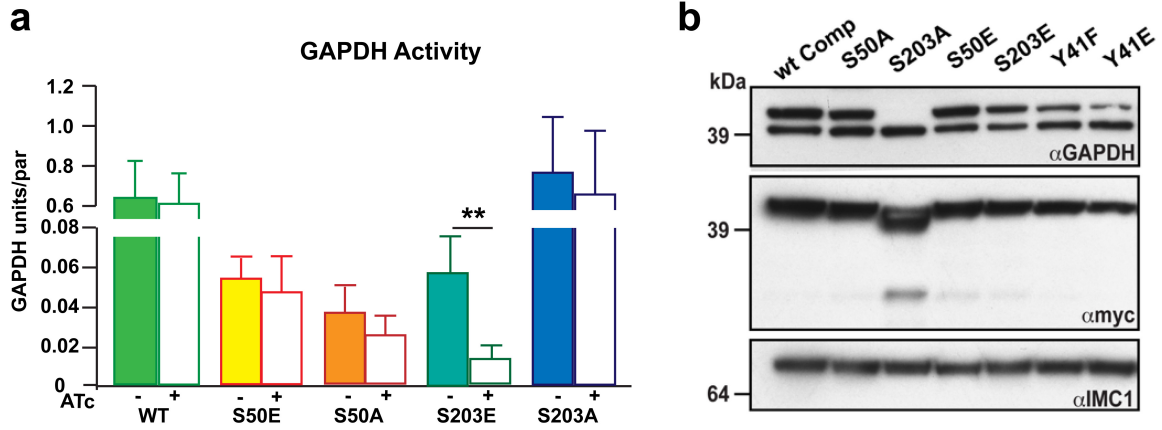
CHAPTER 5: *TOXOPLASMA* GAPDH1 ASSOCIATES TO THE MEMBRANE BY

PALMITOYLATION

5.1. Introduction

Toxoplasma GAPDH1 localizes to the cytosol of intracellular parasites, but is translocated (along with other glycolytic enzymes such as aldolase and lactate dehydrogenase) to the cortical membrane skeleton upon egression from the host cell (Pomel et al., 2008). This association is reversible as upon invasion GAPDH1 is swiftly released into the cytosol. The pellicle of *Toxoplasma* and other apicomplexan parasites is a unique and stable cellular architecture composed of plasma membrane, actinomysosin, and a quilt of flattened vesicles undergirded by microtubules and intermediate filaments that is termed the inner membrane complex (IMC) (Anderson-White et al., 2012). Cortical translocation of the glycolytic enzymes is postulated to enhance ATP delivery for active membrane transport and to power the motility apparatus in *Toxoplasma* (Pomel et al., 2008). The specific signal and mechanism of cortical skeletal association of GAPDH1 and other glycolytic proteins in the extracellular parasites has not been identified.

During *Plasmodium falciparum* schizogony, GAPDH associates with the plasma membrane of the schizont. The membrane association of *Plasmodium* GAPDH has been shown to rely on an interaction of the GAPDH N-terminus with Rab2 in an *in vitro* heterologous system employing human Rab2 and rabbit microsomes (Daubenberger et al., 2003). For the orthologous interaction between GAPDH and Rab2 in humans for the retrograde transport of Rab2-vesciles to the endoplasmic reticulum (Daubenberger et al., 2003), phosphorylation of GAPDH on Tyr41 by Src kinase is required (Tisdale and Artalejo, 2007). This Tyr residue is positionally conserved in *Toxoplasma* GAPDH1

indicating this could be a potential mechanism underlying cortical membrane skeleton association.

An alternative or concurrent mechanism could be that association of GAPDH1 with the membrane skeleton is mediated by reversible acylation: palmitoylation is a reversible modification that enables target proteins to associate with membranes. This modification involves the enzymatic attachment of a fatty acid (i.e. palmitic acid) to a sulfhydryl group on a protein, i.e. cysteine residues. Notably, a family of *Toxoplasma* palmitoyltransferases was recently reported and some of these enzymes do indeed reside in the IMC (Frenal et al., 2014a), and moreover, membrane association by palmitoylation has been demonstrated for other proteins residing in the membrane skeleton (Beck et al., 2010; Garrison et al., 2012). *Toxoplasma* GAPDH1 contains several cysteine residues that could be palmitoylated. We considered the role of these modifications in understanding the mechanism of GAPDH1 translocation in the extracellular parasites. Our studies show that Cys3 residue is not critical for viability of the parasites but is essential for relocation (Dubey et al., 2016).

5.2. Results

5.2.1. *GAPDH1 translocation is not mediated by tyrosine phosphorylation*

Tyr41 is conserved in *Toxoplasma* GAPDH1 and is located in a surface helix α2 (Figure 5.1. a). This residue can interact with the S-loop of the adjacent R dyad monomer; Tyr41 of the R subunit can form hydrogen bonds with Gly190 and Ser192 of S the loop in the O subunit (Figure 5.1. b). Tyr41 is phosphorylated in human GAPDH (Tisdale et al., 2004), but accessibility for kinase and Rab2 may be hindered sterically by the apicomplexan dipeptide insertion (DI) in the S-Loop (Figure 5.1. c-d). Phosphomimetic (Y41E) and phosphonull (Y41F) alleles were generated and in the GAPDH1cKD background to examine whether Tyr41 phosphorylation is involved in GAPDH1 translocation to the cortical membrane skeleton (Dubey et al., 2016). Neither allele alters cortical translocation (Figure 5.3. b) and thus negates the hypothesis that Y41 regulates GAPDH1 translocation to cortical membrane skeleton. Furthermore, both alleles support viability of the parasite as assessed by plaque assay (Figure 5.2. a), although we observe a nearly 4-fold reduction in plaque size for the Y41E allele (Figure 5.2. b). Reduction in plaque size is likely due to a dramatic reduction in GAPDH1 catalytic activity (Figure 5.3. a) by altering the dynamic S-loop (Dubey et al., 2016).

5.2.2. *GAPDH1 is predicted to be palmitoylated*

Next we considered the putative role of palmitoylation in membrane skeleton translocation. To identify putative palmitoylation sites we first subjected Toxoplasma GAPDH1 to a bioinformatics prediction of palmitoylation sites using CSS Palm (Ren et al., 2008). We identified two putative palmitoylation sites; Cys3, which is unique to

Toxoplasma and other coccidians like *Neospora*, *Eimeria* etc., (Figure 5.4. a) and Cys249, which is widely conserved and also found in human GAPDH (Yang et al., 2005) (Figure 3.1). The crystallographic structure of GAPDH1 indicates that Cys249 is not surface exposed in the GAPDH1 tetramer and its modification would block multimerization and thus enzymatic activity. However, Cys3 is surface exposed (Figure 5.4. b). We studied the role of Cys3 in cortical membrane skeleton association by replacement with Ser in a GAPDH1 allele fused at the N-terminus to a tandem Myc. This allele was used for genetic complementation of the GAPDH1cKD line as described in chapter 3. These complemented mutants were tested by Dr. Matt Bogyo's lab at Stanford to obtain direct proof of GAPDH1 palmitoylation using a chemically manipulatable palmitate mimic, 17- octadecynoic acid (17-ODYA) (Martin and Cravatt, 2009). In case C249 would be palmitoylated, we also generated a C249S mutant parasite line so we can discern it from C3S palmitoylation. From these data, we observe strong signals for wild type, C3S and C249S mutants (Figure 5.5.) suggesting the presence of multiple sites of modification in GAPDH1 (Dubey et al., 2016). The observed signal was insensitive to hydroxylamine treatment suggesting that the modification does not occur on a cysteine residue. 17-ODYA can also detect O-palmitoylation (Zou et al., 2011), N-palmitoylation (Linder and Deschenes, 2007) as well as other post translational modifications such as GPI anchors (Binder et al., 2008), which are insensitive to hydroxylamine. These results therefore do not allow a conclusive assessment of whether C3 is palmitoylated in *Toxoplasma*.

5.2.3. *Palmitoylation is critical for translocation but not activity or viability*

To assess the role of GAPDH1^{C3S} in the parasite, we tested the viability of the complemented mutant line by plaque assay. We observed that loss of Cys3 palmitoylation capacity has no effect on the lytic cycle (Figure 5.6. a). Next we tested the GAPDH activity in the parasites, which was not affected by the C3S mutation (Figure 5.6. b). Subsequently we tested translocation and observed that Myc2-GAPDH^{WT} is efficiently targeted to the cortical skeleton in extracellular parasites, however this association is reduced by 80% in Myc2-GAPDH1^{C3S} expressing parasites (Figure 5.7. a). Thus, C3S is critical for efficient membrane skeleton association.

To consolidate the observation that Cys3 is critical for membrane association we directly determined the fractions of WT and C3S mutants associated with membrane through differential centrifugation and detergent extractions as shown in the schematic (Figure 5.7. b). Following osmotic and mechanical lysis of extracellular parasites in presence of minimal salt (5 mM) and low speed centrifugation, we observed slightly more material in the supernatant (S1) than in the pellet fractions (P1) for both WT and C3S parasites (Figure 5.7. c, d). This is somewhat unexpected since only non-lysed parasites and the cytoskeleton were expected to pellet. Probing for the cytoplasmic proteins actin (majority cytoplasmic) and CDPK1 (100% cytoplasmic) demonstrated that lysis was complete (Figure 5.7. d), thus suggesting that GAPDH1 associates with the cytoskeleton IMC1 (Figure 5.7. d). Alternatively, we considered that the membrane skeleton and even plasma membrane could remain associated with the cytoskeleton. Therefore we assessed how plasma membrane (SAG1, GPI-anchored (Burg et al., 1988)) and IMC membrane (ISP2, palmitoylated (Beck et al., 2010)) fractionated. Like GAPDH1, roughly half SAG1 ends up in the pellet (P1) whereas 100% of ISP2 is in the

pellet (P1) suggesting that half of the plasma membrane and all of the IMC membrane tightly associates with the cytoskeleton upon osmotic and mechanical parasite disruption. This complicates the analysis of membrane association.

Next we subjected the low-speed supernatant (S1) to high-speed centrifugation to pellet (P2) all membrane-associated proteins (Taha et al., 2014). While GAPDH1^{WT} resides in the supernatant, suggesting this is mostly cytoplasmic, a significant fraction of GAPDH1^{C3S} fractionates in the pellet, suggesting membrane association (Figure 5.7. c), Since, the majority of the membrane fraction of interest is present in the low-speed pellet, we further deciphered the state of membrane associated proteins in the low speed pellet fraction. We resuspended the pellet in a physiological buffer (150 mM NaCl) and first performed a high-speed spin to release proteins that interact mostly through electrostatic interactions rather than through lipid membrane anchoring. GAPDH1^{WT} remains in the pellet (P3) whereas nearly half of GAPDH1^{C3S} becomes soluble (S3) (Figure 5.7. c). This suggests that the association of GAPDH1^{C3S} with the membrane/cytoskeleton is based largely on electrostatic interactions.

Subsequently we assessed whether we could remove GAPDH1 from the low speed pellet (P1) by detergents. As expected, treatment with 1% SDS solubilizes all proteins probed (Figure 5.7. d S4 and P4). In the control, where no detergent was added C3S again stood out by its significant release from the P1 fraction (Figure 5.7. d S7 and P7). We observed no major difference from the wild type construct using mild detergents (Figure 5.7. d, TX-100 and NP-40). As expected, both membrane-associated proteins SAG1 and ISP2 solubilized with mild detergent whereas the cytoskeletal protein IMC1 did not, which demonstrates that our assay works well. In conclusion, the interpretation

of *Toxoplasma* membrane fractionation is complicated by strong association between the cytoskeleton and membrane structure of interest, but our results are consistent with a critical role for Cys3 in membrane association, potentially through palmitoylation (Dubey et al., 2016).

5.3. Discussion

Tyr41 is conserved in GAPDH of most eukaryotes, with the noted exception of a histidine replacement in *Plasmodium* GAPDH. Whether Tyr phosphorylation is physiologically relevant in *Toxoplasma* is questioned by the absence of conventional Tyr kinases from the genome (Peixoto L, 2010), although the *Toxoplasma* phosphoproteome contains Tyr phosphorylation events (Treeck et al., 2011b). This study does not support the hypothesis that cortical translocation of *Toxoplasma* GAPDH1 is due to Tyr41 phosphorylation and interaction with Rab2 to mediate vesicular trafficking along dynein-powered microtubules as inferred from human GAPDH (Tisdale et al., 2004; Tristan et al., 2011). Tyr41 is replaced by phosphorylatable histidine in *Plasmodium* GAPDH and His41 phosphorylation is not detected in the available *Plasmodium* phosphoproteome (Treeck et al., 2011b). Further investigation is required to examine *Toxoplasma* and *Plasmodium* GAPDH phosphorylation and how it relates to Rab2 interaction (Daubenberger et al., 2003). Nonetheless, molecular disruption of Tyr41 in *Toxoplasma* GAPDH1 alters the dynamic S loop and the primary role of glycolysis.

Both IFA fractionation data strongly implicate Cys3 in membrane skeleton association thereby uncovering a novel GAPDH membrane association mechanism besides the two known mechanisms of GAPDH association through Rab2 association or spectrin-actin association (Tisdale et al., 2004; Waingeh et al., 2006). IMC association is mediated by Cys3 residue of GAPDH1. Since translocation of the GAPDH1[C3S] allele is not completely abolished we are not sure whether GAPDH1 is still able to translocate to some extent by association with glycolytic enzyme complex (Aldrich et al., 1992; Campanella et al., 2005a). Additional mechanisms of cortical membrane skeletal

association may include the PSB domain and secondary palmitoylation at Cys249 of GAPDH1, although palmitoylation at this site would prevent catalytic activity since it is incompatible with protein multimerization.

Our attempt to validate the predicted palmitoylation of C3 residue by 17-ODYA labeling was not successful. Though we are able to show that 17-ODYA modifies GAPDH1, the modification is insensitive to hydroxylamine, suggesting there are residues other than the predicted C3 and C249 that may be palmitoylated and likely not mediated through thio-ester modification. Bioinformatics predictions of other lipid modifications using online tools such as GPS lipid and NMT predictor (myristoylation, prenylation, farnesylation) were also done but did not yield any significant hit. Hence, our data reveal a complex modification picture preventing the direct assessment of whether C3S is palmitoylated.

Data from this study also suggest that cortical translocation of GAPDH1 is not essential for parasite viability. It has been shown that after prolonged extracellular gliding stored ATP becomes depleted (MacRae et al., 2012) and it is therefore feasible that local ATP production at the cortex becomes much more critical in such situation. Alternatively, although our data demonstrate balanced expression of endogenous and complemented GAPDH1 alleles, it is possible that the spurious general cytoplasmic localization of GAPDH1 as a result of overexpression is able to overcome specific membrane association, as has been shown for the CDPK3 kinase anchored in the IMC (Garrison et al., 2012). No effect of palmitoylation mutants is observed on GAPDH activity of the parasites. Overall, our data suggest that cortical translocation is decoupled from glycolytic essentiality.

Figure 5.1. Tyrosine phosphorylation in the S loop may be sterically hindered

a) Surface rendering of *Toxoplasma* GAPDH1 tetramer illustrating the interaction of Tyr41 to S-Loop of neighboring subunit. (b) Tyr41 (red) of R subunit forms 3 hydrogen bonds with Gly190 and Ser192 of the S loop in the O subunit. (c) Apicomplexan dipeptide insertion (DI) in the S-Loop may sterically hinder accessibility for kinase and Rab2. (d) The dipeptide exhibits a positive surface charge as determined by surface electrostatic potential analysis where positively charged residue is rendered as blue and negative charged is red. Attachment to membrane by the predicted PSB patch (magenta) may interfere with access to the S loop and catalytic pocket.

Figure 5.1. Tyrosine phosphorylation in the S loop may be sterically hindered
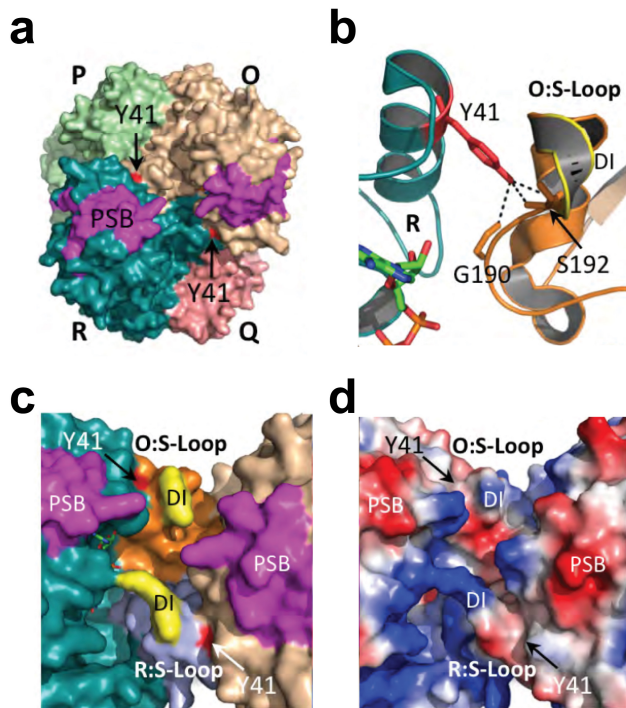
Figure 5.2. Phosphomimic Tyr41 affects parasite lytic cycle

(a) Ten day plaque assay for genetically complemented Y41E and Y41F mutants of GAPDH1cKD. (b) Quantification of plaque size of the mutants was obtained by measuring plaque area of 30 plaques as indicated after 10 days ± ATc. N=3 ± s.e.m. *t*-test **P < 0.02.

Figure 5.2. Phosphomimic Tyr41 affects parasite lytic cycle
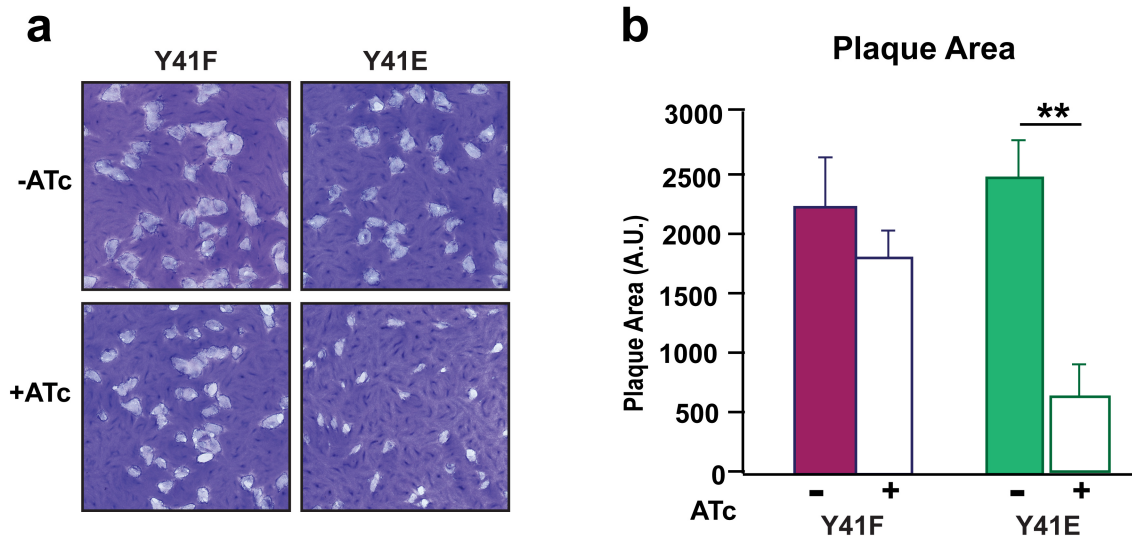
Figure 5.3. Potential tyrosine phosphorylation of the S loop modulates GAPDH activity

(a) GAPDH activity of the phospho-mutants as indicated measured after 60 hours ± ATc. N=3 ± s.e.m. *t*-test, **P < 0.02. (b) Percentage of extracellular parasites displaying cortical GAPDH1 localization of the genetically complemented GAPDH1cKD parasites as indicated was obtained by counting more than 200 parasites. N=3 ± S.D.

Figure 5.3. Potential tyrosine phosphorylation of the S loop modulates GAPDH activity

115
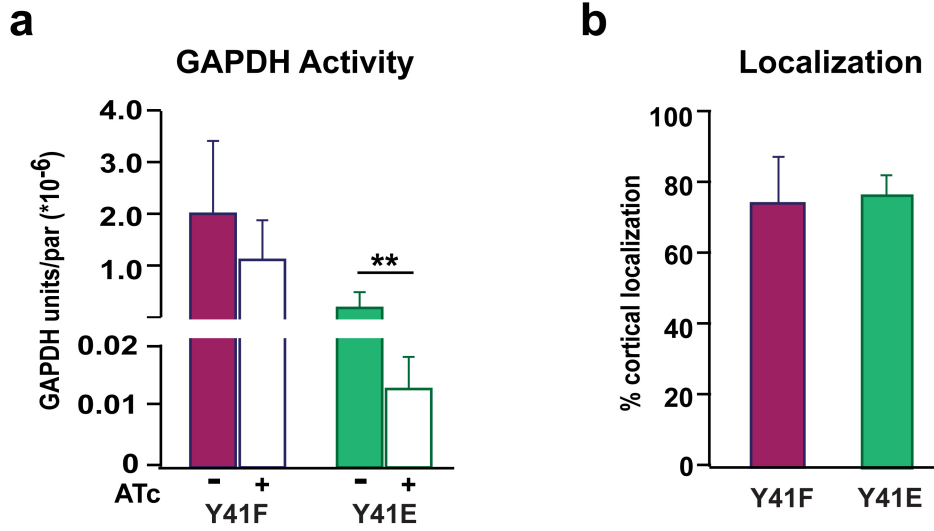
Figure 5.4. GAPDH1 is predicted to be palmitoylated

(a) GAPDH1 sequence alignment of related coccidian parasites with the conserved Cys3 residue highlighted in yellow. (b) Crystallographic structure reveals that the N- and C-termini ends at surface cleft in which the predicted palmitoylation of C3 (red) is surface accessible. This residue is located near the N-terminus of beta-sheet 1. (c) Cys3 is positioned at the edge of the PSB patch. (d) Surface electrostatic potential rendering shows that palmitoylated residue lies in a positive surface patch that may facilitate protein-protein interaction.

Figure 5.4. GAPDH1 is predicted to be palmitoylated
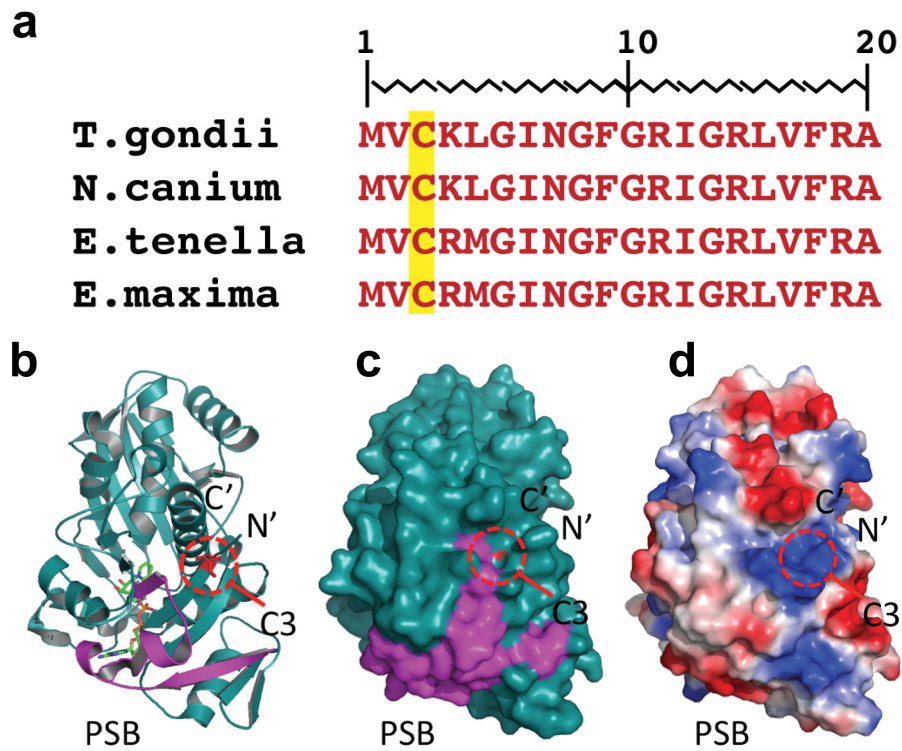
Figure 5.5. 17ODYA labeling to analyze GAPDH1 palmitoylation

Top panel: Rhodamine fluorescence scan of IP optionally followed by hydroxylamine treatment (-/+). Bottom panel: western blot with $\alpha-$myc as a loading control. IP was done as described in the methods section (Dubey et al., 2016) using the following strains parental line Δku80, complemented lines expressing either GAPDH1^{WT} or mutants in the predicted palmitoylation sites, GAPDH1^{C3S} and GAPDH1^{C249S}.

Figure 5.5. 17ODYA labeling to analyze GAPDH1 palmitoylation
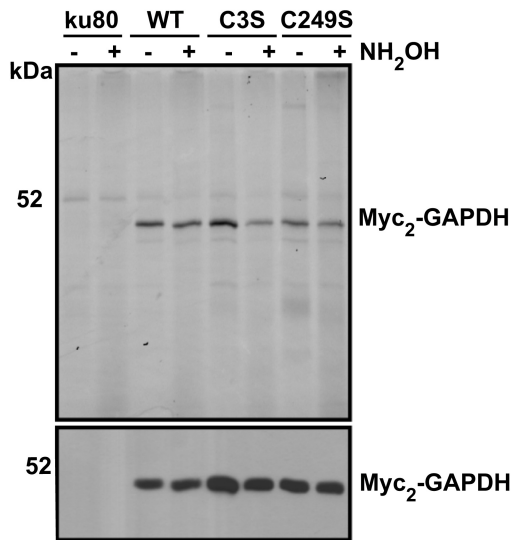
Figure 5.6. The C3S palmitoylation mutant has no effect on viability or activity

(a) Plaque assay of parasites expressing N-terminally-Myc2 tagged GAPDH1^{C3S} variant after 9 days incubation stained with crystal violet. (b) GAPDH activity expressed in GAPDH units in complemented strains after 60 hrs ± ATc. N-terminally-tagged mCherryRFP *Toxoplasma* GAPDH1^{WT} where GAPDH1 translocation is blocked is used as a control for activity assay here.

Figure 5.6. The C3S palmitoylation mutant has no effect on viability or activity
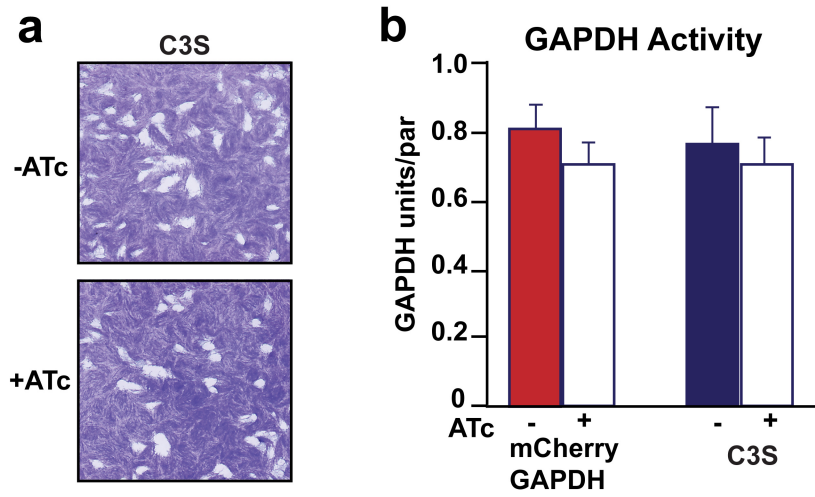
Figure 5.7. GAPDH1 Cys3 is critical for translocation

(a) Cortical translocation of N-terminally Myc2 tagged GAPDH1^{WT} and a GAPDH1^{C3S} variant was quantified by counting more than 200 parasites in the extracellular stage. N=3 ± S.D. *t*-test, ***P < 0.0003. Most representative image probed using α-Myc (green) for GAPDH1^{WT} and mutant GAPDH1^{C3S} corresponding to the bars in the graph is shown below. (b) Flowchart of fractionation and detergent extraction experiment. (c) Western blots of GAPDH1^{WT} and GAPDH1^{C3S} strains after the low speed and high speed spins. The membrane was probed with α-Myc. (d) Detergent extractions of GAPDH1^{WT} and GAPDH1^{C3S} strains using the indicated conditions followed by probing with α-Myc. Samples were probed with the following controls: α-IMC1 (cytoskeleton), α-CDPK1 (cytosolic), α-ACT1 (cytosolic), α-SAG1 (plasma membrane) and α-ISP1 (IMC membrane bound through myristoylation and palmitoylation).

Figure 5.7. GAPDH1 Cys3 is critical for translocation
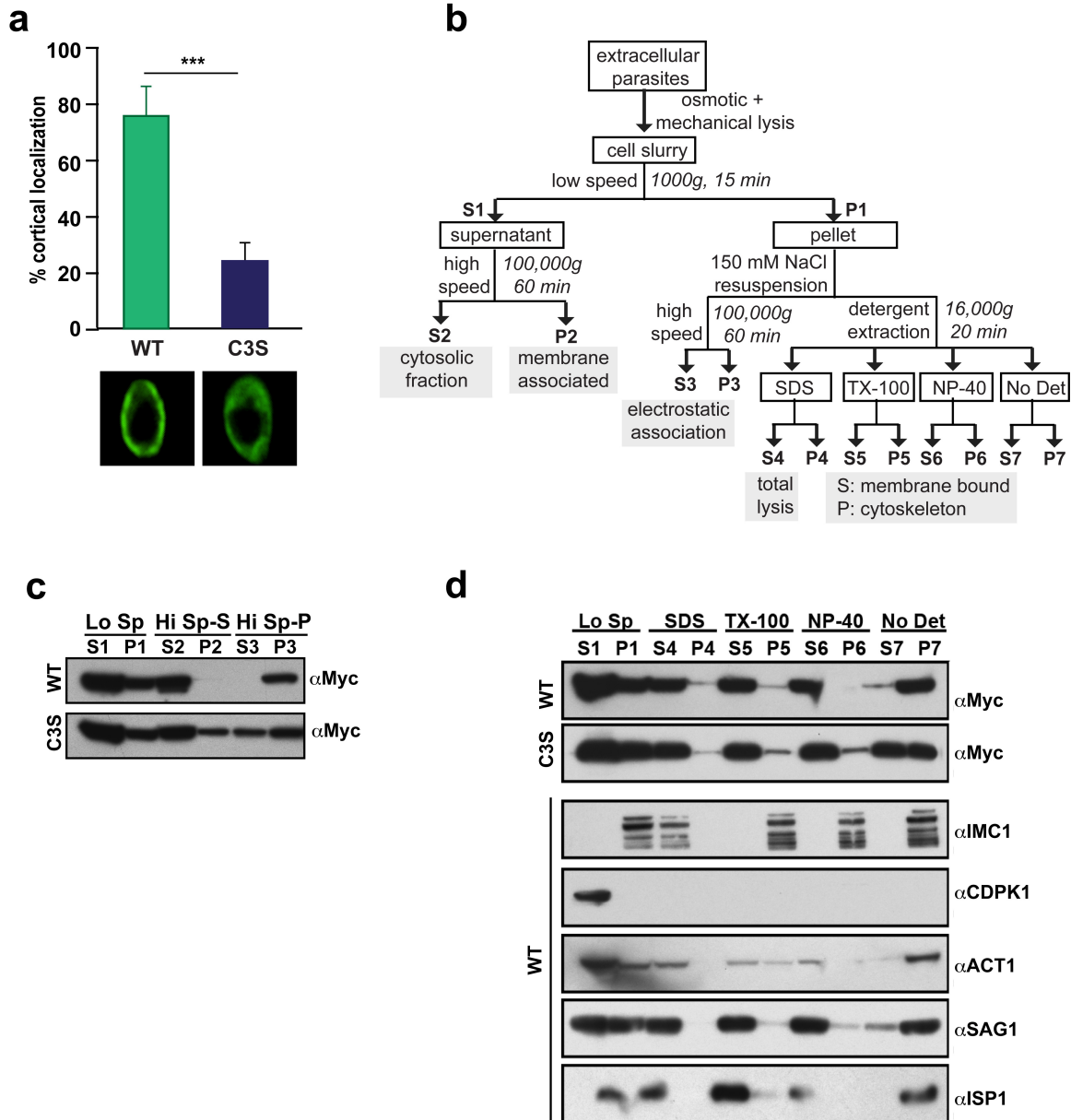
CHAPTER 6: CONCLUSIONS AND FUTURE DIRECTIONS

6.1. Conclusions

Many cortical cytoskeleton building blocks have been identified over the last decade in *Toxoplasma*; however, very few components have been functionally characterized. In the first part of this study, a group of three related intermediate filament-like proteins localizing to the IMC of mature parasites has been studied in detail. I defined the spatio-temporal association of IMC7, 12 and 14 to the cortex of the parasite as occurring in the mid and late G1 phase of the cell cycle. These IMC proteins relocate to the cortex before entering S-phase and distinctly mark the mother cytoskeleton from the forming daughters. Although one of our working models was that this could differentially stabilize mother and daughter cytoskeletons through the final steps of cell division when the mother disassembles, KO studies did not support this model. The alternative model of providing tensile strength to the parasite in the extracellular environment was better supported by the experimental data for IMC7 and IMC14, but not IMC12. Furthermore, we determined that only IMC14 disrupts the synchronous cell division of the parasites but IMC7 and 12 have no effect. This indicates a unique function of IMC14 and may signify a special role in conjunction probably with some other IMC proteins like IMC15, the first cytoskeletal component of budding (Anderson-White et al., 2011) to maintain the timing of budding daughter cells. In absence of IMC14 the parasite begins to enter next nuclear cycle, as the regulated control of the inner and outer core of the centrosome appears to be disrupted leading to a new mitotic cycle before the completion of cytokinesis.

Though we have not established the mechanism of cortical translocation for the IMC proteins, in the case of IMC12 it may be regulated by calcium dependent

phosphorylation in the extracellular stage, as this is the only protein where we observe increasing translocation during increasing time spend outside the host cell. It is also the only protein wherein calcium dependent phosphorylation associated with egress is observed (Nebl et al., 2011). Additionally, phosphoproteome of the peptides enriched from intracellular and extracellular tachyzoites reveal calcium independent phosphorylation sites in IMC7, 12 and 14. These sites may be involved in the translocation of IMC proteins from mid G1 to late G1, but the phosphoproteome data is not resolved through the lytic cycle and does not permit a direct functional association (Treeck et al., 2011a). Only IMC14 is predicted to be palmitoylated but not IMC7 or 12 so this may have some role in IMC14 translocation.

Additionally, our data showed that all three IMC proteins are dispensable for the lytic cycle. It is possible that these proteins are functionally redundant in the parasite and a phenotype, even in differential mother-daughter stability, would only become appreciated upon double or triple gene knockouts. Alternatively, these IMC proteins may be forming oligomers through their conserved alveolin domains and being carried to the cortex in a complex.

Membrane skeletons are commonly found in free living protozoans for maintaining the cell shape and providing mechanical stability, like tetrins in *Tetrahymena* (Brimmer and Weber, 2000)*,* epiplasmins in *Paramecium* (Pomel et al., 2006) and articulins in *euglenoids* (Marrs and Bouck, 1992) *and ciliates* (Huttenlauch et al., 1998)*.* Additionally, it is seen that bacteria like *Caulobacter crescentus* rely on intermediate filament based cytoskeleton for its cell shape. Moreover, in *Plasmodium* IMC proteins function in morphogenesis accompanied by reduced tensile strength of the zoites (Tremp

et al., 2008). However, it is important to note that in *Toxoplasma* the IMC genes expressed is not life cycle specific unlike *Plasmodium* where select alveolin family members are expressed at different life cycle stages such as sporozoite, merozoite, ookinete and gametocytes (Kono et al., 2012; Tremp et al., 2014). So even though the IMC 7, 12 and 14 are not required for the lytic cycle they may have critical roles in merogony, sporogony or gamogony.

The cross disciplinary work spanning parasite molecular biology, biochemistry, cell biology and structural biology in the later part of the thesis gives a comprehensive overview of the role of GAPDH1 in *Toxoplasma* (Dubey et al., 2016). We showed that GAPDH1 is essential for the parasite and that the parasites die within the parasitophorous vacuole between 60 and 84 hours following knockdown of GAPDH1 expression. In addition, we showed that GAPDH1 is not required for invasion or egress (Figure 3.6.) whereas the morphology of parasites without GAPDH1 also did not change (Figure 3.5. c). We concluded that GAPDH1 is required for intracellular growth.

We were able to rescue the viability of the parasite by complementing the GAPDH1cKD with wild type GAPDH1 fused to either a small or large tag. Large tags block the phenomenon of relocation of GAPDH1 from the cytosol to the cortex upon parasite egress but not the complementation capacity indicating that translocation of this glycolytic enzyme is dispensable for the parasite. It could however also be that the overexpression of these constructs can complement the phenotype and support viability likely by also increasing the cortical presence of GAPDH1 as shown for CDPK3 (Garrison et al., 2012). Support for this latter model comes from the high GAPDH activity measured in the complemented strains relative to the wild type line, despite a

fairly balanced protein expression level. We attempted to correct this imbalance by targeting GAPDH1 as a single copy in the UPRT locus or by genetic complementation under the endogenous promoter rather than the strong α-tubulin promoter, but these experiments yielded similar results. Alternatively, it is possible that the tag might drive high enzymatic activity, but we did not make an effort to complement the cKD line with an untagged allele, as we would not be able to distinguish endogenous GAPDH1 from complementing GAPDH1 protein.

The catalytic activity of GAPDH1 is controlled by the conserved active site residue C152. Mutating this residue completely blocks GAPDH activity in the parasite and also disrupts ATP production. This mutant relocates to the cortex but is unable to restore the viability of the cKD line. Additional experiments to rescue viability of the active site mutants with glutamine supplementation (Shen and Sibley, 2014) restored growth to about 50%. In parasites without ALD1, an accumulation of toxic levels of fructose-1-phosphate in presence of glucose was reported that caused parasite death. This effect was alleviated when the parasites were able to salvage energy from glutamine (Shen and Sibley, 2014). We on the other hand did not observe a disruption in replication in presence of glucose, indicating that no accumulation of toxic metabolite occurs, which further indicates that glucose is preferred over L-glutamine as carbon and energy source for the parasite (Figure. 3.11. a-b).

The mechanism of glycolytic enzyme translocation in extracellular parasites was unknown (Pomel et al., 2008). The data presented in this thesis established that translocation is conferred most likely by N-terminal palmitoylation of GAPDH1. We observed that GAPDH1 is palmitoylated and that at least some mode of the modifications

detected by 17-ODYA are not hydroxylamine sensitive. This prevents a direct conclusion toward the palmitoylation of Cys3/Cys249. Using the crystal structure information of TgGAPDH1 and our mutagenesis experiments we know that Cys3 residue is an important residue governing GAPDH1 association with the cortical membrane skeleton of parasite. Our palmitoylation mutants showed significant reduction in translocation as verified by both IFA and fractionation experiments. It is important to note that ALD1 and LDH1 are also predicted to be palmitoylated at several cysteine residues indicating that there may be a common mechanism for translocation of these glycolytic enzymes.

Our data showed that Tyr41 phosphorylation mediating Rab2-dependent cortical translocation as suggested in *Plasmodium* (Daubenberger et al., 2003) does not contribute to GAPDH1 translocation in *Toxoplasma*. Moreover, the timing is different as PfGAPDH1 translocates during the intracellular replication cycle. Since PfGAPGH1 does not contain a Cys at position 3 and has no IMC during schizogony, it is therefore conceivable that both the function and mechanism of cortical translocation is different between *Plasmodium* and *Toxoplasma* GAPDH1.

Our data combined with our knowledge about the TgGAPDH1 structure and phosphoproteome of *Toxoplasma* identified a distinct role for post-translational phosphorylation of the GAPDH1 S-loop. The phosphorylation of the Ser50 residue at the dimer interface of the GAPDH1 offers a novel mechanism of allosteric regulation of protein assembly indicated by their inability to support growth not previously reported. Additionally, another unique residue S203 in the parasite is positioned in the S-loop and is involved in enzyme catalysis. Moreover, Y41 mimics in the S-loop also resulted in a significant reduction in activity. This further underscores the essentiality of the S-loop in

activity, even though this modification may not be physiologically relevant due to the absence of tyrosine kinases in *Toxoplasma* (Peixoto L, 2010). This is the first report of S-loop phosphorylation regulating catalytic function of GAPDH, which may be more universally conserved as Ser50 is conserved across GAPDH evolution.

GAPDH1 is likely to be essential *in vivo* because human serum has high level of glucose that would block the growth of GAPDH1 depleted parasite and also the non-enzymatic roles of GAPDH1 cannot be fulfilled by glutamine supplementation. Our data therefore suggests that GAPDH1 can be a good drug target by directly targeting GAPDH1 activity. Moreover, to our best knowledge regulation of activity by S-loop phosphorylation is absent from the mammalian host; hence drugs targeting the *Toxoplasma* kinase(s) responsible for S-loop phosphorylation might provide specific new drugs. Also, TgGAPDH1 along with its apicomplexan members have a unique dipeptide insertion in the S-loop that constricts the opening of NAD^+ cavity compared to human GAPDH (Satchell et al., 2005). Inhibitors can be designed to target this bulge of the S-loop and hence activity. Such drug leads are also very relevant for other apicomplexan parasites, including the major childhood diarrhea-causing *Cryptosporidium* and the malaria-causing *Plasmodium spp.* for which very limited effective drug options are available.

In summary, the work presented in this thesis shows uncoupling of GAPDH1 functions at both the biological and mechanistic level: glycolysis is essential for replication and mediated by the buried core center and is regulated by the S-loop phosphorylation whereas cortical membrane association occurs in extracellular parasites and is facilitated by palmitoylation at the surface exposed N-terminus.

6.2. Future Directions

To completely understand the functional role of IMC protein cortical association after complete division we need to generate multiple gene knockout lines. With the advent of CRISPR, this is not a very challenging task and we can create a series of double or even triple knockout lines of IMC7, 12 and 14 together to resolve the functional redundancy in the parasite, if any. IMC7 and IMC14 are both involved in maintaining the tensile strength of the parasite. Since we have a conditional knockdown line of IMC7, we can create a direct KO line of IMC14 in that background and decipher if the absence of these proteins incurs severe defects on the lytic cycle of the parasite or whether the tensile strength is more essential in other stages of life cycle. Since IMC7 and IMC12 expression peaks at mid G1 stage, it is possible these are functionally redundant for asexual replication of the parasite. We can further attempt to create a triple knockout of all these proteins since they are exclusively associated with the mother cytoskeleton or use a conditional knock out system using the cre-lox system in case the complete knockout is essential. There is also a possibility that these proteins are not essential in the lytic cycle of the parasite and we will have to further probe their role in merogony, gametogony or sporogony. Since we have already established that these IMC proteins relocate from the cytosol to the cortex completely by late G1 stage and are maintained to the cortex in the extracellular stage, it will be interesting to establish the mechanism of the translocation of IMC proteins. IMC14 is predicted to be palmitoyalted like GAPDH1 where translocation is guided by palmitoylation at the N-terminus. However, IMC12 is known to be phosphorylated both in calcium dependent and independent manner by yet unidentified protein kinases (Nebl et al., 2011; Treeck et al., 2011b) so we can hypothesize that this

phosphorylation may play a critical role in the process. Our initial attempts to complement the IMC12 dKO line with calcium dependent phosphomutants were not successful due to low transfection efficiency making interpretation of data difficult and inconclusive. Generation of clonal lines and quantifying the phosphonull and phosphomimic lines for translocation phenotype can establish if the mechanism is indeed based on this modification. However, it may be that there is a dominant negative effect due to which we were not able to get any stable lines. This can be overcome by conditionally expressing the mutants in the knockout line. Additionally, it could also be possible that IMC12 helps to relocate IMC7 and IMC14 to the cortex by forming a complex.

GAPDH is ubiquitous and is increasingly known for its role in multiple pathways including membrane fusion, microtubule bundling, phosphotransferase activity, nuclear RNA export, DNA replication and DNA repair (Du et al., 2007; Kim et al., 1999; Sirover, 1999), in addition to glycolysis. It will be interesting to establish other moonlighting roles of GAPDH1 in the parasite. GAPDH controls apoptosis in vertebrates via lysine acetylation (Hara et al., 2005; Sen et al., 2008) however; we were not able to detect this phenomenon in *Toxoplasma* upon lysine mutation (Dubey et al., 2016).

It is possible that one of these glycolytic enzymes directly interacts with the cortex and others are bound via them to the membrane. We did observe electrostatic interactions in our fractionation experiments (Figure 5.7, section 5.2.3) indicating protein-protein interaction. The glycolytic enzymes complex would require labile cofactors or depend on low affinity interactions and such physical association of these enzymes would allow for true substrate channeling and hence efficient ATP production

(Pomel et al., 2008). So we can ascertain if this close association of the glycolytic enzyme to the pellicle of the parasite can markedly improve the overall efficiency of local ATP production. GAPDH1 is present on the cytosolic phase of IMC which is probably tethered to the IMC via the glideosome associated proteins GAP40, GAP45 and GAP50 embedded in the opposing membrane by palmitoylation and myristoylation. Missing in this model however, is a channel through the IMC permitting the transport of ATP but the GAPM proteins might be candidates for this function (Bullen et al., 2009). Since the parasites do not require carbon uptake in the first hour of its extracellular life so doing a time point study of extracellular incubation followed by invasion assay could establish if relocation occurs essentially for efficient generation of energy at the site of requirement. Additionally, it will be interesting to explore if GAPDH1 may have a novel moonlighting function in providing resistance to the parasite under osmotic stress like the IMC proteins that are involved in maintaining tensile strength of the extracellular parasite.

From a drug development perspective, identifying the kinases phosphorylating the S-loop should be a priority toward the designing of specific inhibitors whereas other inhibitors might be designed targeting the constricted NAD^+ pocket of enzyme due to dipeptide insertion.

CHAPTER 7: MATERIAL AND METHODS

7.1. Parasites

RH, RHΔku80 (Huynh and Carruthers, 2009) and TATiΔku80 (Sheiner et al., 2011) parasites and their transgenic derivatives were used in this study. All strains were maintained in human foreskin fibroblasts (HFF) as previously described (Roos et al., 1994). All parasites were grown at 37°C and 5% CO_2 except the temperature sensitive mutant FV-P6 which was cultured at 35°C permissive temperature or 40°C restrictive conditions. Stable parasite lines expressing transgenes were selected under 20 μM chloramphenicol or 1 μM pyrimethamine based on the resistance marker and cloned by limiting dilution.

Specifically, IMC7 (conditional knockdown) cKD, IMC12 and IMC14 direct knockout (dKO) and GAPDH1 (cKD) were generated by double homologous recombination under pyrimethamine selection for the purpose of this study. Other parasite lines stably expressing complementing transgenes or GAPDH mutations were selected in presence of chloramphenicol. The cKD lines were induced at a concentration of 1.0 μg/ml anhydrous tetracycline (ATc) for the times specified.

7.2. Plasmids

All primer sequences can be accessed in the Table 6.1. The plasmid p*tub-myc2-GAPDH1/sagCAT,* p*tub-YFP-GAPDH1/sagCAT* and p*tub-mCherry-GAPDH1/sagCAT* were generated by amplifying the GAPDH1 coding sequence using primers #1 and #2 (GAPDH primers section). The insert, digested with AvrII/EcoRV, was cloned into the p*tub-YFP$_2$ (MCS)/sagCAT* plasmid (Anderson-White et al., 2011).

Three-way Gateway cloning (Invitrogen) was employed to generate the IMC7 and GAPDH1 conditional knockdown vector; basically following published protocols (Farrell and Gubbels, 2014). Specifically, the RH genomic DNA was used as a template to amplify the region upstream of the promoter region and beginning of the start codon of the two genes of interest (goi). The entry clone plasmid p*DONR221-goi-R1/R4* was generated by amplifying approximately 1 kb upstream of the promoter region (1.5 kb upstream of start codon) into the p*DONR221 P1/P4* plasmid. The entry clone plasmid p*DONR221-goi-R3/R2* was generated by amplifying a region upstream of the promoter region of the gene and cloned into the p*DONR221 P3/P2* plasmid. The conditional knockout vector p*TgKO2-DHFR-T7S4-goi* was generated by combining the p*TgKO2*, *pDONR221-5'goi-R1/R4, pDONR221-DHFR-T7S4 R4/R3* and p*DONR221-goi R3/R2* plasmid in an LR reaction. The plasmid p*TgKO2-DHFR-T7S4-GAPDH1* was linearized with unique restriction enzyme AflII and p*TgKO2-DHFR-T7S4-IMC7* with ApaI prior to transfection into the TATiΔku80 strain. The stable lines were generated by pyrimethamine selection.

The plasmids *5-pU6-IMC12* and *3-pU6-IMC12* to generate IMC12dKO line and the plasmids *5-pU6-IMC14* and *3-pU6-IMC14* to generate the IMC14dKO line were generated using previously published method. Specifically, sense and antisense protospacers were annealed by boiling them at 98°C for 5 mins in a beaker and slowly cooling by placing the beaker on ice for 2 hrs. The pU6-Sag1 vector was digested with BsaI, dephosphorylated and purified. The purified vector and annealed protospacers are ligated to generate the *pU6-goi*. Sanger sequencing using the primer U6_sequence-F is

then used to verify the sequence of the protospacers in the purified plasmid. For the generation of the IMC12dKO strain the Δku80 line was transfected to with the 20 μg of *5-pU6-IMC12* and *3-pU6-IMC12* plasmid pair alongwith 40 μg of the PCR product of DHFR locus (amplified from the p*DHFR-teto7SAG4* vector) with homologous flanks to IMC12 using the primer pair #8/9 mentioned in Table 6.1 (IMC primers list). Similarly, to generate the IMC14dKO line 20 μg of *5-pU6-IMC14* and *3-pU6-IMC14* and 40 μg PCR product of DHFR locus with homologous flanks to IMC14 (#19/20 primer pairs) were transfected into the Δku80 parasite strain.

Megaprimer mutagenesis was used to generate point mutations in IMC12 and GAPDH1 as described (Gubbels et al., 2006). PCR products were TOPO-cloned, sequence-validated by Sanger sequencing, and ligated into the p*tub-YFP-IMC12/CAT* or p*tub-myc2-GAPDH/CAT* backbone to generate the YFP-IMC12 phosphomutants or the myc2 tagged mutant GAPDH1 plasmid with desired mutation using the primers mentioned in Table 6.1. 50 μg of plasmid was transfected in the IMC12dKO or the GAPDH1cKD strain to generate the mutant lines under chloramphenicol selection.

7.3. PCR verification of parasite genotypes and homologous recombination

All primers used for verification of the integration of the mentioned plasmids in the parasite genome are listed in Table 6.1 split between IMCs and GAPDH1 group of primers. Proper insertion of the T7S4 replacing the gapdh1 promoter was done using the primer pairs 9/10 and 11/12, while the re-insertion was verified by 13/12 (from the

GAPDH primer list). Similarly, using the IMC primer list, the replacement of the imc7 promoter was done using primer pairs 1/2 and 3/4. The replacement of native promoter was tested using the primer pairs 5/12 and 13/6. To test the replacement of the complete locus of IMC12 gene by DHFR selectable marker 10/12 and 13/14 primer pairs were used. Additionally, the reinsertion of the genomic IMC12 was tested using the primer pair 15/16. Similarly, IMC14dKO line was tested for the replacement of the genomic locus with DHFR using pairs 21/12 and 13/22 while the primer pair 23/24 verified the absence of reinsertion. The GAPDH mutations in parasites clones expressing mutant GAPDH1 alleles were validated by PCR amplification of the cMyc-tagged allele and Sanger sequencing.

7.4. Immunofluorescence

Immunofluorescence assays were performed as previously described (Gubbels et al., 2006). Parasite strains of choice were inoculated in six-well plates containing coverslips with HFF cells and fixed with 100% methanol and blocked in 1% BSA in PBS. Alternatively, extracellular parasites were adhered on coverslips coated with poly-Lysine for 1 hr at 37°C. The following primary antibodies were used: rat α-IMC3 (Anderson-White et al., 2011) (1:2000), rat α-IMC7(Anderson-White et al., 2011) (1:2000), mouse MAb 45:36 α-IMC1 (1:1000; kindly provided by Gary Ward, University of Vermont), α-Myc (9E10) conjugated with A488 (1:100; Cell Signaling) and rabbit α-human centrin (1:1000; kindly provided by Iain Cheeseman, Whitehead Institute). Alexa fluorophores A488 and A594 (Invitrogen) conjugated to goat-α-rat, goat-α-rabbit, and goat-α-mouse

secondary antibodies were used (1:400). Nuclear material was co-stained with DAPI (2 µg/ml).

7.5. Fluorescence microscopy

For IFA and live cell microscopy a Zeiss Axiovert 200 M wide-field fluorescence microscope equipped with a α-Plan-Fluar 100X/1.45 NA oil objective and a Hamamatsu C4742-95 CCD camera was used to collect images, which were deconvolved and adjusted for phase-contrast using Volocity software (Improvision/Perkin Elmer). To capture images for the invasion assay an EVOS FS Cell Imaging System (Life Technologies) was used.

7.6. Plaque assay

Six-well plates confluent with HFF cells were inoculated with 50 freshly lysed parasite lines and incubated for 8-10 days ± ATc. Monolayers were fixed with 100% ethanol for 10 min, washed with PBS and stained with crystal violet (Farrell and Gubbels, 2014). Plaques were counted and plaque area quantified using Fiji (Schindelin et al., 2012).

7.7. Osmotic shock assay

Freshly lysed dKO, cKD or parental lines were treated with hypotonic buffer (HBSS diluted to 0.5X or 0.25X in sterile water) as previously described (Harding et al., 2016). Specifically, the strains were filtered and spun at 1000g for 15 min followed by 1X PBS wash before subjecting them to osmotic shock for 5 min. 0.2% saponin was done as a positive control and 1M sorbitol treatment was done to maintain cell rigidity and

represent hypertonic stress condition. Post treatment the cells were stained with 1:200 dil of 488 conjugated Sag1 for 30 min on ice in dark. 1X PBS was done and stained parasites were spun at 1000g for 15 min at room temperature. The pelleted cells were resuspended in 1 mg/ml Propidium iodide (PI) for 10 min on ice. Unstained parasites were used as a control and FITC and PI positive cells were scanned by Flow cytometer.

7.8. Growth assay

Parasitic growth curve based on cytoplasmically expressed YFP-YFP in TATiΔku80 and GAPDH1cKD was recorded basically as described previously (Gubbels et al., 2003) by reading their relative fluorescence every 24 hrs using Molecular Dynamics M5 plate reader at 510 nm excitation and 540 nm emission wavelength using a 530 nm cut off. Stable cytoplasmic YFP-YFP overexpressing GAPDH1cKD lines were selected by two rounds of FACS and cloned by limiting dilution. Three independent experiments were done in triplicate using 5000-parasites/well ± ATc.

7.9. Replication assay

Parasite division in HFF infected with 1.8×10^5 par/well inoculated in a 6 well plate was measured in regular medium ± ATc via IFA using α-IMC3 and α-human centrin as development markers (Szatanek et al., 2012). More than 100 vacuoles per sample were counted in three independent experiments and expressed as average number of parasite/vacuole. Similarly, for assessing division in glutamine supplementation media (MacRae et al., 2012), HFF monolayer was infected with parasites, after washing with DMEM without glucose or glutamine (MacRae et al., 2012) and incubating for 2 hrs in

same media, to make them glucose starved. Also the parasites prior to infection were depleted of residual glucose. The ATc pretreated parasites were washed in DMEM without glucose containing 6 mM L-glutamine (MacRae et al., 2012) (or DMEM without glutamine containing 4.5 g/L glucose as control) and incubated at 37°C for 2 hrs. 1.8×10^5 parasites per well were inoculated in a 6 well plate with the corresponding media ± ATc. Following 24 hrs of incubation, monolayers were fixed with 100% methanol and subjected to IFA using rat α-IMC3 and rabbit α-human centrin antibodies. More than 100 vacuoles were counted in each experiment and values were expressed as cell division.

7.10. Invasion assay

The 'Red-Green-Assay' was done as described previously (Garrison et al., 2012). Briefly, 2.5×10^5 parasites were allowed to invade in HH/FBS (Hank's balanced salt solution, 1 mM Hepes pH 7.0, 1% FBS) medium ± ATc in black well optical bottom 96 well plate in triplicate at 37°C for 1 hr. A488 conjugated mouse α-SAG1/P30 T41E5 (kind gift from J.F. Dubremetz, University of Montpellier) was used to stain all the parasites and post 16% formaldehyde, 8% glutaraldehyde fixation and 0.25% Triton X-100 permeabilization, A594 conjugated mouse α-SAG1/P30 T41E5 was used to stain all extracellular parasites. Three images per well were recorded using EVOS FS Cell Imaging System (Life Technologies) and more than 100 parasites were counted to determine percentage of invaded parasites using Fiji software (Schindelin et al., 2012). Parasites were treated with 1 μM Cytochalasin D for 15 min as positive control for the assay.

7.11. Egress assay

Parasite egress from host cells was assayed as described previously (Garrison et al., 2012). Essentially, 6 well plate-containing coverslips confluent with HFF cells were infected with 6×10^6 parasites ± ATc. 30-34 hrs post-inoculation, 2 μM of A23187 or DMSO vehicle control was used to trigger egress for 5 min at 37°C. Methanol fixation followed by Hemacolor (EMD Chemicals) staining was done as per manufacturer's instructions and over 15 fields were counted for intact vacuoles in each set.

7.12. SDS PAGE and Western blot

Western blot was performed as previously described (Gubbels et al., 2006). Lysate from 5×10^6 parasites was loaded in 12% Bis-Tris gel (Invitrogen), transferred to PVDF membrane (Bio-rad), blocked in 5% milk in 1X PBS + 0.1% Tween40 (PBS-T) and probed with one of the following primary antibodies, rabbit α-human GAPDH antibody conjugated with horse radish peroxidase (HRP) (TGR BioSciences), α-cMyc (9E10) conjugated with HRP (Santa Cruz Biotechnologies), α-IMC7, α-IMC1, α-CDPK1 (1:1000), α-SAG1 (1:1000), α-ACT1 (1:2000) or α-ISP1 (1:1000). Following 1 hr incubation the membrane was washed 3 times with PBS-T for 10 min and probed with corresponding secondary antibody for 1 hr. Washing steps were repeated with PBS-T and once with PBS for 5 min. Signals were detected using chemiluminescent HRP substrate (Millipore) and exposed to X-ray film. To reprobe the membrane with a different antibody, stripping was done after washing with 1X PBS twice for 10 min each. Specifically, the blot was incubated with stripping buffer (62.5 mM Tris-HCl pH 6.7, 2% SDS, 100 mM β-mercaptoethanol) for 30 min at 50°C and washed thrice with 1X PBS.

The blot was blocked again in 5% milk overnight before probing it with the next primary antibody.

7.13. Monolayer lysis assay

To monitor parasite growth in glutamine-supplemented media (see section above), monolayer lysis was done as described earlier (Shen and Sibley, 2014). Essentially, parasite and HFF monolayer were starved in absence of glucose (of L-glutamine as control) for 2 hrs before inoculation as described in the above section. Subsequently, confluent HFF cells in 96 well plates were inoculated with parasite dilutions in triplicate and allowed to grow for 48 hrs under the indicated conditions. Lysis was assessed by crystal violet staining and measuring absorbance at 570 nm using Molecular Dynamics M5 plate reader by well scanning.

7.14. ATP measurement

ATP concentration was determined using the CellTiter-Glo Luminescent Cell Viability Assay (Promega; Madison, WI) according to manufacturer's protocol. In general, intracellular parasites grown 60 hrs ± ATc, were filtered, centrifuged and resuspended in dye free DMEM supplemented with 1% Fetal Bovine serum, 10 U/ml penicillin, 100 μg/ml streptomycin and 1mM glutamine medium to 10^7 parasites/ml. 100 μL parasites were added to a 96 well plate and equilibrated at room temperature for 30 min An equal volume of CellTiter-Glo reagent was added and the plate was shaken for 5 min to allow cell lysis. An M5 plate reader (Molecular Dynamics) was used to record luminescence at

500 ms integration speed after 10 min. ATP (disodium salt) was used to generate the standard curve.

7.15. GAPDH activity assay

GAPDH activity in parasite lines grown ± ATc (60 hrs) was measured by the colorimetric based assay from ScienceCell Research Laboratories as described in the manufacturer's protocol. Basically, GAPDH activity was measured in parasite lysate by assaying the rate of NADH oxidation, which is proportional to the reduction in absorbance at 340 nm over time ($\Delta A_{340\ nm}$/min). In the presence of 3- phosphoglyceric acid (3-PGA), adenosine 5'-triphosphate (ATP) and GAPDH, the oxidation of β-NADH to β-NAD occurs. Specifically, parasite lysate was prepared by syringe-lysis, filtration through a 3 μm polycarbonate filter and centrifugation at 1000g for 15 min. The parasite pellet was washed twice with PBS. The parasite pellet was treated with ice-cold lysis buffer for 20 min at 4°C with gentle agitation. The lysate was centrifuged at 14000 rpm for 5 min and supernatant was carefully collected and stored at -80°C until detection of activity. Cell assay buffer was prepared and initial absorbance was measured using a Molecular Dynamics M5 plate reader. After addition of cell lysate supernatant or GAPDH standard the absorbance was measured over time. The rate of decrease in absorbance was calculated to determine the standard curve and derive the GAPDH activity in the sample, Parasites carrying different GAPDH1 alleles were diluted to the point wherein the activity measured within the dynamic range of the assay and activity was normalized to internal control of the parental and wild type complemented line present in each assay.

Additionally, another kit designed for crude serum and tissue samples (GAPDH Assay kit Cat # E-101) was tested before we used the above-described colorimetric assay for cell lysates. The absorption was measured at 492 nm due to the reduction in NADH was measured by the coupled reaction with the tetrazolium salt. The sensitivity of the assay for the parasite lysate was low and did not detect the range of activity for different GAPDH mutants in the parasite.

7.16. Fractionation assay

7.16.1. *Differential centrifugation*: Fractionation by differential centrifugation was adapted from a previously described method (Taha et al., 2014). To fractionate the membrane bound vs. cytosolic proteins, parasite pellet ($1x10^8$) was cooled in liquid nitrogen for 5 min and then thawed at 37°C before resuspending in hypotonic buffer (10 mM Tris pH 7.8 and 5 mM NaCl). The resuspended pellet was mechanically lysed using 40 strokes of a douncer and centrifuged at low speed (1000g) for 15 min at room temperature in Eppendorf centrifuge 5417C using rotor FA45-30-11. The supernatant was carefully separated (Lo Sp-S1) and the pellet was resuspended in equal volume of resuspension buffer (100 mM Tris pH 7.8 and 150 mM NaCl). A protease inhibitor cocktail (Sigma) was added in a 1:100 ratio and loaded as Lo Sp-P1. The resuspended pellet was equally divided in 5 parts and either centrifuged at 4°C at 100,000g for 60 min in Beckman optima TLX ultracentrifuge (Hi Sp-P) or extracted by detergent as described below. Equivalent volume of the low speed supernatant was also centrifuged at high speed for 60 min (Hi Sp-S).

7.16.2. *Detergent extraction*: Detergent extractions were performed essentially as described previously (Gubbels et al., 2006). The low spin pellet fraction was treated with 1% SDS, 1% TX-100, 0.5% NP-40 or no detergent as control in resuspension buffer. SDS extraction was performed for 10 min at 98°C and then the samples were spun at room temperature for 20 min at 13,000 rpm. All other extractions were performed on ice for 45 min and then spun at 4°C for 20 min at 13,000 rpm. Supernatants were removed as the soluble fraction and the pellets were resuspended in a volume of resuspension buffer equivalent to the supernatant. Following extractions, the pellet and supernatant fractions were separated and western blot was performed as described above.

Table 7.1. PCR Primers and protospacers All protospacers used in the study are phosphorylated at 5' end. In the oligonucleotides, the restriction enzyme sites are italicized and underlined, Att-recombination sites are underlined and mutagenesis sites are represented in bold font.

_____

#	Protospacers name	Sequence

_____

1. 5-IMC12dKO-s   /5Phos/AAGTT GTACTTCGCTCTGTGAATTTGG
2. 5-IMC12dKO-as   /5Phos/AAAAC CAAATTCACAGAGCGAAGTACA
3. 3-IMC12dKO-s   /5Phos/AAGTT GCGTCGACTCCATGCCCCAGTG
4. 3-IMC12dKO-as   /5Phos/AAAAC ACTGGGGCATGGAGTCGACGCA
5. 5-IMC14dKO-s   /5Phos/AAGTT GtaccaatagtggacacgATGG
6. 5-IMC14dKO-as   /5Phos/AAAAC CATcgtgtccactattggtaCA
7. 3-IMC14dKO-s   /5Phos/AAGTT GAGTCCGCAGTCTCGTGAATTG
8. 3-IMC14dKO-as   /5Phos/AAAAC AATTCACGAGACTGCGGACTCA

_____

#	IMCs Primer name	Sequence

_____

1. 5'IMC7-F-B1   GGGG<u>ACAAGTTTGTACAAAAAAGCAGGCT</u>GCGTCCAGTTCACAGCTCCCAACAC
2. 5'IMC7-F-B4   GGGG<u>ACAACTTTGTATAGAAAAGTTGGGT</u>GGCACTGGCAGAACGGCGTCTG
3. 3'IMC7-F-B3   GGGG<u>ACAACTTTGTATAATAAAGTTG</u>cgATGGGAGTTCACTGCTGACAACGTAC
4. 3'IMC7-R-B2   GGGG<u>ACCACTTTGTACAAGAAAGCTGGGT</u>ACGCGATCGTGAATGGTCGGAC
5. 5'IMC7ver-F   GAACGACCAGACATCCGATGTTCT
6. 3'IMC7ver-R   CGTGTACACCAAGTCCAAGGGC
7. 5'U6_sequence-F   ctcgtagagaacaagcactcg
8. 5'IMC12-DHFR-F   cactcctttatttgggaaaccaccttgtctttgctCACGAAACCTTGCATTCAAAC
9. 3'IMC12-DHFR-R   ctggtccacacttcccctctacggaaaagcggttcATCCTGCAAGTGCATAGAAGG
10. 5'IMC12ver-F   cagGTTTAAACCACCAACAAATCCAACAACTTCCG
11. 3'IMC12ver-R   GGGGACCACTTTGTACAAGAAAGCTGGGTAGCTGTCTGATTCGGTTGGACTTC
12. 3'DHFR-CXR   ACTGCGAACAGCAGCAAGATCG
13. 5'DHFR-ver-F   CACACAGTCTCACCTCGCCT
14. 3'IMC12ver-N-R   cgtactacagcgtgttcacg
15. IMC12dko-int-ver-F   GGGGACAAGTTTGTACAAAAAAGCAGGCTGCCAGCATGCTGGCGGTACCCAAC
16. IMC12dko-int-ver-R   GGGGACAACTTTGTATAGAAAGTTGGGTGCGCACAACCGGTGAACAGAATAC
17. IMC12-S249A-S250A-R CTCGCTCACGCGAGAGAAAACCCGCGGTG**CCGC**GGCGAGAGAGCCCACTGCCGCCTC
18. IMC12-S249E-S250E-R CTCGCTCACGCGAGAGAAAACCCGCGG**CTCCTC**GGCGAGAGAGCCCACTGCCGCCTC
19. 5'IMC14-DHFR-F   cttgtgtttcgtgtggaccggaaggaaatcCACGAAACCTTGCATTCAAACC
20. 3'IMC14-DHFR-R   catacggcatctgtatttgaacatactcgcctgcATCCTGCAAGTGCATAGAAGG
21. 5'IMC14ver-F   cagGTTTAAACTCGCATGCTGAGGAACCAACC
22. 3'IMC14ver-R   cgccgctatattaagccttgc
23. IMC14dko-int-ver-F   gtgactgggcgatgagcg
24. IMC14dko-int-ver-R   CGGGACATCACGGTACTTATACTC

_____

#	GAPDH1 Primer name	Sequence

_____

1. GAPDH1-F-Avr   cag<u>*CCTAGG*</u>ATGGTGTGCAAGCTGGG
2. GAPDH1-R-RV   cag<u>*GATATC*</u>TTACGCGCCGTCCTGGACG
3. GAPDH1F-BglII   cag<u>*AGATCT*</u>aaaATGGTGTGCAAGCTGGG
4. GAPDH1-R-AvrII   cag<u>*CCTAGG*</u>CGCGCCGTCCTGGACGG
5. GAPDH1-F-B1   GGGG<u>ACAAGTTTGTACAAAAAAGCAGGCT</u>gcGCGATACAACGGATCACTGTCG
6. GAPDH1-R-B4   GGGG<u>ACAACTTTGTATAGAAAAGTTGGGT</u>GGTCGTGTAACTGCGTCCCGC
7. GAPDH1-F-B3   GGGG<u>ACAACTTTGTATAATAAAGTTG</u>aaATGGTGTGCAAGCTGGGTATTAACG
8. GAPDH1-R-B2   GGGG<u>ACCACTTTGTACAAGAAAGCTGGGT</u>AGTAGTGGCCGTGGACCGAG
9. 5-GAPDH1-ver-F   GTACCGTGAACGGTAGACCTC

```
10. 5-DHFR-CXR         ACTGCGAACAGCAGCAAGATCG
11. 3-DHFR-CVI-F1      GTGCTGGACTGTTGCTGTCTGC
12. 3-GAPDH1-ver-R     CGTTGGTCAAGTGAGCCTGAG
13. GAPDH1-pro-ver     GAGGTGGGAGTTGGTATAGTCAATC
14. GAPDH1-C152G-F     GATGTCATTGTGTCGAACGCCTCT**GGA**ACGACCAACTGCTTGGCTCCTCTCGCC
15. GAPDH1-C152G-R     GGCGAGAGGAGCCAAGCAGTTGGT**CGT**GCAAGAGGCGTTCGACACAATGACATC
16. GAPDH1-S50A-R      GGGGTAGTGGCCGTGGAC**GGC**GTCGTATCTCAGAAGGTACACCATGTAGTC
17. GAPDH1-S203A-R     GGCAGGGATGATGTTGACGCCTGC**GGC**CCGGCCAGCGCGCCAATCTTTGCC
18. GAPDH1-S50E-R      GGGGTAGTGGCCGTGGAC**CT**CGTCGTATCTCAGAAGGTACACCATGTAGTC
19. GAPDH1-S203E-R     GGCAGGGATGATGTTGACGCCTGC**CT**CCCGGCCAGCGCGCCAATCTTTGCC
20. GAPDH1-Y41F-R      GTATCTCAGAAGGTACACCATG**A**AGTCCAGGGACATGAACGGGTC
21. GAPDH1-Y41E-R      GTATCTCAGAAGGTACACCAT**CTC**GTCCAGGGACATGAACGGGTC
22. GAPDH1-K162R-R     GCCGAACTTATCGTGGACAATT**C**TGGCGAGAGGAGCCAAGCAGTT
23. GAPDH1-K162Q-R     GCCGAACTTATCGTGGACAAT**CTG**GGCGAGAGGAGCCAAGCAGTT
24. GAPDH1-C3S-F       ATGGTG**A**GCAAGCTGGGTATTAACGGTTTTGGC
25. GAPDH1-C249S-R     CTTCGCGGGCTTGGCCAGCTTGC**T**GGTCAGATCAACCACAGACAC
```

APPENDIX A: Functional characterization of IMC15, the first known cytoskeletal

component of *Toxoplasma gondii* daughter buds

A.1. Introduction

The unique division of the intracellular apicomplexan parasite *Toxoplasma gondii* involves the assembly of two daughter cells within the mother (Sheffield and Melton, 1968). This process of endodyogeny or internal budding unfolds with the initiation of a new inner membrane complex (IMC), a series of flattened, cortical vesicles or alveoli (Hu et al., 2002). On the cytoplasmic side of the IMC lies a network of 8-10 nm intermediate filament-like proteins called alveolar IMC proteins (Mann and Beckers, 2001). These proteins contain a repeat of valine and proline rich domains called alveolin motifs conserved throughout the super-phylum alveolates that includes ciliates, dinoflagellates and apicomplexans (Gould et al., 2008). *Toxoplasma* has a family of 14 alveolin domain IMC proteins all containing alveolin repeat motifs. Their assembly dynamics resolved previously unappreciated discrete spatio-temporal events in the division process of this parasite (Anderson-White et al., 2011). Specifically, IMC15 was identified as the earliest cytoskeleton marker of budding. IMC15 is first recruited to the duplicated centrosomes, which are the staging hub for daughter assembly (Anderson-White et al., 2011) and subsequently translocates to the newly assembling buds (Gubbels et al., 2006). Hence, we propose that IMC15 is a scaffolding protein and recruits cytoskeletal proteins to complete daughter cell budding.

Division in *Toxoplasma* unfolds with the duplication of the Golgi apparatus and centrosome followed by the assembly of the cortical cytoskeleton on the duplicated centrosomes. The new cytoskeleton forms the scaffold for anchoring new organelles in the daughter buds within the mother (Nishi et al., 2008). Previous studies have established a timeline of early budding (Anderson-White et al., 2012). In addition to

IMC15, Rab11B, an alveolate specific subfamily member of Rab11-GTPases, localizes early to the growing IMC of the replicating parasites (Agop-Nersesian et al., 2010). Rab11B is required for transporting the vesicles from the Golgi to the IMC during daughter cell assembly and biogenesis of the IMC (Agop-Nersesian et al., 2010). Additionally, actin-like protein1 (ALP1) is localized to the apical end of dividing daughter cells and is required for the daughter IMC formation (Gordon et al., 2008). In the early budding stages, a family of ISP proteins organized along the IMC sub-compartments are recruited to the bud (Beck et al., 2010). Moreover, the glideosome-associated proteins GAP40 and GAP50 also appear in the early stage of budding and are required for completing the assembly of the new daughters and maintaining their stability (Harding et al., 2016). Overall, the early appearance of IMC15 in daughter cell formation suggests it could function as an essential scaffolding protein required to recruit the subsequent building blocks, which we pursued here by disrupting IMC15 expression.

The exact mechanism of the budding process has not been deciphered and therefore we pursued the functional characterization of IMC15, the first cytoskeletal component of budding. Previous attempts to directly knockout this gene in the parasite were unsuccessful suggesting that it may be essential (Anderson-White and Gubbels, 2011). Several additional strategies to create a conditional knockdown of IMC15 were equally unsuccessful due to background expression near the low natural expression level of this gene (Anderson-White and Gubbels, 2011). Here we have used new powerful genome editing technology to overcome the previous problems since it offers robust experimental paths to test and characterize any gene in the parasite. In this study, we were able to generate an IMC15 direct knockout (dKO) line through CRISPR/Cas9

genome editing (Sidik et al., 2014)[,] (Shen et al., 2014). We explored the role of this gene in the lytic cycle of the parasite. We discover that although loss of IMC15 is not critical for the lytic cycle of the parasite, it is critical for a correct execution of endodyogeny as we observe an increased frequency of more than two daughters per division round. This suggests IMC15 could be a scaffolding protein serving as a checkpoint or regulator of the endodyogeny process.

A.2. Results

A.2.1. *IMC15 is not essential for completing the lytic cycle of Toxoplasma*

To probe the function of IMC15 in the initiation of daughter cell budding we adopted a direct knockout strategy using CRISPR/Cas9 genome editing (Sidik et al., 2014). CRISPR/Cas9 was used to create a targeted double stranded break at the gene locus which was repaired using a template with homologous flanks to replace the IMC15 coding sequence generated by PCR and encoding the drug selectable marker DHFR-TS (Figure A.1. a). Successful replacement of the locus and absence of reintegration of the IMC15 coding sequence elsewhere in the genome was validated by diagnostic PCR reactions (Fig A.1b). The ability to generate an IMC15 dKO clonal line is an indication, in itself, that IMC15 is not essential for the lytic cycle of the parasite. However, to measure subtle effects on replicative efficiency we performed a plaque assay on the dKO line and the WT parent line, which measure integrated growth over a period of nine days (Figure A.2. a). Indeed we observed plaques of comparable numbers supporting that IMC15 is not essential. However, IMC15 dKO plaques appeared slightly larger, but upon careful quantification this effect was not statistically significant (Figure A.2. b).

A.2.2. *IMC15 is not required for initiation of daughter cells*

Based on previously published data, we hypothesized that IMC15 acts as a cue for initiation of budding in the parasite (Anderson-White et al., 2011). We assessed the effect of loss of IMC15 on the early budding process by IFA using the IMC3 marker for daughter development (Anderson-White et al., 2011). We observed no defect in daughter cell formation as indicated by incorporation of IMC3 in the dKO line (Fig A.3. a). Our

data suggest that IMC15 is not an essential scaffolding protein for incorporation of other cytoskeletal or membrane components in the budding daughter.

A.2.3. *Loss of IMC15 results in endopolygeny*

The increased plaque size upon loss of IMC15 prompted us to evaluate this intriguing phenotype by IFA using a centrosome (centrin) and daughter scaffold (IMC3) marker for daughter development (Szatanek et al., 2012). As a control we used the WT line and as expected it showed normal internal budding with duplicated centrosomes associated with two budding daughters within the mother (Figure A.3. b). In our dKO line, on the other hand, we frequently observed four centrosomes and four daughters in one mother (Figure A.3. a). At a lower frequency, three daughters and four centrosomes per mother were observed (lower panel Figure A.3. a). The multiple centrosomes each give rise to new daughters thereby generating more than two offspring per division round (i.e. endopolygeny). Although multiple (>2) daughters form at a low 1-2% frequency in normal parasites (Hu et al., 2004), quantification of this phenotype in parasites without IMC15 revealed the incidence increased to 25% (Figure A.3. c). Taken together, our data suggest that IMC15 is critical in regulating or controlling the number of daughter buds per division round.

.

A.3. Discussion

IMC15, the earliest known cytoskeletal component of daughter cell budding in *Toxoplasma,* is surprisingly not essential for the lytic cycle of the parasite (Figure A.2. a). Multiple attempts at depleting IMC15 protein in the parasite by various techniques were unsuccessful in the past, which suggested a critical role in parasite viability. But with novel CRISPR/Cas9 mediated high efficiency genome editing we were able to create an IMC15 dKO line. These results appear contradictory and it is feasible that efficiency of CRISPR permits selection for compensatory mechanisms counteracting the loss of IMC15. At this point we are unable to assess this possibility directly. However, we do see a disregulatory effect on the endodyogeny due to ablation of IMC15 as we observe an increase in multiple daughters per division round (Figure A.3. c).

To understand this phenotype we have to consider the controls underlying cell division cycle progression. The division of the parasite starts with the duplication of Golgi followed by the centrosome duplication. The *Toxoplasma* centrosome is a functionally bipartite structure (Suvorova et al., 2015). The inner core is thought to regulate the mitotic cycle in the nucleus, whereas the outer core functions in daughter cell assembly. By separately controlling the inner and outer cores, the parasite is able to successfully uncouple mitosis from daughter budding, thereby enabling endopolygeny. The formation of multiple daughters within a mother is reminiscent of another division mode of *Toxoplasma* i.e. endopolygeny that occurs in the definitive hosts (cats) or in other apicomplexans like *Sarcocystis* (Speer and Dubey, 1999). Furthermore, multiple daughters naturally form in tachyzoite tissue culture at a low frequency, under mild experimental stimuli (Hu et al., 2004). Since IMC15 is assembled on the duplicated

centrosome our initial hypothesis was that it served as a scaffolding protein recruiting additional cytoskeleton proteins. However, our data indicate that this is not the case since additional IMC proteins are added to the forming daughters and the budding process is completed (Figure A.3. a). The unexpected observation of multiple daughters in absence of IMC15 suggests a different role, most likely in timely activation or control of the outer core centrosome cycle.

Similar multi-daughter phenotypes have been observed with other mutants. E.g., in the absence of the GTPase activity of Rab6 (Stedman et al., 2003). Rab6 regulates the retrograde transport of proteins between post Golgi secretory granules to the parasite's Golgi apparatus, and functional disruption shifts cytokinesis toward endopolygeny in 24% of the parasites (Stedman et al., 2003), a percentage closely reflecting our observations upon loss of IMC15. In addition, TgNCR1, a protein containing a canonical sterol-sensing domain in the parasite related to the Niemann-Pick, type C1-related protein (NPC1) with significant identity to Human NPC1, is required for stimulation of lipid storage, membrane biosynthesis and parasite division. The deletion of TgNCR1 shows endopolygeny at an incidence of about 75% due to deregulation of trafficking of the lipids necessary for daughter formation (Lige et al., 2011). Furthermore, deletion of IMC sub-compartment protein ISP2 also leads to a high frequency (60%) of multiple daughters per mother along with loss in fitness (Beck et al., 2010). Although the function of ISP2 is unknown, both Rab6 and NPC1 are involved in membrane trafficking or biogenesis. It therefore appears that timely availability of membrane is critical for the daughter bud initiation function of the outer centrosome core. Since IMC15 is predicted to be palmitoylated and the IMC meshwork is anchored in the alveolar membranes, a feasible

model is that IMC15 assists in recruiting, anchoring or fusing vesicles trafficking from the Golgi to start assembly of the new daughter. Thus, if the efficiency of this process is reduced by deleting of IMC15 it can easily be envisioned that the outer core will not properly execute its job and subsequently the parasite will forgo daughter development eventually leading to another mitotic round producing a total of four centrosomes. This would assign in essence an assistant scaffolding function to IMC15, though not an essential one. In conclusion, this part of my thesis sheds significant light on understanding the role of IMC15 in the initiation of daughter budding. Additionally, similar expression level of IMC15 in all zoite forms (Hehl et al., 2015) identifies it as a potential regulator of daughter formation in the parasite.

Figure legend A.1. Generation of IMC15 dKO and validation by PCR

(a) IMC15 dKO strategy by homologous recombination using CRISPR/Cas9 based technology. Protospacers targeting gDNA of IMC15 after the start and stop codon were used to direct the DNA cleavage by Cas9. Using 35 bp homologous regions (red) flanking the DHFR selectable marker the IMC15 coding sequence was replaced. Recombination was performed in the Δku80 background (WT). Pyrimethamine resistant parasites were selected and cloned by limiting dilution. (b) Diagnostic PCR reaction to verify the IMC15 dKO line genotype. As expected, pair I PCR is present both in the WT and dKO line, but generates a different sized band indicating integration at the correct locus. Pair II additionally validates correct genomic integration. No PCR product in Pair III for the dKO line shows that the IMC15 gDNA is not randomly reintegrated else where in the genome.

Figure A.1. Generation of IMC15 dKO and validation by PCR
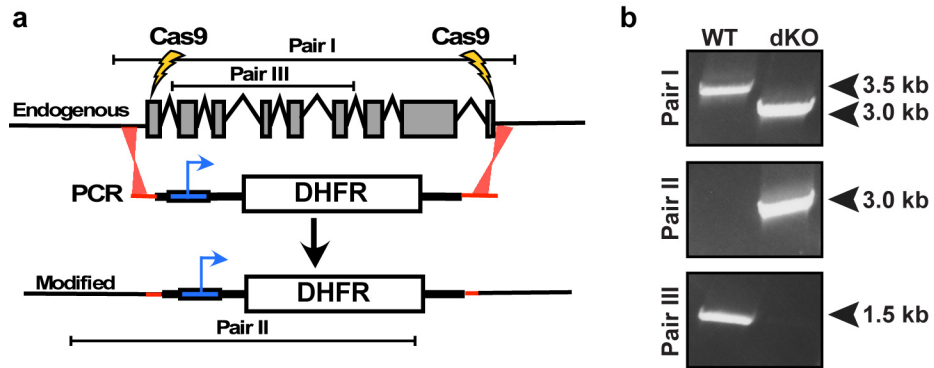
Figure legend A.2. IMC15 is not essential for the lytic cycle

(a) Representative image of plaque assays of WT and IMC15 dKO line after nine days incubation. (b) Quantification of plaque size of both the lines by measuring their plaque area of 30 plaques in each experiment. N=3 ± s.e.m. The data is not statistically significant using the unpaired t-test.

Figure A.2. IMC15 is not essential for the lytic cycle
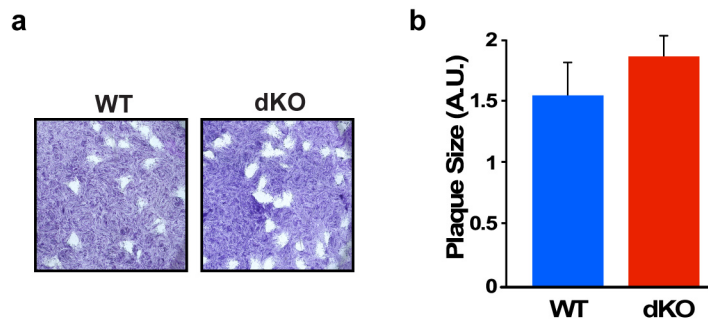
Figure legend A.3. Loss of IMC15 causes multi-daughter phenotype

IFA images of (a) IMC15dKO (dKO) and (b) Wild type (WT) parasite lines using α−IMC3 and α−h-Centrin antibodies after methanol fixation. The top panel shows the vacuoles with initiating and early daughter buds, middle panel has budding daughters in mid-phase and in the bottom panel the daughters are late phase of maturation. (c) Graph showing the quantification of the multiple-daughter phenotype in the marked lines by counting 200 vacuoles in each experiment. N=3 ± s.e.m. The statistical significance was calculated using unpaired two-tailed t-test.

Figure A.3. Loss of IMC15 causes multi-daughter phenotype
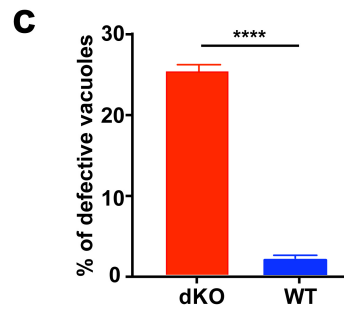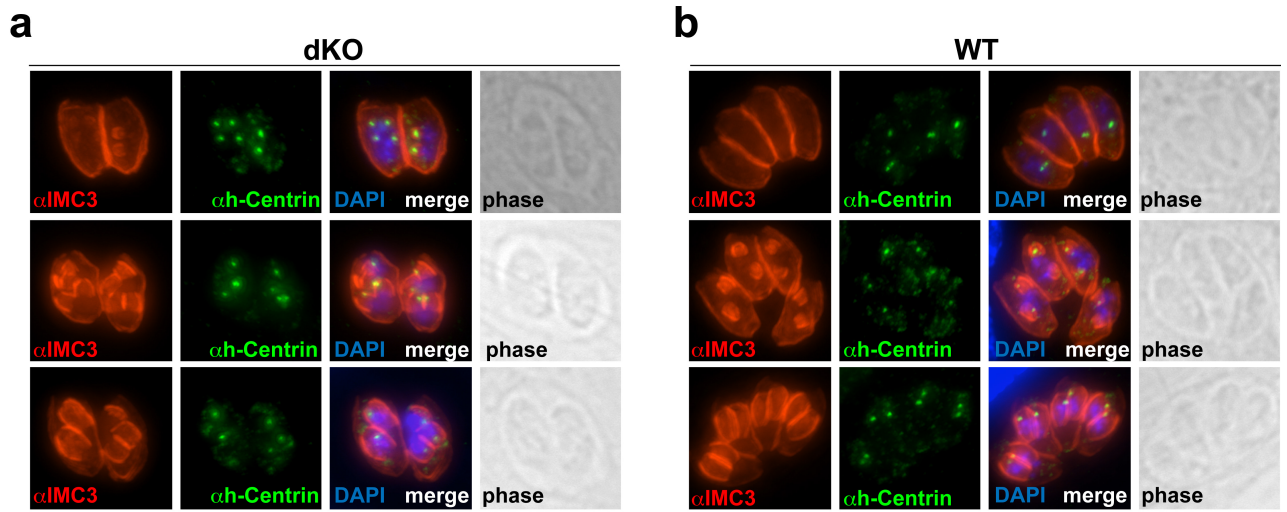
A.4. Material and Methods

A.4.1. Parasites

RH strain parasites and their transgenic derivatives were cultured and maintained as described in Chapter 6 (Material and Methods). Specifically, the double stranded breaks generated by Cas9 must be repaired by Homologous Recombination (HR) (Fox et al., 2009; Huynh and Carruthers, 2009), hence KU80, a Non-Homologous End-Joining (NHEJ) facilitating DNA-binding protein, lacking parasite line (Δku80) was used to facilitate this.

A.4.2. Plasmids

All primer sequences used in this study are listed in Table A.1. IMC15 dKO line was generated using the CRISPR/Cas9 system. A 20 base pair unique protospacer or guide sequence beside the protospacer-adjacent motif (PAM) was designed using the program ProtoMatchv2.0 (script by Sebastian Lourido: http://louridolab.wi.mit.edu/) at the 5' and 3' end of the IMC15 gDNA. The annealed phosphorylated oligonucleotides corresponding to these unique protospacer were then cloned into the pU6 plasmid (kindly donated by Sebastian Lourido Lab, Whitehead Institute) between the BsaI sites to generate the pU6-IMC15 plasmid. Sanger sequencing using the U6_sequence forward primer was used to sequence the final plasmids and verify the protospacers. DHFR locus was amplified from the DHFR-teto7SAG4 vector (kind gift from Wassim Daher (Morlon-Guyot et al., 2014)) using the primers (#2 and #3) with homologous flanks to IMC15 mentioned in Table A.1. 20 μg each plasmid was transfected into the Δku80 parasite line alongwith 40 μg PCR product of the DHFR resistant marker for drug

selection. 1 µg/ml of pyrimithine was added the following day to select the resistant parasites.

A.4.3. Verification of the knockout line

Within a week of transfection and drug selection using pyrimethamine, stable lines resistant to the drug were obtained. The gDNA was isolated and purified from the parasite using the Zymo gDNA isolation kit and diagnostic PCR reactions were done. The sets of primers used to verify the genotype are listed in Table A.1. After obtaining the parasite lines with successful integration of the DHFR cassette within the IMC15 locus, cloning by limiting dilution was done in a 384 well plate. A clone was used for all subsequent assays.

A.4.4. Plaque assay

Plaque assay was done as described in detail in the Chapter 6. Both WT and dKO line were incubated for 9 days before fixation and staining. The stained plaque assay plates were scanned and plaque size was measured in Fiji in three independent experiments.

A.4.5. Immunofluorescence

IFAs were performed as previously described in Chapter 6, 18 hpi (hours post infection). The following primary antibody was used rat α-IMC3 (1:2000) to mark the daughter buds and mother IMCs and rabbit α-human centrin (1:1000) to label the centrosomes. Alexa fluorophores (1:400) A594 conjugated to a goat-α-rat secondary antibody and

A488 conjugated to a goat-α–rabbit secondary antibody were used. Nuclear material was co-stained using DAPI (2 μg/ml).

A.4.6. Fluorescence microscopy and phenotype quantification

Wide field fluorescence microscope was used as previously described in Chapter 6. After IFA for quantification of the phenotype, more than 100 random vacuoles in budding stage were counted for both IMC15 dKO line and Δku80 parental parasite line. Statistical significance was calculated using two-tailed unpaired t-test on PRISM graphpad software.

Table A.1. Appendix protospacers and primer sequences

_____

# Protospacers name	Sequence

_____

1.	5-IMC15dKO-s	/5Phos/AAGTTGAGAGAATTTTTCTAAAATGG
2.	5-IMC15dKO-as	/5Phos/AAAACCATTTTAGAAAAATTCTCTCA
3.	3-IMC15dKO-s	/5Phos/AAGTTGCACAGTGTTGCCAGTCACCGG
4.	3-IMC15dKO-as	/5Phos/AAAACCGGTGACTGGCAACACTGTGCA

_____

# Primer name	Sequence

_____

1.	U6_sequence-F	ctcgtagagaacaagcactcg
2.	5'IMC15-DHFR-F	gaaaggacacgctttgcacacaccggcgtcacagcCACGAAACCTTGCATTCAAACC
3.	3'IMC15-DHFR-R	cgtttcctagacaatccgtctcctcaaggaggagcATCCTGCAAGTGCATAGAAGG
4.	5'IMC15ver-F	GTGTACTGGTGTTCGAGGCTATG
5.	5'DHFR-CXR	ACTGCGAACAGCAGCAAGATCG
6.	3'IMC15ver-R	CAAACCAAATGATGCGGTCCCTG
7.	IMC15dko-int-ver-F	cagaactgcaagagacaccg
8.	IMC15dko-int-ver-R	ctgcagtgcaagaattccgc

_____

167

References

Agop-Nersesian, C., Egarter, S., Langsley, G., Foth, B.J., Ferguson, D.J.P., and Meissner, M. (2010). Biogenesis of the inner membrane complex is dependent on vesicular transport by the alveolate specific GTPase Rab11B. PLoS Pathog *6*, e1001029.

Aingaran, M., Zhang, R., Law, S.K., Peng, Z., Undisz, A., Meyer, E., Diez-Silva, M., Burke, T.A., Spielmann, T., Lim, C.T., *et al.* (2012). Host cell deformability is linked to transmission in the human malaria parasite Plasmodium falciparum. Cell Microbiol *14*, 983-993.

Akella, R., Min, X., Wu, Q., Gardner, K.H., and Goldsmith, E.J. (2010). The third conformation of p38alpha MAP kinase observed in phosphorylated p38alpha and in solution. Structure *18*, 1571-1578.

Akinyi, S., Gaona, J., Meyer, E.V., Barnwell, J.W., Galinski, M.R., and Corredor, V. (2008). Phylogenetic and structural information on glyceraldehyde-3-phosphate dehydrogenase (G3PDH) in Plasmodium provides functional insights. Infect Genet Evol *8*, 205-212.

Aldrich, H.C., McDowell, L., Barbosa, M.F., Yomano, L.P., Scopes, R.K., and Ingram, L.O. (1992). Immunocytochemical localization of glycolytic and fermentative enzymes in Zymomonas mobilis. J Bacteriol *174*, 4504-4508.

Alexander, D.L., Mital, J., Ward, G.E., Bradley, P., and Boothroyd, J.C. (2005). Identification of the moving junction complex of Toxoplasma gondii: a collaboration between distinct secretory organelles. PLoS Pathog *1*, e17.

Andenmatten, N., Egarter, S., Jackson, A.J., Jullien, N., Herman, J.P., and Meissner, M. (2013). Conditional genome engineering in Toxoplasma gondii uncovers alternative invasion mechanisms. Nature methods *10*, 125-127.

Anderson-White, B., Beck, J.R., Chen, C.T., Meissner, M., Bradley, P.J., and Gubbels, M.J. (2012). Cytoskeleton assembly in Toxoplasma gondii cell division. Int Rev Cell Mol Biol *298*, 1-31.

Anderson-White, B.R., Ivey, F.D., Cheng, K., Szatanek, T., Lorestani, A., Beckers, C.J., Ferguson, D.J., Sahoo, N., and Gubbels, M.J. (2011). A family of intermediate filament-like proteins is sequentially assembled into the cytoskeleton of Toxoplasma gondii. Cell Microbiol *13*, 18-31.

Anderson-White, B.R.A., and Gubbels, M.-J.T.a. (2011). Identification and Characterization of the IMC Protein Family in Toxoplasma gondii (Boston College).

Azam, S., Jouvet, N., Jilani, A., Vongsamphanh, R., Yang, X., Yang, S., and Ramotar, D. (2008). Human glyceraldehyde-3-phosphate dehydrogenase plays a direct role in reactivating oxidized forms of the DNA repair enzyme APE1. J Biol Chem *283*, 30632-30641.

Bargieri, D.Y., Andenmatten, N., Lagal, V., Thiberge, S., Whitelaw, J.A., Tardieux, I., Meissner, M., and Menard, R. (2013). Apical membrane antigen 1 mediates apicomplexan parasite attachment but is dispensable for host cell invasion. Nature communications *4*, 2552.

Barsoum, R.S. (2004). Parasitic infections in organ transplantation. Exp Clin Transplant *2*, 258-267.

Beck, J.R., Rodriguez-Fernandez, I.A., de Leon, J.C., Huynh, M.H., Carruthers, V.B., Morrissette, N.S., and Bradley, P.J. (2010). A novel family of Toxoplasma IMC proteins displays a hierarchical organization and functions in coordinating parasite division. PLoS Pathog *6*, e1001094.

Behnke, M.S., Wootton, J.C., Lehmann, M.M., Radke, J.B., Lucas, O., Nawas, J., Sibley, L.D., and White, M.W. (2010). Coordinated progression through two subtranscriptomes underlies the tachyzoite cycle of Toxoplasma gondii. PLoS One *5*, e12354.

Bichet, M., Touquet, B., Gonzalez, V., Florent, I., Meissner, M., and Tardieux, I. (2016). Genetic impairment of parasite myosin motors uncovers the contribution of host cell membrane dynamics to Toxoplasma invasion forces. BMC Biol *14*, 97.

Biesecker, G., Harris, J.I., Thierry, J.C., Walker, J.E., and Wonacott, A.J. (1977). Sequence and structure of D-glyceraldehyde 3-phosphate dehydrogenase from Bacillus stearothermophilus. Nature *266*, 328-333.

Binder, E.M., Lagal, V., and Kim, K. (2008). The prodomain of Toxoplasma gondii GPI-anchored subtilase TgSUB1 mediates its targeting to micronemes. Traffic *9*, 1485-1496.

Bishop, R., Musoke, A., Morzaria, S., Gardner, M., and Nene, V. (2004). Theileria: intracellular protozoan parasites of wild and domestic ruminants transmitted by ixodid ticks. Parasitology *129 Suppl*, S271-283.

Blader, I.J., Coleman, B.I., Chen, C.T., and Gubbels, M.J. (2015). Lytic Cycle of Toxoplasma gondii: 15 Years Later. Annu Rev Microbiol *69*, 463-485.

Blume, M., Rodriguez-Contreras, D., Landfear, S., Fleige, T., Soldati-Favre, D., Lucius, R., and Gupta, N. (2009). Host-derived glucose and its transporter in the obligate intracellular pathogen Toxoplasma gondii are dispensable by glutaminolysis. Proc Natl Acad Sci U S A *106*, 12998-13003.

Bonafe, N., Gilmore-Hebert, M., Folk, N.L., Azodi, M., Zhou, Y., and Chambers, S.K. (2005). Glyceraldehyde-3-phosphate dehydrogenase binds to the AU-Rich 3' untranslated region of colony-stimulating factor-1 (CSF-1) messenger RNA in human ovarian cancer cells: possible role in CSF-1 posttranscriptional regulation and tumor phenotype. Cancer Res *65*, 3762-3771.

Brimmer, A., and Weber, K. (2000). The cDNA sequences of three tetrins, the structural proteins of the Tetrahymena oral filaments, show that they are novel cytoskeletal proteins. Protist *151*, 171-180.

Bullen, H.E., Tonkin, C.J., O'Donnell, R.A., Tham, W.H., Papenfuss, A.T., Gould, S., Cowman, A.F., Crabb, B.S., and Gilson, P.R. (2009). A novel family of Apicomplexan glideosome-associated proteins with an inner membrane-anchoring role. J Biol Chem *284*, 25353-25363.

Burg, J.L., Perelman, D., Kasper, L.H., Ware, P.L., and Boothroyd, J.C. (1988). Molecular analysis of the gene encoding the major surface antigen of Toxoplasma gondii. J Immunol *141*, 3584-3591.

Campanella, M.E., Chu, H., and Low, P.S. (2005). Assembly and regulation of a glycolytic enzyme complex on the human erythrocyte membrane. Proc Natl Acad Sci U S A *102*, 2402-2407.

Chen, A.L., Kim, E.W., Toh, J.Y., Vashisht, A.A., Rashoff, A.Q., Van, C., Huang, A.S., Moon, A.S., Bell, H.N., Bentolila, L.A.*, et al.* (2015). Novel components of the Toxoplasma inner membrane complex revealed by BioID. MBio *6*, e02357-02314.

Chen, C.T., and Gubbels, M.J. (2013). The Toxoplasma gondii centrosome is the platform for internal daughter budding as revealed by a Nek1 kinase mutant. J Cell Sci *126*, 3344-3355.

Cook, W.J., Senkovich, O., and Chattopadhyay, D. (2009). An unexpected phosphate binding site in glyceraldehyde 3-phosphate dehydrogenase: crystal structures of apo, holo and ternary complex of Cryptosporidium parvum enzyme. BMC structural biology *9*, 9.

Daubenberger, C.A., Tisdale, E.J., Curcic, M., Diaz, D., Silvie, O., Mazier, D., Eling, W., Bohrmann, B., Matile, H., and Pluschke, G. (2003). The N'-terminal domain of glyceraldehyde-3-phosphate dehydrogenase of the apicomplexan Plasmodium falciparum mediates GTPase Rab2-dependent recruitment to membranes. Biological chemistry *384*, 1227-1237.

Del Carmen, M.G., Mondragon, M., Gonzalez, S., and Mondragon, R. (2009). Induction and regulation of conoid extrusion in Toxoplasma gondii. Cell Microbiol *11*, 967-982.

Demarse, N.A., Ponnusamy, S., Spicer, E.K., Apohan, E., Baatz, J.E., Ogretmen, B., and Davies, C. (2009). Direct binding of glyceraldehyde 3-phosphate dehydrogenase to telomeric DNA protects telomeres against chemotherapy-induced rapid degradation. Journal of molecular biology *394*, 789-803.

Dobrowolski, J., and Sibley, L.D. (1997). The role of the cytoskeleton in host cell invasion by Toxoplasma gondii. Behring Inst Mitt, 90-96.

Dobrowolski, J.M., and Sibley, L.D. (1996). Toxoplasma invasion of mammalian cells is powered by the actin cytoskeleton of the parasite. Cell *84*, 933-939.

Du, Z.X., Wang, H.Q., Zhang, H.Y., and Gao, D.X. (2007). Involvement of glyceraldehyde-3-phosphate dehydrogenase in tumor necrosis factor-related apoptosis-inducing ligand-mediated death of thyroid cancer cells. Endocrinology *148*, 4352-4361.

Dubey, R., Staker, B.L., Foe, I.T., Bogyo, M., Myler, P.J., Ngo, H.M., and Gubbels, M.J. (2016). Membrane skeletal association and post-translational allosteric regulation of Toxoplasma gondii GAPDH1. Mol Microbiol.

Dubremetz, J.F., and Elsner, Y.Y. (1979). Ultrastructural study of schizogony of Eimeria bovis in cell cultures. J Protozool *26*, 367-376.

Dubremetz, J.F., and Torpier, G. (1978). Freeze fracture study of the pellicle of an eimerian sporozoite (Protozoa, Coccidia). J Ultrastruct Res *62*, 94-109.

Egarter, S., Andenmatten, N., Jackson, A.J., Whitelaw, J.A., Pall, G., Black, J.A., Ferguson, D.J., Tardieux, I., Mogilner, A., and Meissner, M. (2014). The toxoplasma Acto-MyoA motor complex is important but not essential for gliding motility and host cell invasion. PLoS One *9*, e91819.

Farrell, M., and Gubbels, M.J. (2014). The Toxoplasma gondii kinetochore is required for centrosome association with the centrocone (spindle pole). Cell Microbiol *16*, 78-94.

Fast, N.M., Kissinger, J.C., Roos, D.S., and Keeling, P.J. (2001). Nuclear-encoded, plastid-targeted genes suggest a single common origin for apicomplexan and dinoflagellate plastids. Mol Biol Evol *18*, 418-426.

Fleige T, F.K., Ferguson DJP, Gross U, Bohne W (2007). Carbohydrate metabolism in the Toxoplasma gondii apicoplast: localization of three glycolytic isoenzymes, the single pyruvate dehydrogenase complex, and a plastid phosphate translocator.

Foussard, F., Gallois, Y., Tronchin, G., Robert, R., and Mauras, G. (1990). Isolation of the pellicle of Toxoplasma gondii (Protozoa, Coccidia): characterization by electron microscopy and protein composition. Parasitol Res *76*, 563-565.

Fox, B.A., Ristuccia, J.G., Gigley, J.P., and Bzik, D.J. (2009). Efficient gene replacements in Toxoplasma gondii strains deficient for nonhomologous end joining. Eukaryot Cell *8*, 520-529.

Francia, M.E., and Striepen, B. (2014). Cell division in apicomplexan parasites. Nat Rev Microbiol *12*, 125-136.

Frenal, K., Kemp, L.E., and Soldati-Favre, D. (2014a). Emerging roles for protein S-palmitoylation in Toxoplasma biology. Int J Parasitol *44*, 121-131.

Frenal, K., Marq, J.B., Jacot, D., Polonais, V., and Soldati-Favre, D. (2014b). Plasticity between MyoC- and MyoA-glideosomes: an example of functional compensation in Toxoplasma gondii invasion. PLoS Pathog *10*, e1004504.

Frenkel, J.K. (1973). Toxoplasma In and Around Us. BioScience *23*, 343-352.

Frenkel, J.K., Dubey, J.P., and Miller, N.L. (1970). Toxoplasma gondii in cats: fecal stages identified as coccidian oocysts. Science *167*, 893-896.

Fritz, H.M., Buchholz, K.R., Chen, X., Durbin-Johnson, B., Rocke, D.M., Conrad, P.A., and Boothroyd, J.C. (2012). Transcriptomic analysis of toxoplasma development reveals many novel functions and structures specific to sporozoites and oocysts. PLoS One *7*, e29998.

Gaji, R.Y., Behnke, M.S., Lehmann, M.M., White, M.W., and Carruthers, V.B. (2011). Cell cycle-dependent, intercellular transmission of Toxoplasma gondii is accompanied by marked changes in parasite gene expression. Mol Microbiol *79*, 192-204.

Gajria, B., Bahl, A., Brestelli, J., Dommer, J., Fischer, S., Gao, X., Heiges, M., Iodice, J., Kissinger, J.C., Mackey, A.J.*, et al.* (2008). ToxoDB: an integrated Toxoplasma gondii database resource. Nucleic Acids Res *36*, D553-556.

Garrison, E., Treeck, M., Ehret, E., Butz, H., Garbuz, T., Oswald, B.P., Settles, M., Boothroyd, J., and Arrizabalaga, G. (2012). A forward genetic screen reveals that calcium-dependent protein kinase 3 regulates egress in Toxoplasma. PLoS Pathog *8*, e1003049.

Glaser, P.E., and Gross, R.W. (1995). Rapid plasmenylethanolamine-selective fusion of membrane bilayers catalyzed by an isoform of glyceraldehyde-3-phosphate dehydrogenase: discrimination between glycolytic and fusogenic roles of individual isoforms. Biochemistry *34*, 12193-12203.

Gordon, J.L., Beatty, W.L., and Sibley, L.D. (2008). A novel actin-related protein is associated with daughter cell formation in Toxoplasma gondii. Eukaryot Cell *7*, 1500-1512.

Gould, S.B., Tham, W.H., Cowman, A.F., McFadden, G.I., and Waller, R.F. (2008). Alveolins, a new family of cortical proteins that define the protist infrakingdom Alveolata. Mol Biol Evol *25*, 1219-1230.

Gubbels, M.J., Li, C., and Striepen, B. (2003). High-throughput growth assay for Toxoplasma gondii using yellow fluorescent protein. Antimicrob Agents Chemother *47*, 309-316.

Gubbels, M.J., Vaishnava, S., Boot, N., Dubremetz, J.F., and Striepen, B. (2006). A MORN-repeat protein is a dynamic component of the Toxoplasma gondii cell division apparatus. J Cell Sci *119*, 2236-2245.

Gupta, R., Kumar, V., Kushawaha, P.K., Tripathi, C.P., Joshi, S., Sahasrabuddhe, A.A., Mitra, K., Sundar, S., Siddiqi, M.I., and Dube, A. (2014). Characterization of glycolytic enzymes--rAldolase and rEnolase of Leishmania donovani, identified as Th1 stimulatory proteins, for their immunogenicity and immunoprophylactic efficacies against experimental visceral leishmaniasis. PLoS One *9*, e86073.

Gutierrez, J., O'Donovan, J., Williams, E., Proctor, A., Brady, C., Marques, P.X., Worrall, S., Nally, J.E., McElroy, M., Bassett, H.*, et al.* (2010). Detection and quantification of Toxoplasma gondii in ovine maternal and foetal tissues from experimentally infected pregnant ewes using real-time PCR. Vet Parasitol *172*, 8-15.

Hager, K.M., Striepen, B., Tilney, L.G., and Roos, D.S. (1999). The nuclear envelope serves as an intermediary between the ER and Golgi complex in the intracellular parasite Toxoplasma gondii. J Cell Sci *112 (Pt 16)*, 2631-2638.

Hara, M.R., Agrawal, N., Kim, S.F., Cascio, M.B., Fujimuro, M., Ozeki, Y., Takahashi, M., Cheah, J.H., Tankou, S.K., Hester, L.D.*, et al.* (2005). S-nitrosylated GAPDH initiates apoptotic cell death by nuclear translocation following Siah1 binding. Nat Cell Biol *7*, 665-674.

Harding, C.R., Egarter, S., Gow, M., Jimenez-Ruiz, E., Ferguson, D.J., and Meissner, M. (2016). Gliding Associated Proteins Play Essential Roles during the Formation of the Inner Membrane Complex of Toxoplasma gondii. PLoS Pathog *12*, e1005403.

Hartmann, J., Hu, K., He, C.Y., Pelletier, L., Roos, D.S., and Warren, G. (2006). Golgi and centrosome cycles in Toxoplasma gondii. Mol Biochem Parasitol *145*, 125-127.

Hehl, A.B., Basso, W.U., Lippuner, C., Ramakrishnan, C., Okoniewski, M., Walker, R.A., Grigg, M.E., Smith, N.C., and Deplazes, P. (2015). Asexual expansion of Toxoplasma gondii merozoites is distinct from tachyzoites and entails expression of non-overlapping gene families to attach, invade, and replicate within feline enterocytes. BMC Genomics *16*, 66.

Hoff, E.F., and Carruthers, V.B. (2002). Is Toxoplasma egress the first step in invasion? Trends Parasitol *18*, 251-255.

Hu, K., Johnson, J., Florens, L., Fraunholz, M., Suravajjala, S., DiLullo, C., Yates, J., Roos, D.S., and Murray, J.M. (2006). Cytoskeletal components of an invasion machine-The apical complex of Toxoplasma gondii. PLoS Pathog *2*, e13.

Hu, K., Mann, T., Striepen, B., Beckers, C.J.M., Roos, D.S., and Murray, J.M. (2002). Daughter Cell Assembly in the Protozoan ParasiteToxoplasma gondii. Mol Biol Cell *13*, 593-606.

Hu, K., Roos, D.S., Angel, S.O., and Murray, J.M. (2004). Variability and heritability of cell division pathways in Toxoplasma gondii. J Cell Sci *117*, 5697-5705.

Huttenlauch, I., Peck, R.K., and Stick, R. (1998). Articulins and epiplasmins: two distinct classes of cytoskeletal proteins of the membrane skeleton in protists. J Cell Sci *111 (Pt 22)*, 3367-3378.

Huynh, M.H., and Carruthers, V.B. (2009). Tagging of endogenous genes in a Toxoplasma gondii strain lacking Ku80. Eukaryot Cell *8*, 530-539.

Huynh, M.H., Rabenau, K.E., Harper, J.M., Beatty, W.L., Sibley, L.D., and Carruthers, V.B. (2003). Rapid invasion of host cells by Toxoplasma requires secretion of the MIC2-M2AP adhesive protein complex. Embo J *22*, 2082-2090.

Jenkins, J.L., and Tanner, J.J. (2006). High-resolution structure of human D-glyceraldehyde-3-phosphate dehydrogenase. Acta crystallographica Section D, Biological crystallography *62*, 290-301.

Joiner, K.A., and Dubremetz, J.F. (1993). Toxoplasma gondii: a protozoan for the nineties. Infect Immun *61*, 1169-1172.

Jones, J.L., and Holland, G.N. (2010). Annual burden of ocular toxoplasmosis in the US. Am J Trop Med Hyg *82*, 464-465.

Jones, J.L., Parise, M.E., and Fiore, A.E. (2014). Neglected parasitic infections in the United States: toxoplasmosis. Am J Trop Med Hyg *90*, 794-799.

Kafsack, B.F., Carruthers, V.B., and Pineda, F.J. (2007). Kinetic modeling of Toxoplasma gondii invasion. J Theor Biol *249*, 817-825.

Kaye, A. (2011). Toxoplasmosis: diagnosis, treatment, and prevention in congenitally exposed infants. J Pediatr Health Care *25*, 355-364.

Keeley, A., and Soldati, D. (2004). The glideosome: a molecular machine powering motility and host-cell invasion by Apicomplexa. Trends Cell Biol *14*, 528-532.

Khater, E.I., Sinden, R.E., and Dessens, J.T. (2004). A malaria membrane skeletal protein is essential for normal morphogenesis, motility, and infectivity of sporozoites. J Cell Biol *167*, 425-432.

Kim, J.W., Kim, T.E., Kim, Y.K., Kim, Y.W., Kim, S.J., Lee, J.M., Kim, I.K., and Namkoong, S.E. (1999). Antisense oligodeoxynucleotide of glyceraldehyde-3-phosphate dehydrogenase gene inhibits cell proliferation and induces apoptosis in human cervical carcinoma cell lines. Antisense Nucleic Acid Drug Dev *9*, 507-513.

Kono, M., Herrmann, S., Loughran, N.B., Cabrera, A., Engelberg, K., Lehmann, C., Sinha, D., Prinz, B., Ruch, U., Heussler, V.*, et al.* (2012). Evolution and architecture of the inner membrane complex in asexual and sexual stages of the malaria parasite. Mol Biol Evol *29*, 2113-2132.

Kumagai, H., and Sakai, H. (1983). A porcine brain protein (35 K protein) which bundles microtubules and its identification as glyceraldehyde 3-phosphate dehydrogenase. Journal of biochemistry *93*, 1259-1269.

Lakhdar-Ghazal, F., Blonski, C., Willson, M., Michels, P., and Perie, J. (2002). Glycolysis and proteases as targets for the design of new anti-trypanosome drugs. Curr Top Med Chem *2*, 439-456.

Lescault, P.J., Thompson, A.B., Patil, V., Lirussi, D., Burton, A., Margarit, J., Bond, J., and Matrajt, M. (2010). Genomic data reveal Toxoplasma gondii differentiation mutants are also impaired with respect to switching into a novel extracellular tachyzoite state. PLoS One *5*, e14463.

Levine, N.D. (1988). Progress in taxonomy of the Apicomplexan protozoa. J Protozool *35*, 518-520.

Lige, B., Romano, J.D., Bandaru, V.V., Ehrenman, K., Levitskaya, J., Sampels, V., Haughey, N.J., and Coppens, I. (2011). Deficiency of a Niemann-Pick, type C1-related protein in toxoplasma is associated with multiple lipidoses and increased pathogenicity. PLoS Pathog *7*, e1002410.

Lin, S.S., Blume, M., von Ahsen, N., Gross, U., and Bohne, W. (2011). Extracellular Toxoplasma gondii tachyzoites do not require carbon source uptake for ATP maintenance, gliding motility and invasion in the first hour of their extracellular life. Int J Parasitol *41*, 835-841.

Linder, M.E., and Deschenes, R.J. (2007). Palmitoylation: policing protein stability and traffic. Nat Rev Mol Cell Biol *8*, 74-84.

Lirussi, D., and Matrajt, M. (2011). RNA granules present only in extracellular toxoplasma gondii increase parasite viability. Int J Biol Sci *7*, 960-967.

Liu, J., He, Y., Benmerzouga, I., Sullivan, W.J., Jr., Morrissette, N.S., Murray, J.M., and Hu, K. (2016). An ensemble of specifically targeted proteins stabilizes cortical microtubules in the human parasite Toxoplasma gondii. Mol Biol Cell *27*, 549-571.

Luft, B.J., and Remington, J.S. (1992). Toxoplasmic encephalitis in AIDS. Clin Infect Dis *15*, 211-222.

MacRae, J.I., Sheiner, L., Nahid, A., Tonkin, C., Striepen, B., and McConville, M.J. (2012). Mitochondrial metabolism of glucose and glutamine is required for intracellular growth of Toxoplasma gondii. Cell Host Microbe *12*, 682-692.

Mann, T., and Beckers, C. (2001). Characterization of the subpellicular network, a filamentous membrane skeletal component in the parasite Toxoplasma gondii. Mol Biochem Parasitol *115*, 257-268.

Mansfield, L.S., and Gajadhar, A.A. (2004). Cyclospora cayetanensis, a food- and waterborne coccidian parasite. Vet Parasitol *126*, 73-90.

Marrs, J.A., and Bouck, G.B. (1992). The two major membrane skeletal proteins (articulins) of Euglena gracilis define a novel class of cytoskeletal proteins. J Cell Biol *118*, 1465-1475.

Martin, B.R., and Cravatt, B.F. (2009). Large-scale profiling of protein palmitoylation in mammalian cells. Nat Methods *6*, 135-138.

McDonald, V., and Shirley, M.W. (2009). Past and future: vaccination against Eimeria. Parasitology *136*, 1477-1489.

Meissner, M., Schluter, D., and Soldati, D. (2002). Role of Toxoplasma gondii myosin A in powering parasite gliding and host cell invasion. Science *298*, 837-840.

Montoya, J.G., and Liesenfeld, O. (2004). Toxoplasmosis. Lancet *363*, 1965-1976.

Moras, D., Olsen, K.W., Sabesan, M.N., Buehner, M., Ford, G.C., and Rossmann, M.G. (1975). Studies of asymmetry in the three-dimensional structure of lobster D-glyceraldehyde-3-phosphate dehydrogenase. J Biol Chem *250*, 9137-9162.

Morlon-Guyot, J., Berry, L., Chen, C.T., Gubbels, M.J., Lebrun, M., and Daher, W. (2014). The Toxoplasma gondii calcium-dependent protein kinase 7 is involved in early steps of parasite division and is crucial for parasite survival. Cell Microbiol *16*, 95-114.

Morrissette, N.S., Murray, J.M., and Roos, D.S. (1997). Subpellicular microtubules associate with an intramembranous particle lattice in the protozoan parasite Toxoplasma gondii. J Cell Sci *110*, 35-42.

Morrissette, N.S., and Sibley, L.D. (2002). Cytoskeleton of apicomplexan parasites. Microbiol Mol Biol Rev *66*, 21-38; table of contents.

Nakagawa, T., Hirano, Y., Inomata, A., Yokota, S., Miyachi, K., Kaneda, M., Umeda, M., Furukawa, K., Omata, S., and Horigome, T. (2003). Participation of a fusogenic protein, glyceraldehyde-3-phosphate dehydrogenase, in nuclear membrane assembly. J Biol Chem *278*, 20395-20404.

Nebl, T., Prieto, J.H., Kapp, E., Smith, B.J., Williams, M.J., Yates, J.R., 3rd, Cowman, A.F., and Tonkin, C.J. (2011). Quantitative in vivo analyses reveal calcium-dependent phosphorylation sites and identifies a novel component of the Toxoplasma invasion motor complex. PLoS Pathog *7*, e1002222.

Nichols, B.A., and Chiappino, M.L. (1987). Cytoskeleton of Toxoplasma gondii. J Protozool *34*, 217-226.

Nishi, M., Hu, K., Murray, J.M., and Roos, D.S. (2008). Organellar dynamics during the cell cycle of Toxoplasma gondii. J Cell Sci *121*, 1559-1568.

Nitzsche, R., Zagoriy, V., Lucius, R., and Gupta, N. (2015). Metabolic cooperation of glucose and glutamine is essential for the lytic cycle of obligate intracellular parasite Toxoplasma gondii. J Biol Chem.

Opperdoes, F.R., and Michels, P.A. (2001). Enzymes of carbohydrate metabolism as potential drug targets. Int J Parasitol *31*, 482-490.

Overman, R.C., Debreczeni, J.E., Truman, C.M., McAlister, M.S., and Attwood, T.K. (2014). Completing the structural family portrait of the human EphB tyrosine kinase domains. Protein Sci *23*, 627-638.

Peixoto L, C.F., Harb OS, Davis PH, Beiting DP, Brownback CS, Ouloguem D, Roos DS (2010). Integrative genomic approaches highlight a family of parasite-specific kinases that regulate host responses.

Pomel, S., Diogon, M., Bouchard, P., Pradel, L., Ravet, V., Coffe, G., and Vigues, B. (2006). The membrane skeleton in Paramecium: Molecular characterization of a novel epiplasmin family and preliminary GFP expression results. Protist *157*, 61-75.

Pomel, S., Luk, F.C., and Beckers, C.J. (2008). Host cell egress and invasion induce marked relocations of glycolytic enzymes in Toxoplasma gondii tachyzoites. PLoS Pathog *4*, e1000188.

Porchet, E., and Torpier, G. (1977). [Freeze fracture study of Toxoplasma and Sarcocystis infective stages (author's transl)]. Z Parasitenkd *54*, 101-124.

Radke, J.R., Striepen, B., Guerini, M.N., Jerome, M.E., Roos, D.S., and White, M.W. (2001). Defining the cell cycle for the tachyzoite stage of Toxoplasma gondii. Mol Biochem Parasitol *115*, 165-175.

Rajapakse, S., Chrishan Shivanthan, M., Samaranayake, N., Rodrigo, C., and Deepika Fernando, S. (2013). Antibiotics for human toxoplasmosis: a systematic review of randomized trials. Pathog Glob Health *107*, 162-169.

Ramakrishnan, S., Docampo, M.D., MacRae, J.I., Ralton, J.E., Rupasinghe, T., McConville, M.J., and Striepen, B. (2015). The intracellular parasite Toxoplasma gondii depends on the synthesis of long-chain and very long-chain unsaturated fatty acids not supplied by the host cell. Mol Microbiol *97*, 64-76.

Reiss, N., Oplatka, A., Hermon, J., and Naor, Z. (1996). Phosphatidylserine directs differential phosphorylation of actin and glyceraldehyde-3-phosphate dehydrogenase by protein kinase C: possible implications for regulation of actin polymerization. Biochemistry and molecular biology international *40*, 1191-1200.

Ren, J., Wen, L., Gao, X., Jin, C., Xue, Y., and Yao, X. (2008). CSS-Palm 2.0: an updated software for palmitoylation sites prediction. Protein Eng Des Sel *21*, 639-644.

Robien, M.A., Bosch, J., Buckner, F.S., Van Voorhis, W.C., Worthey, E.A., Myler, P., Mehlin, C., Boni, E.E., Kalyuzhniy, O., Anderson, L., *et al.* (2006). Crystal structure of glyceraldehyde-3-phosphate dehydrogenase from Plasmodium falciparum at 2.25 A resolution reveals intriguing extra electron density in the active site. Proteins *62*, 570-577.

Roitel, O., Vachette, P., Azza, S., and Branlant, G. (2003). P but not R-axis interface is involved in cooperative binding of NAD on tetrameric phosphorylating glyceraldehyde-3-phosphate dehydrogenase from Bacillus stearothermophilus. J Mol Biol *326*, 1513-1522.

Roos, D.S., Donald, R.G., Morrissette, N.S., and Moulton, A.L. (1994). Molecular tools for genetic dissection of the protozoan parasite Toxoplasma gondii. Methods Cell Biol *45*, 27-63.

Sahasrabudhe, N.S., Jadhav, M.V., Deshmukh, S.D., and Holla, V.V. (2003). Pathology of Toxoplasma myocarditis in acquired immunodeficiency syndrome. Indian J Pathol Microbiol *46*, 649-651.

Satchell, J.F., Malby, R.L., Luo, C.S., Adisa, A., Alpyurek, A.E., Klonis, N., Smith, B.J., Tilley, L., and Colman, P.M. (2005). Structure of glyceraldehyde-3-phosphate dehydrogenase from Plasmodium falciparum. Acta crystallographica Section D, Biological crystallography *61*, 1213-1221.

Schindelin, J., Arganda-Carreras, I., Frise, E., Kaynig, V., Longair, M., Pietzsch, T., Preibisch, S., Rueden, C., Saalfeld, S., Schmid, B., *et al.* (2012). Fiji: an open-source platform for biological-image analysis. Nat Methods *9*, 676-682.

Schnittger, L., Rodriguez, A.E., Florin-Christensen, M., and Morrison, D.A. (2012). Babesia: a world emerging. Infect Genet Evol *12*, 1788-1809.

Segal, H.L., and Boyer, P.D. (1953). The role of sulfhydryl groups in the activity of D-glyceraldehyde 3-phosphate dehydrogenase. J Biol Chem *204*, 265-281.

Sen, N., Hara, M.R., Kornberg, M.D., Cascio, M.B., Bae, B.I., Shahani, N., Thomas, B., Dawson, T.M., Dawson, V.L., Snyder, S.H.*, et al.* (2008). Nitric oxide-induced nuclear GAPDH activates p300/CBP and mediates apoptosis. Nat Cell Biol *10*, 866-873.

Sheffield, H.G., and Melton, M.L. (1968). The fine structure and reproduction of Toxoplasma gondii. The Journal of parasitology, 209-226.

Sheiner, L., Demerly, J.L., Poulsen, N., Beatty, W.L., Lucas, O., Behnke, M.S., White, M.W., and Striepen, B. (2011). A systematic screen to discover and analyze apicoplast proteins identifies a conserved and essential protein import factor. PLoS Pathog *7*, e1002392.

Shen, B., Brown, K.M., Lee, T.D., and Sibley, L.D. (2014). Efficient gene disruption in diverse strains of Toxoplasma gondii using CRISPR/CAS9. MBio *5*, e01114-01114.

Shen, B., and Sibley, L.D. (2014). Toxoplasma aldolase is required for metabolism but dispensable for host-cell invasion. Proc Natl Acad Sci U S A *111*, 3567-3572.

Sibley, L.D. (2004). Intracellular parasite invasion strategies. Science *304*, 248-253.

Sidik, S.M., Hackett, C.G., Tran, F., Westwood, N.J., and Lourido, S. (2014). Efficient genome engineering of Toxoplasma gondii using CRISPR/Cas9. PLoS One *9*, e100450.

Sirover, M.A. (1999). New insights into an old protein: the functional diversity of mammalian glyceraldehyde-3-phosphate dehydrogenase. Biochim Biophys Acta *1432*, 159-184.

Sirover, M.A. (2011). On the functional diversity of glyceraldehyde-3-phosphate dehydrogenase: biochemical mechanisms and regulatory control.

Soldati, D., Dubremetz, J.F., and Lebrun, M. (2001). Microneme proteins: structural and functional requirements to promote adhesion and invasion by the apicomplexan parasite Toxoplasma gondii. Int J Parasitol *31*, 1293-1302.

Speer, C.A., and Dubey, J.P. (1999). Ultrastructure of shizonts and merozoites of Sarcocystis falcatula in the lungs of budgerigars (Melopsittacus undulatus). J Parasitol *85*, 630-637.

Starkl Renar, K., Iskra, J., and Krizaj, I. (2016). Understanding malarial toxins. Toxicon *119*, 319-329.

Starnes, G. L., Coincon, M., Sygusch, J. and Sibley, L. D. (2009). Aldolase is essential for energy production and bridging adhesin-actin cytoskeletal interactions during parasite invasion of host cells. Cell Host Microbe *5*, 353-364.

Stedman, T.T., Sussmann, A.R., and Joiner, K.A. (2003). Toxoplasma gondii Rab6 mediates a retrograde pathway for sorting of constitutively secreted proteins to the Golgi complex. J Biol Chem *278*, 5433-5443.

Striepen, B., Crawford, M.J., Shaw, M.K., Tilney, L.G., Seeber, F., and Roos, D.S. (2000). The plastid of Toxoplasma gondii is divided by association with the centrosomes. J Cell Biol *151*, 1423-1434.

Striepen, B., Jordan, C.N., Reiff, S., and Van Dooren, G.G. (2007). Building the perfect parasite: cell division in apicomplexa. PLoS Pathog *3*, e78.

Sundararaj, K.P., Wood, R.E., Ponnusamy, S., Salas, A.M., Szulc, Z., Bielawska, A., Obeid, L.M., Hannun, Y.A., and Ogretmen, B. (2004). Rapid shortening of telomere length in response to ceramide involves the inhibition of telomere binding activity of nuclear glyceraldehyde-3-phosphate dehydrogenase. Journal of Biological Chemistry *279*, 6152-6162.

Suvorova, E.S., Francia, M., Striepen, B., and White, M.W. (2015). A novel bipartite centrosome coordinates the apicomplexan cell cycle. PLoS Biol *13*, e1002093.

Szatanek, T., Anderson-White, B.R., Faugno-Fusci, D.M., White, M., Saeij, J.P., and Gubbels, M.J. (2012). Cactin is essential for G1 progression in Toxoplasma gondii. Mol Microbiol *84*, 566-577.

Taha, M.S., Nouri, K., Milroy, L.G., Moll, J.M., Herrmann, C., Brunsveld, L., Piekorz, R.P., and Ahmadian, M.R. (2014). Subcellular fractionation and localization studies reveal a direct interaction of the fragile X mental retardation protein (FMRP) with nucleolin. PLoS One *9*, e91465.

Tisdale, E.J. (2001). Glyceraldehyde-3-phosphate dehydrogenase is required for vesicular transport in the early secretory pathway. J Biol Chem *276*, 2480-2486.

Tisdale, E.J. (2002). Glyceraldehyde-3-phosphate dehydrogenase is phosphorylated by protein kinase Ciota /lambda and plays a role in microtubule dynamics in the early secretory pathway. J Biol Chem *277*, 3334-3341.

Tisdale, E.J., and Artalejo, C.R. (2006). Src-dependent aprotein kinase C iota/lambda (aPKCiota/lambda) tyrosine phosphorylation is required for aPKCiota/lambda association with Rab2 and glyceraldehyde-3-phosphate dehydrogenase on pre-golgi intermediates. J Biol Chem *281*, 8436-8442.

Tisdale, E.J., and Artalejo, C.R. (2007). A GAPDH mutant defective in Src-dependent tyrosine phosphorylation impedes Rab2-mediated events. Traffic *8*, 733-741.

Tisdale, E.J., Azizi, F., and Artalejo, C.R. (2009). Rab2 utilizes glyceraldehyde-3-phosphate dehydrogenase and protein kinase C{iota} to associate with microtubules and to recruit dynein. J Biol Chem *284*, 5876-5884.

Tisdale, E.J., Kelly, C., and Artalejo, C.R. (2004). Glyceraldehyde-3-phosphate dehydrogenase interacts with Rab2 and plays an essential role in endoplasmic reticulum to Golgi transport exclusive of its glycolytic activity. J Biol Chem *279*, 54046-54052.

Treeck, M., Sanders, J.L., Elias, J.E., and Boothroyd, J.C. (2011a). The phosphoproteomes of Plasmodium falciparum and Toxoplasma gondii reveal unusual adaptations within and beyond the parasites' boundaries. Cell Host Microbe *10*, 410-419.

Treeck, M., Sanders, J.L., Elias, J.E., and Boothroyd, J.C. (2011b). The phosphoproteomes of Plasmodium falciparum and Toxoplasma gondii reveal unusual adaptations within and beyond the parasites' boundaries. Cell Host Microbe *10*, 410-419.

Tremp, A.Z., Al-Khattaf, F.S., and Dessens, J.T. (2014). Distinct temporal recruitment of Plasmodium alveolins to the subpellicular network. Parasitol Res *113*, 4177-4188.

Tremp, A.Z., Khater, E.I., and Dessens, J.T. (2008). IMC1b is a putative membrane skeleton protein involved in cell shape, mechanical strength, motility, and infectivity of malaria ookinetes. J Biol Chem *283*, 27604-27611.

Tristan, C., Shahani, N., Sedlak, T.W., and Sawa, A. (2011). The diverse functions of GAPDH: views from different subcellular compartments. Cellular signalling *23*, 317-323.

Verlinde, C.L., Hannaert, V., Blonski, C., Willson, M., Perie, J.J., Fothergill-Gilmore, L.A., Opperdoes, F.R., Gelb, M.H., Hol, W.G., and Michels, P.A. (2001). Glycolysis as a target for the design of new anti-trypanosome drugs. Drug Resist Updat *4*, 50-65.

Waingeh, V.F., Gustafson, C.D., Kozliak, E.I., Lowe, S.L., Knull, H.R., and Thomasson, K.A. (2006). Glycolytic Enzyme Interactions with Yeast and Skeletal Muscle F-Actin. Biophysical Journal *90*, 1371-1384.

Wang, Y., Karnataki, A., Parsons, M., Weiss, L.M., and Orlofsky, A. (2010). 3-Methyladenine blocks Toxoplasma gondii division prior to centrosome replication. Mol Biochem Parasitol *173*, 142-153.

Wong, S.Y., and Remington, J.S. (1994). Toxoplasmosis in pregnancy. Clin Infect Dis *18*, 853-861; quiz 862.

Yang, J., Gibson, B., Snider, J., Jenkins, C.M., Han, X., and Gross, R.W. (2005). Submicromolar concentrations of palmitoyl-CoA specifically thioesterify cysteine 244 in glyceraldehyde-3-phosphate dehydrogenase inhibiting enzyme activity: a novel mechanism potentially underlying fatty acid induced insulin resistance. Biochemistry *44*, 11903-11912.

Zorba, A., Buosi, V., Kutter, S., Kern, N., Pontiggia, F., Cho, Y.J., and Kern, D. (2014). Molecular mechanism of Aurora A kinase autophosphorylation and its allosteric activation by TPX2. Elife *3*, e02667.

Zou, C., Ellis, B.M., Smith, R.M., Chen, B.B., Zhao, Y., and Mallampalli, R.K. (2011). Acyl-CoA:lysophosphatidylcholine acyltransferase I (Lpcat1) catalyzes histone protein O-palmitoylation to regulate mRNA synthesis. J Biol Chem *286*, 28019-28025.